CALIFORNIA INSTITUTE OF TECHNOLOGY

EARTHQUAKE ENGINEERING RESEARCH LABORATORY

STRUCTURAL DAMAGE EVALUATION: THEORY AND APPLICATIONS TO EARTHQUAKE ENGINEERING

THESIS BY

RUSTEM SHAIKHUTDINOV

REPORT NO. EERL 2004-06

PASADENA, CALIFORNIA
MAY 2004

(DEFENDED FEBRUARY 17, 2004)

STRUCTURAL DAMAGE EVALUATION: THEORY AND APPLICATIONS TO EARTHQUAKE ENGINEERING

Thesis by

Rustem Shaikhutdinov

In Partial Fulfillment of the Requirements

for the Degree of

Doctor of Philosophy

Report No. EERL 2004-06

California Institute of Technology

Pasadena, California

2004

(Defended February 17, 2004)

Acknowledgments

My sincere gratitude goes to my adviser Professor James L. Beck for his direction and encouragement throughout the course of this investigation. Without his invaluable guidance and support, this thesis would not have been possible. I am also truly grateful to Keith A. Porter for the suggestions and input that were most helpful. I am thankful for the delightful time we spent working together.

I truly appreciate the time and input of Professors Wilfred D. Iwan, John F. Hall in reviewing my thesis and delegating their time to serve on my thesis examination committee. It has been a really enriching experience to be their student, as well.

My studies were financially supported by funds from California Institute of Technology; California Universities for Research in Earthquake Engineering under the CUREe-Kajima joint research program, Phase IV; the Earthquake Engineering Research Centers Program of the National Science Foundation under Award Number EEC-9701568 through the Pacific Earthquake Engineering Research Center (PEER). These supports are gratefully acknowledged. Any opinions, findings and conclusions or recommendations expressed in this material are those of the authors and do not necessarily reflect those of the support providers.

I am thankful to Carolina Oseguera and Connie Yehle for always being so thoughtful and supportive throughout all the years of my staying at Caltech.

My special thanks go out to my lovely wife Julia, who gave me strength and determination to pursue on the road of research and instilled my days with joy and happiness.

Abstract

The further development of performance-based earthquake engineering (PBEE) is on the current agenda of the earthquake engineering community. A part of assessing the seismic performance of civil engineering structures involves estimation of seismic damage. The conventional approach to damage estimation is based on fragility functions that relate some chosen parameters of structural response to incurred damage. Therefore, damage prediction is based exclusively on the knowledge of the chosen structural response parameters, meaning that damage analysis is uncoupled from the structural analysis. The structural response parameters selected for use in damage analysis are usually referred to as engineering demand parameters (*EDP*). In the present study, it is shown that for structural damage estimation, the uncoupled damage analysis has deficiencies that lead to less accurate damage prediction. These shortcomings originate from two sources: first, dependence of practically all *EDP*s on structural damage and second, inexact damage description. To overcome these deficiencies, another approach to structural damage estimation is proposed. The proposed approach, besides using an *EDP*, uses all information available from structural analysis that is relevant to the damage to be assessed, implying that damage analysis is coupled with structural analysis. It is shown that utilization of this additional information provides more accurate damage prediction. The difference between the two approaches is studied by comparison of results of damage estimation performed for a 2-D structural model of a reinforced-concrete frame. The results show that difference between uncoupled and coupled damage analysis estimates could be significant and that it depends on specific characteristics of the chosen structural model and the damage model in a complex way, preventing the possibility of

estimating this error in a general form that is applicable to all practically possible cases. Damage estimation is performed for various damage models that include both single and multiple damage states. Since the final goal of seismic performance evaluation is estimation of decision variables such as repair cost, downtime, etc., the two approaches to damage estimation are also compared in terms of repair cost that is calculated for the reinforced-concrete frame. A case where structural damage prediction is based on observation of *EDP* alone, without a structural model available, is also studied. It is shown that incorporating site-specific information can significantly change the damage estimates and, therefore, may be worth doing.

Table of contents

Table of Figures

1 Introduction

The primary focus of the present study is structural damage estimation. Damage estimation is a vital part of the seismic performance evaluation of buildings and other structures with respect to multiple performance objectives. In turn, the proper evaluation of seismic performance is essential for decision making involved in managing the risk to building, bridges, and other infrastructure in seismically active areas. Today, the earthquake engineering community faces new challenges that are brought about by the latest needs of the real estate development and management industries. The safety of buildings and other structures used to be the main concern of designers, owners, and regulators. The development of modern building codes has provided society with guidelines that serve well for achieving the required safety levels. However, nowadays other issues are becoming significant for owners and risk managers. Providing that safety requirements are met, the questions being asked now are "how much does it cost to repair?", "how long it will be shut down in case of the earthquake?", etc. These questions relate to the economic aspect of the seismic performance of real estate. Given the multiple performance objectives, accurate damage estimation becomes more important than ever. The issues involved in the decision-making process with respect to various performance objectives and the role of damage estimation in this process are discussed in detail in Sections 2.1 and 2.2, respectively.

Depending on the decision maker's needs, a building's seismic performance can be evaluated on different levels of accuracy. A rough performance estimate can be obtained by category-based techniques, where all facilities are subdivided into classes

that are specified by some formal feature and/or parameters. For example, such classes may be: reinforced-concrete shear-wall building higher than 7 stories, or single-span bridge with monolithic abutment. Then a performance prediction model is built on the observed seismic performance of all available samples within the category. This approach is used, among others, by Hart and Srinivasan (1994) and by Basoz and Kiremidjian (1999).

More advanced techniques include specific building information in the damage analysis, such as particular design features and the site seismic hazard. The information about structural design is usually included in a finite element structural model. The structural model is used for carrying out a structural analysis. Damage analysis is then executed based on the results of the structural analysis. If better performance prediction is desired by the decision maker, then more site-specific information can be incorporated in the structural analysis and the analysis can be closer to the real-life behavior of the structure. For a relatively rough analysis, a simplified building model, like a shear beam, can be used in a pushover analysis. If more accurate results are desired, then more sophisticated structural models should be used, such as detailed finite-element models together with dynamic time-history simulation. Accordingly, the damage estimation technique should match the accuracy of the structural analysis.

Here is where the key point of the present study lies. It is apparent that structural analysis tools are making steady progress in increasing the accuracy of models. More and more features of real structure behavior are included in the mathematical models, such as shear-flexure interaction or complex load interaction in 3-D. However, it will be shown that current damage analysis techniques in some cases do not match the enhanced

performance of the advanced structural analysis tools, making these advances largely wasted for loss estimation studies. Indeed, since the seismic performance assessment is based both on structural analysis and damage analysis, the inaccurate damage evaluation prevents reliable performance estimation from being achieved. The highly accurate structural analysis will not contribute to the final goal – accurate performance estimation, because the structural analysis results will be diluted by the larger errors at the stage of the damage estimation. Thus, the goal here is to develop improved methods of damage estimation that are capable of providing the results with an accuracy that matches the accuracy of the most sophisticated structural models.

From a practical perspective, as it is mentioned before, if more precise performance estimation is desired, then more site-specific information should be included in the analysis and more complicated analysis should be performed. It is true for the structural analysis and it is true for the damage analysis. In general, this means that the better performance estimation requires more effort and expense to perform the analysis. Such efforts are not justified for all real estate risk management problems. In most cases a high-end solution is unnecessary. However, there are problems when maximum accuracy is necessary despite the cost of achieving it. This is the case when calibration of less complex methods of performance analysis is needed; that is, the sophisticated method must provide the most accurate solution so that the performance of simplified techniques may be judged by how close their results are to the “exact” one. This is also the case when evaluation of the unique and expensive facilities is performed, where the additional expense for the more complicated analysis is justified.

Before we proceed with the introduction to the different damage estimation approaches, we want to point out that increasing utilization of site-specific information in the seismic performance analysis can lead to a potential problem, related to the inherent difficulty of experimental verification of the site-specific analysis results. A more detailed discussion of this problem is given in Section 2.3. Another problem of seismic performance evaluation that can arise is due to the different sensitivity of the decision-making process to the errors in performance assessment for different decision criteria. The issues relevant to this problem are also considered in Section 2.3

At the present time, the common tools of general purpose damage analysis are fragility functions that are used for uncoupled damage analysis. These functions establish a probabilistic relation between structural response to seismic loading and the resulting damage to individual components. Historically, fragility functions were developed within nuclear engineering to evaluate the seismic resistance of nuclear reactors with respect to operational or safety failure. Later, their area of application was extended to other fields, such as estimation of the seismic resistance of electrical equipment or the seismic performance of civil engineering structures such as bridges and buildings. For all these applications, fragility functions proved to be convenient, versatile and reasonably accurate tools of damage estimation.

In order to use fragility functions for a general, multiple criteria performance analysis, they must be applied to a broader range of objects than previously and serve for evaluation of a broader range of issues. The objects for damage evaluation can be any damageable piece of the structure or nonstructural components, such as beams, columns, partitions, windows, equipment, furniture, etc. The loading parameters (input to a

fragility function) can be spectral acceleration S_a, inter-story drift ratio (IDR), ductility demand, peak ground acceleration (PGA), etc., with the latter having been most heavily utilized before. The assessed damage can be fracture, full or partial loss of functionality, toppling, leakage, cracking, spalling, etc. As we can see, this amounts to a significant extension of fragility functions' applications. The adequacy of fragility functions and uncoupled damage analysis as tools to handle all of this newly introduced variety of problems can not be taken for granted. Indeed, we shall see that fragility functions as a part of uncoupled damage analysis have certain limitations, especially in the area of structural damage estimation. Chapter 3 provides a rigorous mathematical description of fragility functions from the perspective of structural reliability theory. The theory identifies the limitations of fragility functions and provides a foundation for devising a coupled approach to structural response and damage estimation.

Using the results presented in Chapter 3, we have developed a coupled approach to structural analysis and damage estimation that does not have the shortcomings of the uncoupled damage analysis. Within the proposed approach, we have developed a method of damage estimation that is referred to as Method 1 henceforth. Seismic damage has been estimated for some chosen case-study facilities by the proposed method and also by the uncoupled method. Chapter 4 describes the case studies and provides the results of damage estimation performed by the different techniques.

The problem with multiple damage states is explored in Section 3.2 and Chapters 5 and 6. Section 3.2 discusses theoretical issues arising from the multiple damage state case. Chapter 5 presents a case study of structures that consist of members with multiple damage states. Damage of the structure is evaluated by the existing methods and by the

proposed method of damage analysis. The same chapter describes how repair cost can be calculated based on the known damage state. The repair cost estimates are obtained for damage states that have been evaluated by different damage analysis methods. Results are compared in terms of both a damage measure (number of damaged members) and repair cost. A combined approach to damage analysis is developed in Chapter 6. To demonstrate a practical value of the proposed combined damage evaluation technique, the repair cost of an example structure is evaluated.

Chapter 7 deals with the problem of using fragility functions for structural health monitoring applications. It considers a model of a reinforced-concrete column and demonstrates that fragility functions applicable to in-situ structural members may differ from fragility functions that are developed using experimental data from in-lab test results.

2 Methods and challenges of performance-based earthquake engineering

2.1 Decision making for a real estate owner

Seismic performance is a vital characteristic of buildings and other structures for all agents that are involved in operations with real estate located in seismically affected areas. How well a particular building will perform during an earthquake at some point in the future is important because it affects the present value of the property. In particular, at any present time, a real estate owner can face a set of seismic risk-management options to choose from: do nothing, sell the property, perform seismic retrofit or buy earthquake insurance. Likewise, a potential owner (a person who wants to buy a real estate property) faces similar choices: do not buy, buy and do nothing, buy and retrofit, buy and insure.

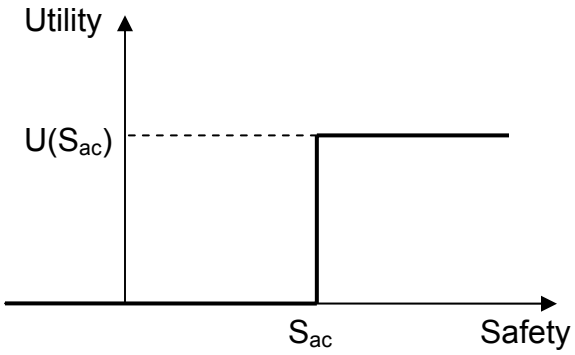

Figure 2.1 Example of utility function for decision making based on safety.

The process of making a choice between several alternatives can be analyzed by decision theory. Here we outline a simple procedure of formal decision making process. This analysis does not consider uncertainty in the outcomes or risk preferences of decision makers. The general approach of decision theory states that the best choice is the one that gives the highest utility among different options (for details about utility and

decision theory see, for example, Resnik 1987). Calculation of utilities for different options depends on the decision maker's objectives and preferences. When applying this concept to the case of a real estate owner or a buyer, usually the most prevalent concern is safety. In terms of decision theory, this means that the higher the safety of some option, the higher is its utility, meaning that utility is the increasing function of safety. Normally, it suffices to use a very simplistic utility function to account for the matter of safety. It is convenient to utilize a step function like one shown in the Figure 2.1. Such function basically states that any option with the safety less than some acceptable level should be rejected. When the safety is higher than S_{ac}, the utility is constant, implying that there is no marginal benefit from increasing safety beyond the acceptable level. This situation reflects an approach of real estate owners, where S_{ac} represents the safety level provided by modern building codes. Alternatively, for some owners, the acceptable level of safety is the one that meets minimum legal requirements. In both cases, once the safety requirement is satisfied, he or she does not care if the safety level is significantly higher than S_{ac} or just barely exceeds the threshold value.

If several options meet the safety requirement, then the owner can use some other criteria in order to choose between these options. For many owners, it appears that the other important issue that affects decision making is economic performance. There are different ways one can measure the economic performance of buildings and other structures with respect to seismic activity. Some of the quantities that are important for economic performance are repair cost and downtime. The repair cost represents the direct losses that the owner can incur – it is an uncertain expense associated with owning real estate. Downtime is the total time required to make the facility operational again and it

can be related to both direct and indirect losses, where “direct” losses are understood as decrease of value (e.g., cash outflow) and “indirect” losses refer to missed opportunities to acquire value (loss of profit due to business shut down). For example, for the residential owner, the downtime could be the time when the building is not livable. Therefore, temporary lodging would be needed, which means that the owner would bear the direct rental expenses associated with the lodging. For the commercial real estate, the downtime induces a loss of profit, which may be considered as the indirect loss. Clearly, both direct and indirect potential seismic losses associated with different options can affect the owner’s choice. Depending on the preferences of a particular owner, a utility function can be defined for repair cost and downtime.

Implementation of the decision choices usually involves some cost for the decision maker. For example, if a potential buyer decides to buy a property he will have to pay the purchase price. Similarly, if he resolves in favor of retrofitting measures or purchasing earthquake insurance, he will have to bear the price of the retrofit or insurance premium. The cost of each choice has a certain negative utility for the decision maker as well. Summing the utilities of the implementation cost and the future benefits, the option with the highest utility can be found. An illustration of the decision-making procedure for a current building owner is shown in Figure 2.2. In this example, the building owner can choose between three options: retrofit, insure or do nothing. By analysis, the owner can determine the option that maximizes his utility. In this case, all choices are associated with losing value: retrofit cost, insurance premium, future deductible and future losses that can include repair cost and downtime. Therefore, the best option minimizes the total loss.

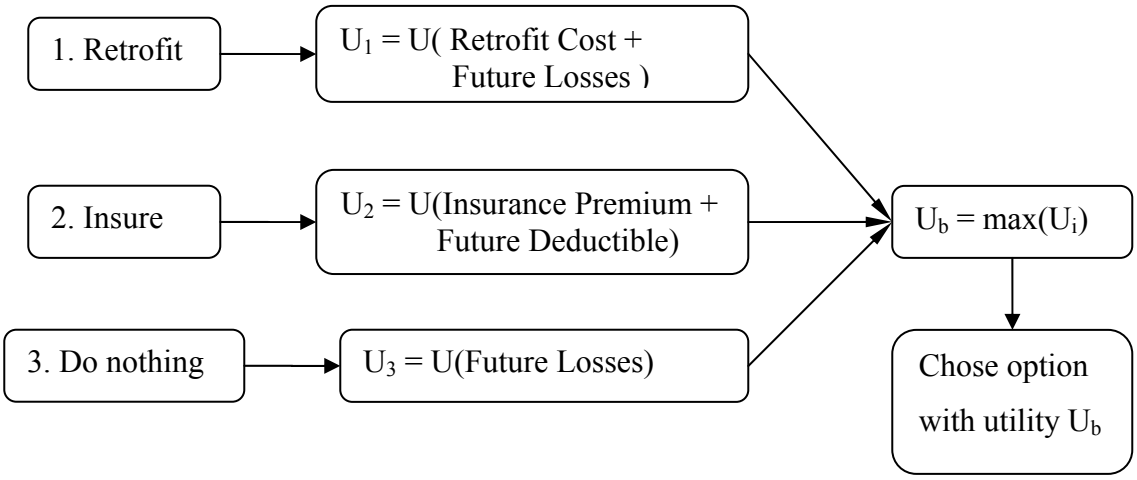

Figure 2.2 Example of a decision making process for a real estate owner.

The decision making process presented by Figure 2.2 disregards the uncertainty of the future losses and discounting of the future losses. A more sophisticated analysis would use the expected value of the utility of the future losses and benefits discounted to the present time, that is, use their present value (PV); see, for example, Beck et al. 2002. For the purpose of the present study it suffices to note that the optimal choice is based on a formal decision making process. An essential part of this process is evaluation of future losses that can be expressed in terms of repair cost or downtime or some other parameters. In the following chapters, we shall consider the ways to calculate these parameters.

2.2 Methods of performance-based earthquake engineering

The decision-making procedure described in Chapter 2.1 can be performed only if reliable estimates of building performance are available. Obtaining such estimates is not a trivial problem. The quantities of interest, such as the expected number of lives lost, repair cost and downtime depend on a huge number of uncertain variables. The number

of lives lost is one of the measures of the safety performance of buildings. The analysis of the safety of buildings and other structures has long been the subject of study of structural reliability theory. We give here a brief overview of the structural reliability approach.

2.2.1 Overview of structural reliability theory for seismic safety

Structural reliability theory for analysis of seismic safety usually does not directly consider such safety measures as expected number of lost lives. Instead, it deals with the events that can be directly related to the deaths caused by an earthquake. Such events are usually referred to as life safety failure (LSF). Two examples of LSF are total structural collapse and partial structural collapse. The problem of interest for practical applications is finding the probability of LSF. In general, this probability can be calculated according to the following probability integral

$$P(LSF) = \int_{\Omega_F} f_{\underline{Q},\underline{X}^S}\left(\underline{q},\underline{x}^S\right) d\underline{q} d\underline{x}^S \tag{2.1}$$

where $\underline{Q}$ is a vector of random variables that fully define the seismic excitation (ground acceleration time history is commonly used); $\underline{X}^S$ is a vector of random variables defining the values of all relevant structural properties; $\underline{q}$ and $\underline{x}^S$ are particular values of the random vectors $\underline{Q}$ and $\underline{X}^S$, respectively; $f_{\underline{Q},\underline{X}^S}\left(\underline{q},\underline{x}^S\right)$ is the joint probability density function of random vectors $\underline{Q}$ and $\underline{X}^S$; and Ω_F is the failure region comprising all the values of $\underline{Q}$ and $\underline{X}^S$ for which LSF occurs.

For convenience of calculation, the failure region is usually given a mathematical description as follows. Define a function $g\left(\underline{q},\underline{x}^S\right)$ in such a way that it possesses the following property

$$g\left(\underline{q},\underline{x}^S\right)<0 \;\Leftrightarrow [\underline{q},\underline{x}^S]\in\Omega_F \tag{2.2}$$

meaning that region of negative values of $g\left(\underline{q},\underline{x}^S\right)$ coincides with the failure region. Function $g\left(\underline{q},\underline{x}^S\right)$ is called a limit-state function for the LSF. Then the probability of LSF becomes

$$P(LSF)=\int_{g\left(\underline{q},\underline{x}^S\right)<0} f_{\underline{Q},\underline{X}^S}\left(\underline{q},\underline{x}^S\right)d\underline{q}d\underline{x}^S \tag{2.3}$$

Limit-state functions can be defined in a number of ways. One example is to define it in terms of maximum inter-story drift ratio (IDR)

$$g\left(\underline{q},\underline{x}^S\right)=d_l-d_m\left(\underline{q},\underline{x}^S\right) \tag{2.4}$$

where d_m is the maximum IDR resulting from a particular earthquake excitation $\underline{q}$ applied to a structure with properties $\underline{x}^S$; d_l is a chosen threshold value. This limit-state function implies that life safety failure occurs once the threshold value is exceeded: $d_m > d_l$. Therefore, this approach assumes that it is likely that the structure undergoes partial or complete collapse once the maximum IDR exceeds the threshold value. The choice of threshold value depends on a structure type and may be based on experimental or field observations. Substituting (2.4) into (2.3), we obtain a special case of the structural reliability integral

$$P(LSF)=\int_{d_l<d_m\left(\underline{q},\underline{x}^S\right)} f_{\underline{Q},\underline{X}^S}\left(\underline{q},\underline{x}^S\right)d\underline{q}d\underline{x}^S \tag{2.5}$$

Evaluation of integral 2.3 (or 2.5) is not a trivial task because vectors $\underline{Q}$ and $\underline{X}^S$ can contain up to several thousand variables and calculation of the function $g\left(\underline{q},\underline{x}^S\right)$ is

often computationally expensive because it involves a nonlinear structural analysis. A number of methods have been developed to estimate integral (2.3). Some of them are FORM, SORM and various Monte Carlo simulation based techniques (see, for example, Au and Beck, 2001a and Au and Beck, 2001b).

The well-developed methods of structural reliability are designed for estimation of the safety performance of structures. They do not provide ready tools for estimation of the economic performance of real estate. The development of such tools is on the current agenda of the earthquake engineering community. In this work, we shall discuss the approaches and methods used for development of such tools in detail.

2.2.2 Performance-based earthquake engineering framing equation

2.2.2.1 Standard integral form for arbitrary decision variables

Economic performance of real estate depends on more variables than safety performance. From Equation 2.1, it can be seen that in dealing with safety issues, structural reliability theory considers the sets of random variables that describe the ground motion and the structural properties. However, the knowledge of these variables is not sufficient for estimation of many important performance criteria, such as repair cost or downtime. For example, parameters like equipment price or labor cost are essential for estimation of the building repair/replacement cost. Including all the variables that affect the economic performance of the real estate into (2.1) leads to

$$P(EF) = \int_{\Omega_{EF}} f_{\underline{Q},\underline{X},\underline{M}}\left(\underline{q},\underline{x},\underline{m}\right) d\underline{q} d\underline{x} d\underline{m} \tag{2.6}$$

where $\underline{Q}$ defines ground motion time history as before, $\underline{X}$ contains both structural and nonstructural properties of the real estate (nonstructural properties can be the properties

of the building nonstructural elements or the building contents), $\underline{M}$ is composed of variables that represents market conditions (prices, availability of materials and contractors, etc.); $f_{\underline{Q},\underline{X},\underline{M}}(\underline{q},\underline{x},\underline{m})$ is a joint probability density function of all the variables; *EF* is an event that is classified as an economic failure and Ω_{EF} is the failure region for *EF*. The term "economic failure" is chosen to be consistent with "life safety failure." For different decision makers, *EF* can mean different things. For example, for an owner of commercial real estate, economic failure can mean that the repair cost is higher than some acceptable level. Alternatively, the owner may be intolerant to a downtime that is too long.

The limit function for *EF* is defined in a way similar to (2.2), with nonstructural properties and market conditions included in the independent variables

$$g(\underline{q},\underline{x},\underline{m}) < 0 \;\Leftrightarrow [\underline{q},\underline{x},\underline{m}] \in \Omega_{EF} \tag{2.7}$$

Depending on the priorities of the decision maker, the limit-state function can be defined in various ways. For example, it can be expressed in terms of repair cost or some other performance criteria. For repair cost, the limit-state function can be defined similarly to (2.4) as: $g(\underline{q},\underline{x},\underline{m}) = C_l - C_R(\underline{q},\underline{x},\underline{m})$. For the present study, we shall use a general formulation of the limit-state function

$$g(\underline{q},\underline{x},\underline{m}) = DV_l - DV(\underline{q},\underline{x},\underline{m}) \tag{2.8}$$

where *DV* (decision variable) stands for repair cost, downtime or any other variable that is important for a decision maker and DV_l is a chosen threshold value. The name "decision variable" is adopted because it is involved in the performance criterion that is

used in the decision making process subsequent to the building evaluation. Using (2.7) and (2.8), we can rewrite (2.6) in the following way

$$P(DV > DV_l) = \int_{DV(\underline{q},\underline{x},\underline{m})>DV_l} f_{\underline{Q},\underline{X},\underline{M}}(\underline{q},\underline{x},\underline{m})\, d\underline{q} d\underline{x} d\underline{m} \tag{2.9}$$

Comparing (2.9) and (2.5), it can be seen that in general the problem of economic performance evaluation is more complex than the problem of safety performance evaluation. First, the number of integration variables is larger, implying a corresponding increase in the dimensions of the integration space and the computational effort. The second hurdle stems from the fact that the limit function (2.8) is more difficult to evaluate for economic decision variables than for decision variables that are typically used in safety performance analysis. We shall now discuss this problem in more detail.

2.2.2.2 Evaluation of damage and decision variables

Consider the limit function (2.4) for the safety integral (2.5). Besides the designated threshold value of IDR d_l, it contains the maximum IDR which is a function of the ground motion and structural properties ($d_m(\underline{q},\underline{x}^S)$). The problem of evaluation of $d_m(\underline{q},\underline{x}^S)$ is equivalent to the problem of evaluation of the structural response of the building with the properties defined by $\underline{x}^S$ subjected to the seismic excitation $\underline{q}$. This problem has been extensively addressed in the past. A number of structural simulation software packages are freely or commercially available. New tools (e.g., OpenSees, PEERC, 2004) are under development to provide better accuracy in structural simulation. Therefore, the limit-state function (2.4) can be readily evaluated with existing tools.

Consider now the limit function (2.8) with the repair cost as DV. The repair cost of the whole structure can be found as a function of the repair or replacement cost of each

of its damaged components. Therefore, in order to evaluate (2.8), we need to know the repair or replacement cost of each building assembly as a function of vector $[\underline{q},\underline{x},\underline{m}]$, where small letters, as before, stand for particular values of the corresponding random variables $[\underline{Q},\underline{X},\underline{M}]$. For instance, take the repair/replacement cost of a window pane. The question to answer is: what is this cost for the particular window given that the building is subjected to the ground motion $\underline{q}$, properties of the building structural and non-structural components are $\underline{x}$, and market prices for parts and labor are $\underline{m}$? Let us assume that the window is not repairable, meaning that it can only be left as it is (if intact) or it can be replaced (if broken). Then if the market conditions are known, we know the cost of replacement of the window with the known dimensions and quality. Also, given the ground motion $\underline{q}$ and building properties $\underline{x}$, we can utilize structural properties $\underline{x}^S$ to obtain the structural response of the building (standard structural simulation packages can be used). With this kind of information, it is still unknown what has happened to the window. The window may or may not need replacement, meaning that the window replacement cost may be the market price of the replacement or zero. Therefore, we can not determine the exact value of the window repair/replacement cost and, consequently, we can not evaluate the limit-state function (2.8).

To find the window repair/replacement cost, we need additional information. This additional information is associated with the damage of the window. It can be easily seen that once we know how badly the window is damaged, we can determine the consequences with a high degree of certainty. For the window example, the repair/replacement cost can be defined with absolute certainty if the market conditions are also known, where the known market conditions mean that a particular supplier has

been chosen from the market participants and the supplier's price for the window (c_R) is fixed. Therefore, if the window is broken, then it needs to be replaced (repair/replacement cost equals the market price of the replacement), while if the window is intact then it does not need replacement (repair/replacement cost equals zero). Thus, for a particular window we have

$$C_R = \begin{cases} 0 & DS = "intact" \\ c_R & DS = "broken" \end{cases} \tag{2.10}$$

where $c_R \in \underline{m}$ is the known market window replacement price and DS denotes the damage state of the window. A similar relation between damage and repair cost (or any other DV) can be obtained for every assembly. Such a relation for repair costs is routinely established by cost estimators for post-earthquake conditions once the damage to the building is known.

Therefore, once the damage state of the window is known, the repair/replacement cost can be easily found. We can use the concept of damage states for the estimation of the limit-state function (2.8). We assume that the damage state of a component is independent of the market conditions $\underline{m}$ (for example, damage state of a window does not depend on how much the window replacement cost is). It is also obvious that the damage to the window depends on the magnitude of the applied damaging factor and the ability of the window to resist this damaging factor, that is, its "strength." In our problem, the magnitude of the damaging factor (or factors) depends on the seismic excitation $\underline{q}$ and the strength of the members and other relevant structural properties that are contained in $\underline{x}$. Therefore, it is reasonable to assume that the damage state of the window is a function of

$\underline{x}$ and $\underline{q}$: $DS = g_{DS}(\underline{q}, \underline{x})$. The general expression for the window repair/replacement cost can be rewritten as follows

$$\begin{aligned} C_R(\underline{q}, \underline{x}, \underline{m},) &= C_R(g_{DS}(\underline{q}, \underline{x}), \underline{m}) \\ &= C_R(DS, c_R) \end{aligned} \tag{2.11}$$

It is easy to see that (2.10) gives the repair replacement cost (2.11) for the particular assembly (a window), leading to the limit-state function (2.8) trivially.

2.2.2.3 Performance-based earthquake engineering framing equation

Applying the idea of damage states to the general case, we can find the probability of DV exceeding the threshold value DV_l in a way that is different from (2.9). Consider now a case of arbitrary DV estimated for the structure under consideration and the limit-state function in the form (2.8). Suppose that the damage state is some function of the seismic excitation $\underline{Q}$ and building properties $\underline{X}$: $DS = g_{\underline{DS}}(\underline{Q}, \underline{X})$. Suppose further that damage states are defined in such a way that DV is a function of the damage state and market conditions only

$$\begin{aligned} DV(\underline{Q}, \underline{X}, \underline{M}) &= DV(g_{\underline{DS}}(\underline{Q}, \underline{X}), \underline{M}) \\ &= DV(\underline{DS}, \underline{M}) \end{aligned} \tag{2.12}$$

where $\underline{DS}$ is a vector of damage states of all the assemblies that affects the value of DV. Clearly, (2.12) is generalization of (2.11) for the DV of the whole structure as opposed to the DV of a particular assembly (a window).

DV is a function of random variables and so it is a random variable itself. Thus, the probability of exceeding threshold value DV_l can be found through integration of the probability density function (PDF) of DV

$$P(DV > DV_L) = \int_{DV_L}^{\infty} f_{DV}(v)dv \tag{2.13}$$

where $f_{DV}(v)$ is the PDF of DV. Using (2.12), it is possible to find the PDF of DV as a marginal PDF of the joint PDF of DV and the damage measure $\underline{DS}$

$$f_{DV}(v) = \int_{-\infty}^{\infty} f_{DV,\underline{DS}}(v, \underline{ds})\, d\,\underline{ds} \tag{2.14}$$

where $\underline{DS}$ is a vector of the damage states of all the damageable components. Actually, $\underline{DS}$ is a discrete random variable whose positive values range over all the combinations of the damage states of all components. Therefore, we can count all the possible combinations and number them in some order. If there exist N different values of $\underline{DS}$ (N different combinations of damage states), then (2.14) can be rewritten as

$$f_{DV}(v) = \sum_{i=1}^{N} f_{DV,\underline{DS}}(v, \underline{ds}_i) \tag{2.15}$$

For the i-th value of the damage state vector $\underline{DS}$, we can find the joint PDF as a product of the joint probability mass function of $\underline{DS}$ and the conditional PDF of DV given $\underline{DS} = \underline{ds}_i$

$$f_{DV,\underline{DS}}(v, \underline{ds}_i) = f_{DV|\underline{DS}}(v \mid \underline{ds}_i) p_{\underline{DS}}(\underline{ds}_i) \tag{2.16}$$

Consider the conditional PDF: $f_{DV|\underline{DS}}(v \mid \underline{ds}_i)$. It can be found by differentiating the corresponding conditional cumulative distribution function CDF: $F_{DV|\underline{DS}}(v \mid \underline{ds}_i)$. This CDF can be evaluated in the following way

$$F_{DV|\underline{DS}}(v \mid \underline{ds}_i) = P(DV \le v \mid \underline{DS} = \underline{ds}_i)$$

Substituting (2.12), and assuming independence of damage state and market conditions, we obtain

$$\begin{aligned} F_{DV|\underline{DS}}(v \mid \underline{ds}_i) &= P(DV(\underline{M}, \underline{DS}) \le v \mid \underline{DS} = \underline{ds}_i) \\ &= P(DV(\underline{M}, \underline{ds}_i) \le v \mid \underline{DS} = \underline{ds}_i) \\ &= P(DV(\underline{M}, \underline{ds}_i) \le v) \\ &= P(\underline{M} \in \Omega_{v,i}) \end{aligned}$$

where $\Omega_{v,i}$ is the domain in the space of market conditions variables $\underline{M}$, which satisfies the following properties: $\underline{M} \in \Omega_{v,i}$ if and only if the inequality $DV(\underline{M}, \underline{ds}_i) \le v$ holds. Thus, assuming that the joint PDF of the market conditions variables is known, the conditional CDF is found as

$$F_{DV|\underline{DS}}(v \mid \underline{ds}_i) = \int_{\Omega_{v,i}} f_{\underline{M}}(\underline{m}) d\underline{m}$$

and the conditional PDF is

$$f_{DV|\underline{DS}}(v \mid \underline{ds}_i) = \frac{d}{dv} \int_{\Omega_{v,i}} f_{\underline{M}}(\underline{m}) d\underline{m} \tag{2.17}$$

Therefore once the function $DV(\underline{M},\underline{DS})$ is defined, the conditional PDF $f_{DV|\underline{DS}}(v \mid \underline{ds}_i)$ can be evaluated. Substituting (2.16) and (2.15) into (2.13), the probability of DV exceeding a threshold value DV_l can be written as

$$P(DV > DV_L) = \int_{DV_L}^{\infty} \sum_{i=0}^{N} f_{DV|\underline{DS}}(v \mid \underline{ds}_i) p_{\underline{DS}}(\underline{ds}_i) dv \tag{2.18}$$

where $f_{DV|\underline{DS}}(v \mid \underline{ds}_i)$ is obtained according to (2.17).

The joint probability mass function $p_{\underline{DS}}(\underline{ds}_i)$ can be found by the approach similar to one that is used for the estimation of $f_{\underline{DV}}(v)$. Thus, the set of structural response parameters that are vital for determining *DS* should be chosen. This kind of idea has been used for further modification of (2.18). As a result, the analytical methods of seismic performance evaluation for civil engineering structures with respect to multiple performance objectives have been proposed (Porter 2000, Porter et al. 2001, Beck et al. 1999, Irfanoglu 2000). Also, the integral (2.18) is rewritten in the form that is proposed to be the basis of performance-based earthquake engineering (PBEE) (Cornell and Krawinkler 2000, Krawinkler 2002, Miranda and Aslani 2003) as follows

$$P(DV > DV_l) = \sum_{i=1}^{N} \int_0^\infty \int_0^\infty \{P(DV > DV_l \mid \underline{DM} = \underline{dm}_i) p_{\underline{DM}|\underline{EDP}}(\underline{dm}_i \mid \underline{edp}) f_{\underline{EDP}|IM}(\underline{edp} \mid im) f_{IM}(im)\} d(\underline{edp}) d(im) \tag{2.19}$$

where damage measure (*DM*) is the authors' term for *DS* used before, that is, a vector containing the discrete damage states of all damageable components (henceforth, we shall use *DM* while considering a whole structure and *DS* for a separate component of the structure); *EDP* is a vector of engineering demand parameters containing structural response characteristics such as inter-story drift ratio (IDR), peak diaphragm acceleration (PDA), etc.; *IM* is an intensity measure of the ground motion such as spectral acceleration (S_a), peak ground acceleration (PGA), etc.; $P(DV > DV_l \mid \underline{DM} = \underline{dm}_i)$ is the probability of the decision variable being greater than DV_l conditioned on knowledge of the component damage states, $i = 1...N$, where N is the number of possible damage states for vector *DM*; $p_{\underline{DM}|\underline{EDP}}(\underline{dm}_i \mid \underline{edp})$ is the conditional probability mass function that is equal to the probability that the structure suffered the damage defined by $\underline{dm}_i$ given that it

has been subjected to the $\underline{EDP}$ whose value is equal to $\underline{edp}$; $f_{\underline{EDP}|IM}(\underline{edp}\,|\,im)$ is the conditional PDF of the structural response ($\underline{EDP}$) given that the intensity of the ground motion is im; $f_{IM}(im)$ is the PDF of the seismic event intensity measure (IM) given that an earthquake has occurred. Equation (2.19) gives the probability of a decision variable being greater than some threshold value given that an earthquake has happened.

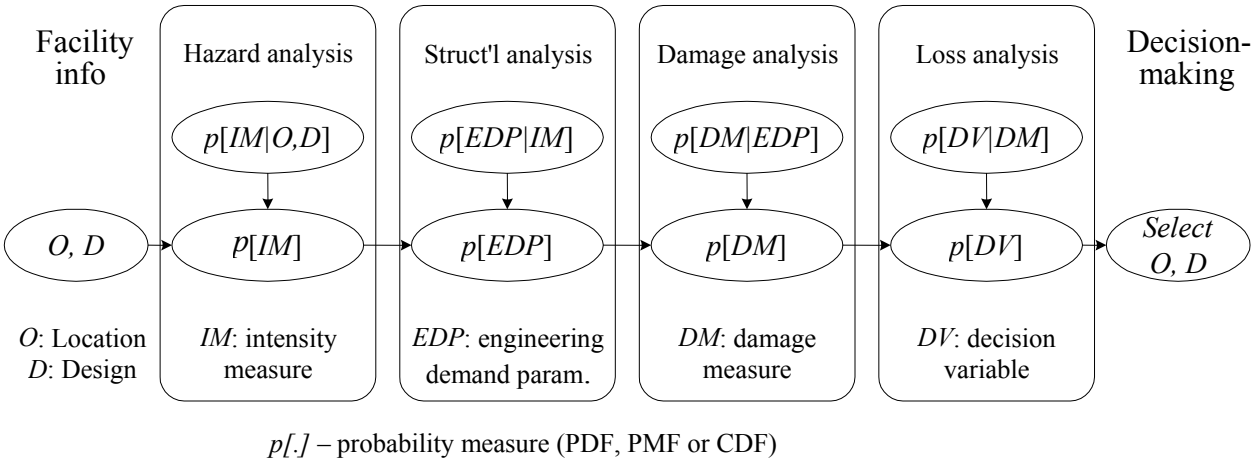

Figure 2.3 Implementation structure of the PEER PBEE framing equation.

Note that the left-hand sides of (2.9) and (2.19) are the same and so the integrals on the right-hand side must be also equal. However, the equality of two integrals can not be taken for granted. The integration over state space variables $\underline{Q}$, $\underline{X}$, $\underline{M}$ is implicit in (2.19) as opposed to the explicit integral form (2.9). Whether the implicit integration scheme is equivalent to the explicit integral depends on the choice of the intermediate variables used in the analysis: $\underline{EDP}$, $\underline{DM}$. One of the goals of the present study is to develop guidelines that can be used for adopting the proper $\underline{EDP}$ and $\underline{DM}$.

The factoring of the joint PDF in (2.9) into the product chain of conditional joint PDFs (2.19) provides an additional advantage. The whole problem can be divided into four separate parts as shown Figure 2.3. Each part can be analyzed independently of the

others, by the experts that are most qualified in the related area: seismic hazard analysis, structural analysis, damage analysis and loss analysis. Also, the analysis can be performed in parallel to provide a quicker result.

2.2.2.4 Fragility functions in PBEE framework

One of the essential parts of the PBEE framing equation is the conditional probability of being in particular damage state given the response: $p_{\underline{DM}|\underline{EDP}}\left(\underline{dm}_i \mid \underline{edp}\right)$. We shall investigate this expression in detail. The vector $\underline{DM}$ is a collection of damage states of every damageable component, where damage state is a discrete variable defining the severity of the damage for each component: $\underline{DM} = [DS_1, DS_2, \ldots DS_{Na}]$, where DS_i is the random variable that is equal to the damage state (DS) of the i-th damageable assembly, and N_a is the total number of the damageable assemblies in the structure. In practice, it usually suffices to deal with the state of each component of $\underline{DM}$ independently rather than with the whole vector at once. Therefore, we consider the j-th damageable component: $P\left(DS_j = n \mid \underline{EDP} = \underline{edp}\right)$, where $n = 1 \ldots k$ is the damage state number, k being the number of possible damage states of the j-th component. It is also reasonable to chose EDPs in such a way that only one variable in the vector $\underline{EDP}$ is relevant for evaluation of the damage of the j-th component. Denote this variable by EDP_j. Note that in general the number of damageable components is not equal to the number of EDPs, making the adopted indexing not quite general. However, we shall use the notation for simplicity, since it does not adversely affect the following considerations. Assuming that none of the other members of $\underline{EDP}$ except EDP_j provides any information about the damage state of the j-th component, it is easy to see

$$P\left(DS_j = n \mid \underline{EDP} = \underline{edp}\right) = P\left(DS_j = n \mid EDP_j = z\right) \tag{2.20}$$

where z is the known value of the j-th member of $\underline{EDP}$: EDP_j.

Damage states for each component are numbered according to the severity of the damage, giving higher numbers to the more severe damage. For example, for a window we can define three damage states: "undamaged," "cracked" and "broken." Then if the j-th component happens to be a window, the damage measure is defined as follows: DS_j = 0 means that the window is undamaged, DS_j = 1 corresponds to the window being "cracked" and DS_j = 2 corresponds to the window being "broken." These damage states are mutually exclusive and collectively exhaustive, meaning that none of them can happen together with the any of the others and there are no other outcomes that can happen to the window. For such damage states, the conditional probability of the j-th component being in n-th damage state can be found as follows

$$P\left(DS_j = n \mid EDP_j = z\right) = P\left(DS_j \geq n \mid EDP_j = z\right) - P\left(DS_j \geq n+1 \mid EDP_j = z\right) \tag{2.21}$$

where $P\left(DS_j \geq n \mid EDP_j = z\right)$ is the fragility function of the j-th component with respect to n-th damage state, expressed in terms of EDP_j. Therefore, fragility functions in PBEE are used to relate structural response and the induced damage. In the present study, we shall examine how well the fragility functions can serve this purpose for commonly encountered earthquake engineering applications.

2.3 Challenges of PBEE design

The difficulty in making seismic performance predictions for real estate comes, in the first place, from the incomplete knowledge about factors that define the seismic performance. The most important factors are associated with the seismic loading and the

ability of the structure to resist this loading. All the particular characteristics of both the seismic load and the structure are important for obtaining accurate estimates of decision variables. Different sites are capable of producing ground motions with different characteristics, such as intensity or frequency content. These characteristics define the destructive potential of the seismic event. Similarly, different structures have different strengths to resist the seismic loading. Destructiveness of the seismic event and the strength of the structure are the key factors that determine the overall seismic performance. Therefore, by including the knowledge of the particular characteristics of the ground motions specific to the site under consideration, one can improve the accuracy of seismic performance analysis. The same is true for the details of a particular building design. Indeed, the incorporation of site-specific seismic hazard information and building-specific structural information into seismic performance analysis is an increasingly popular way to improve the accuracy of seismic performance predictions.

However, the site-specific approach has a shortcoming: the more site-specific information is included in the mathematical models of seismic performance, the less verifiable those models are. For example, suppose that a decision maker uses a future repair cost as a criterion for his decision regarding a shear wall high-rise building located at a distance of 5 miles from a fault. Suppose further, that some estimate of the expected facility repair cost is obtained as a result of the seismic performance evaluation carried out by a method that is based on detailed information about the site hazard, such as soil conditions and seismicity of the fault, and a detailed structural model of the building. It turns out that the estimate can be confirmed by neither real-life observations nor experimental results. This can be seen from the following considerations.

In general, mathematical model results are verified by comparison with the results of experimental testing, where all the conditions of the test set up are equivalent to the conditions used in the mathematical model. Alternatively, verification can be performed through observations of naturally occurring phenomena in conditions similar to the ones used in the mathematical models. In the present example, the mathematical model includes the properties of the whole structure and surrounding terrain, therefore, exactly the same building and its environment must be recreated for the full-scale experimental program, which is practically impossible. Similarly, it is unrealistic to find a set of identical buildings and seismic conditions somewhere among already existing civil engineering structures, due to the great variety of designs and site conditions. Therefore, reliable verification of the mathematical model results is practically impossible.

The other potential problem comes from the increasing number of performance criteria. For example, consider two cases of decision making: one is based on safety and the other is based on money losses. Suppose in both cases a decision maker has a choice between two options: mitigate or do not mitigate.

First, consider safety-based decision making. Suppose, as a measure of safety, the number of lost lives is used. The performance analysis provides the following estimates for the two decision options: if mitigation is chosen then the future life losses are estimated to be from 2 to 4; if "do nothing" option is chosen then the life losses can be from 3 to 7. The usual decision making approach in such situation is conservative: choose the option with the best worst outcome. The outcomes include both implementation expenses and future losses

Option: "mitigate," the worst outcome: – (cost of mitigation + 4 lives)

Option “do nothing,” the worst outcome: – 7 lives

Clearly, the “mitigate” option would be preferable if the cost of mitigation is less than “cost” of three lives. The cost of mitigation is estimated $1.75M. Putting a price tag on a human life is a very sensitive issue that is usually avoided. At best, a very broad range of numbers can be inferred based on some real-life situations, such as court decisions. Facing the uncertainty of human life “cost,” one usually uses a conservative approach picking up a value from high end of the cost range. For most of the practical applications, this value is much higher than the mitigation cost. Therefore, the cost of mitigation might be assumed to be negligible in comparison with the value of human life, justifying the implementation of mitigation measures irrespective of the cost of such measures. Now, suppose we have developed a more accurate performance estimation method that gives a narrower range than in the original loss estimates: in case of mitigation, the future life losses are from 2.5 to 3; in case of no action, the future life losses can be from 3.5 to 4.5. The worst case outcomes become

Option: “mitigate,” the worst outcome: – (cost of mitigation + 3 lives)

Option: “do nothing,” the worst outcome: – 4.5 lives

The rational decision would be to choose the mitigate option if the cost of mitigation is less than the “cost” of 1.5 lives. However, since the human life is assumed to be practically invaluable, the mitigation option has to be chosen again, disregarding its cost. Therefore, in this case the decision making process that is based on safety criteria is insensitive to the accuracy of the seismic performance estimation method.

Second, consider economic-based decision making. Suppose the performance analysis provides the following estimates for the two decision options: if mitigation is

chosen then the future money losses are estimated to be from \$2.0 M to \$4.0 M; if "do nothing" option is chosen then the money losses can be from \$3.0 M to \$7.0 M. Exploiting the same conservative approach, we have the worst case estimates

Option: "mitigate," the worst outcome: $-(1.75 + 4.0) = -\$5.75$ M

Option: "do nothing," the worst outcome: $-\$7.0$ M

Clearly, the mitigation option is more attractive, since it provides lesser total losses. Now, suppose we have developed a more accurate performance estimation method that provides the following loss estimates: in case of mitigation, the future money losses are from \$2.5 M to \$3.0 M; in case of no action the future money losses can be from \$3.5 M to \$4.5 M. The worst case outcomes become:

Option: "mitigate," the worst outcome: $-(1.75 + 3.0) = -\$4.75$ M

Option: "do nothing," the worst outcome: $-\$4.5$ M

It can be seen that the optimal choice has changed. The best strategy in this case is to do nothing. Therefore, in this case the decision making process that is based on economic criteria is sensitive to the accuracy of the seismic performance estimation technique.

The same conclusion may also be derived from the following considerations. The economic performance is determined by a monetary value that is expected to be lost in the future due to seismic activity. The money equivalent life safety performance is defined by a number of lives lost and the value of a human life. Therefore, uncertainty of the monetary value loss contributes directly to uncertainty of the overall economic performance. But uncertainty of the overall money equivalent life safety performance combines both uncertainty of lives lost and very high uncertainty of the life value. Thus,

an increase of accuracy of the future money lost estimation (decrease of uncertainty) has an immediate impact on estimation of economic performance, possibly affecting a decision making process. The same increase of accuracy of the estimated future lives lost has a lesser impact on estimation of life safety performance, because it is swamped by the high uncertainty of human life value. Consequently, the impact on decision making should be less significant.

As we have seen, there are at least two reasons for a more thorough examination of seismic performance estimation techniques. First, since the results of a site-specific analysis are practically unverifiable, the number of assumptions and simplifications made in the mathematical model has to be minimized and each assumption has to be accurately estimated in terms of the margin of error that it introduces. Second, utilization of economic performance criteria in decision making makes the optimal choice more sensitive to the accuracy of the seismic performance estimation. Therefore, it is especially important for presumably "more accurate" performance estimates to be reliable and unbiased, which again depends on the assumptions that are made during the development of a particular method of seismic performance estimation.

3 Theory of fragility functions

The PBEE methodology should be applicable to any type of structure that is exposed to seismic risk, so equation (2.19) is relevant for buildings, bridges and other structures of concern. Usually such structures consist of many substructures, assemblies and subassemblies. Since an arbitrary *DV* is considered, damage to any of the structural components may affect the value of the *DV*. Therefore, fragility functions should be developed for any kind of component that can be damaged: building structural and nonstructural members, building contents, etc. This is a significant extension from the original area of application of the fragility functions in nuclear engineering, where fragility functions are primarily used to estimate damage to nuclear reactors. We investigate henceforth whether such an extension can lead to potential problems.

3.1 Single damage state

In this section, we shall consider the fragility functions of a component with respect to a single damage state. However, for generality, we use a notation that is consistent with the multiple damage state case but we do not discuss in this section the specific issues arising from the possible multiplicity of the damage states, leaving these problems for Section 3.2.

By definition, the fragility function of an arbitrary element is the probability of the element being in the n-th or higher damage state, given that EDP is equal to *z*

$$F^{n}(z) = P\left(DS \geq n \mid EDP = z\right) \tag{3.1}$$

We apply this definition to a generic type of component, meaning that it may apply to structural or nonstructural components or building contents. We refer to this

generic component as "an element." Thus, consider an element under seismic loading, which has k damage states. In general, the occurrence of damage to the element depends on various conditions: the earthquake characteristics, design of the structure affected by the earthquake, property of the elements of the structure including the properties of the element under consideration. As before, we denote the variables that define the earthquake properties (time history) by the vector $\underline{Q}$, and variables that define the structural properties by the vector $\underline{X}$. For the vector $\underline{X}$, we can write $\underline{X} = [\underline{X}_1, \underline{X}_2, \ldots, \underline{X}_i, \ldots]$, where vectors $\underline{X}_j$ contains the properties of the j-th element, $j = 1,2 \ldots m$, and m is the number of elements in the structure. Suppose there exists a function $g_n(\underline{X}, \underline{Q})$ with the following property

$$g_n(\underline{X}, \underline{Q}) < 0 \quad \Leftrightarrow \quad DS \geq n \tag{3.2}$$

It is said in structural reliability theory that the function $g_n(\underline{X}, \underline{Q})$ defines the limit state of the n-th damage state. Given that (3.2) holds, we can rewrite (3.1) as follows

$$F^n(z) = P(g_n(\underline{X}, \underline{Q}) < 0 \mid EDP = z) \tag{3.3}$$

Consider the conditioning part $EDP = z$. Normally, EDP is chosen in a way to provide some information about the damage state, that is, the knowledge that $EDP = z$ gives some information about the event $g_n(\underline{X}, \underline{Q}) < 0$. In other words, once we know that $EDP = z$, the conditional probability of the event $g_n(\underline{X}, \underline{Q}) < 0$ is different from the probability of the event $g_n(\underline{X}, \underline{Q}) < 0$ without knowledge of the value of EDP. Therefore, the limit-state function and EDP are probabilistically related. It is convenient to assume that the limit-state function and EDP are also functionally related, meaning that the limit-state function $g_n(\underline{X}, \underline{Q})$ can be written as an explicit function of EDP: $g_n(EDP, \underline{X}, \underline{Q})$. Then the fragility function assumes the following form

$$F^{n}(z) = P(g_n(EDP, \underline{X}, \underline{Q}) < 0 \mid EDP = z)$$

$$= P\,(g_n\,(z, \underline{X}, \underline{Q}) < 0 \mid EDP = z) \tag{3.4}$$

The conditioning part in (3.4) can be dropped in the case that there is no more relevant information in the event $EDP = z$, or, using the theory of probability terminology, events $g_n(z, \underline{X}, \underline{Q}) < 0$ and $EDP = z$ are independent

$$F^{n}(z) = P(g_n(z, \underline{X}, \underline{Q}) < 0) \tag{3.5}$$

However, the general form of fragility function (3.5) is very inconvenient for practical use. In order to find the probability of the event $g_n(z, \underline{X}, \underline{Q}) < 0$, it is necessary to integrate over the whole space of random variables $\{\underline{X}, \underline{Q}\}$

$$P(g_n(z, \underline{X}, \underline{Q}) < 0) = \int_{g_n\left(z, \underline{X}, \underline{Q}\right)<0} f_{\underline{X},\underline{Q}}(\underline{x}, \underline{q})\, d\underline{x}\, d\underline{q} \tag{3.6}$$

where $f_{\underline{X},\underline{Q}}\left(\underline{x}, \underline{q}\right)$ is the joint probability density function of the random variables that are contained in vectors $\underline{X}$ and $\underline{Q}$. The calculation of the integral (3.6) for the purpose of finding the fragility function is computationally expensive (we have to calculate the whole integral for each value of z). Also, the resulting fragility function has little practical value. Vectors $\underline{X}$ and $\underline{Q}$ and their joint PDF are different for each particular site and for each particular structure. Therefore, the fragility function calculated according to (3.6) is valid only for that particular element within the particular structure at the particular site. This leaves no room for utilizing the obtained fragility function for estimation of the fragility of the same element as part of another structure at some other site. Effectively, it means that the computational effort that is necessary for estimation of (3.6) would not be transferable.

To avoid this problem, let us assume that the limit function $g_n(\underline{X}, \underline{Q})$ can be rewritten in the following way

$$g_n(\underline{X}, \underline{Q}) = g_n(EDP(\underline{X}, \underline{Q}), \underline{X}_i), \tag{3.7}$$

where $\underline{X}_i$ are the properties of the element under consideration. Therefore, (3.5) can be rewritten

$$F^n(z) = P(g_n(z, \underline{X}_i) < 0) \tag{3.8}$$

and the fragility function can be estimated by the following integral

$$P\left(g_n\left(z, \underline{X}_i\right) < 0\right) = \int_{g_n\left(z, \underline{X}_i\right)<0} f_{\underline{X}_i}\left(\underline{x}_i\right) d\underline{x}_i \tag{3.9}$$

where $f_{\underline{X}_i}\left(\underline{x}_i\right)$ is the joint probability density of the element properties $\underline{X}_i$. Since $\underline{X}_i$ includes just a small fraction of the random variables that are contained in the vectors $\underline{X}$ and $\underline{Q}$, the integral (3.9) can be calculated much more easily than (3.6). Moreover, the fragility function calculated by (3.9) remains the same for all elements with the equivalent properties (same $\underline{X}_i$ and $f_{\underline{X}_i,}\left(\underline{x}_i\right)$) and does not depend on any external conditions. Therefore, the problem is made very generic and more convenient to treat.

However, such simplification can lead to potential problems that can be seen by considering the key step of the solution: the assumption that $g_n(\underline{X}, \underline{Q}) = g_n(EDP(\underline{X}, \underline{Q}), \underline{X}_i)$. Making this transformation, we need to satisfy the assumption (3.2), which for the current case takes the form

$$g_n(EDP(\underline{X}, \underline{Q}), \underline{X}_i) < 0 \;\Leftrightarrow\; DS \geq n \tag{3.10}$$

Whether (3.10) is satisfied obviously depends on the choice of EDP and possibly some other conditions. Note that violation of (3.10) effectively invalidates (3.9), since

once the event $g_n(EDP(\underline{X}, \underline{Q}), \underline{X}_i) < 0$ is not equivalent to the event $DS \geq n$, the corresponding probabilities are not guaranteed to be equal either. Therefore, the consequence of violation of (3.10) will be that the function estimated by (3.9) is not equal to the desired function (3.3). In Chapter 4, we shall consider the problems of the appropriate choice of *EDP* and conditions to ensure assumption (3.10) is valid. Also, we shall deal with the estimation of the possible error arising from its violation.

Assuming that (3.10) holds, it is convenient to introduce a new random variable that is usually called "capacity." The capacity is assumed to be the only property of the element that is relevant for determining its damage. Therefore, all the rest of the properties of the element, which are contained in $\underline{X}_i$, are used only for calculating the capacity: $C = C(\underline{X}_i)$. Then the limit-state function is usually formulated as follows

$$g_n(\underline{X}, \underline{Q}) = g_n(EDP(\underline{X}, \underline{Q}), C(\underline{X}_i)) \tag{3.11}$$

$$= C(\underline{X}_i) - EDP(\underline{X}, \underline{Q})$$

We shall use this model to estimate the fragility function. Substituting (3.11) into (3.3)

$$F^n(z) = P(C(\underline{X}_i) - EDP(\underline{X}, \underline{Q}) < 0 \mid EDP = z) \tag{3.12}$$

$$= P(C(\underline{X}_i) - z < 0 \mid EDP = z)$$

$$= P(C(\underline{X}_i) < z \mid EDP = z)$$

Assuming that $C(\underline{X}_i) < z$ and $EDP = z$ are independent, we find the fragility function as

$$F^n(z) = P(C(\underline{X}_i) < z) \tag{3.13}$$

We can conclude that if all of the aforementioned conditions are satisfied, then the fragility function of the element is a cumulative distribution function of its capacity, providing that capacity is a continuous random variable. To distinguish the particular

capacity defined in (3.11) – (3.13) from other properties of the element that are similar in nature we call it "capacity with respect to *n*-th damage state, formulated in terms of *EDP*."

3.1.1 Fragility functions of the structural members

So far, all assumptions that have been made to arrive at formulation (3.13) have not involved any special provisions regarding the particular characteristics of the element under consideration. The derivation is made for an abstract, generic element. From now on we shall consider elements that represent the structural members of a facility, where we define structural member as a component that significantly affects structural response. Examples of structural members are beams, columns, shear walls, etc.

We start by exploring the general functional form of engineering demand parameters: $EDP(\underline{X}, \underline{Q})$. In practice, all *EDP* that are used in earthquake engineering can be subdivided into two groups: the parameters that depend purely on the excitation $\underline{Q}$, such as PGA, PGV, and other similar characteristics of ground motion, and *EDP*s that depend on the structural response and so both on the excitation $\underline{Q}$ and the properties of the structure $\underline{X}$. Some of the latter *EDP*s are: Inter-story Drift Ratio (IDR), ductility demand, peak diaphragm acceleration (PDA), spectral acceleration S_a (since it depends on the first natural period and damping of the structure), various damage indices – the list includes practically all of the structural response parameters that are being used by the earthquake engineering community. We shall consider the *EDP*s of the second type as "structure-dependent." Since such *EDP*s depend on the structure ($\underline{X}$) in general, it is reasonable to assume that they depend on the each structural member ($\underline{X}_i$) in particular. Otherwise, if an element does not have any effect on the structural response (*EDP* does

not depend on $\underline{X}_i$), then that element is not a structural member. Therefore we can write down *EDP* in the unfolded form

$$EDP(\underline{X},\underline{Q}) = EDP(\underline{X}_1,\underline{X}_2,\ldots,\underline{X}_i,\ldots,\underline{Q}) \tag{3.14}$$

Substitute (3.14) into (3.12)

$$F^n(z) = P(C(\underline{X}_i) < z \mid EDP(\underline{X}_1,\underline{X}_2,\ldots,\underline{X}_i,\ldots,\underline{Q}) = z) \tag{3.15}$$

The classic understanding of conditioning presumes no other knowledge beside the value of *EDP*: *EDP* = z. It corresponds to the case of observation of actual structural behavior, where *EDP* is the only relevant observable parameter and we know neither the properties of the structural members ($\underline{X}_j$, j = 1…*m*) nor the earthquake time history ($\underline{Q}$). In that case, the only available information is that an earthquake has happened and *EDP* = z. This situation is applicable to structural health monitoring.

Recall that the conditioning part in (3.15) can be ignored if and only if events $EDP(\underline{X}_1, \underline{X}_2,\ldots, \underline{X}_i ,\ldots, \underline{Q}) = z$ and $C(\underline{X}_i) < z$ are independent. Equivalently, the conditioning in (3.15) can be discarded if and only if event $EDP(\underline{X}_1, \underline{X}_2,\ldots, \underline{X}_i ,\ldots, \underline{Q}) = z$ does not contain any information about the event $C(\underline{X}_i) < z$. In the present case, the events at issue are not independent in general, because both of them depend on the properties of the element, for which the fragility function is estimated. Therefore, there is some information in the event $EDP(\underline{X}_1, \underline{X}_2,\ldots, \underline{X}_i ,\ldots, \underline{Q}) = z$, which can change the probability of the event $C(\underline{X}_i) < z$. Mathematically, a certain care is needed for the proper application of conditioning in the multivariate state space ($\underline{X}$, $\underline{Q}$). A standard way to do it is by transformation to a different coordinate system. Let us introduce a coordinate system $\underline{Y}$ =

$\psi(\underline{X}, \underline{Q})$ with total number of coordinates (y_i) equal to the total number of variables in vectors $\underline{X}$ and $\underline{Q}$. The transformation ψ is defined as follows

$$\psi: \quad y_1 = EDP, \qquad y_i = e_i,\ i = 2..n_p \tag{3.16}$$

where e_i are the members of the vector $[\underline{X}, \underline{Q}]$ and n_p is the length of the vector $[\underline{X}, \underline{Q}]$. Therefore, the new coordinates $\underline{Y}$ are equal to the old coordinates $[\underline{X}, \underline{Q}]$ except that the first variable is equal to *EDP*. In $\underline{Y}$ coordinates, (3.15) takes form

$$F^n(z) = P(C(\underline{Y}_i) < z \mid Y_1 = z) \tag{3.17}$$

where $\underline{Y}_i = \underline{X}_i$ - the properties of the i-th element. Equation (3.17) can be evaluated with the standard integral expression

$$F^n(z) = \int_{C(\underline{y}_i)<z} f_{\underline{Y}_i|Y_1}(\underline{y}_i \mid z)\, d\underline{y}_i \tag{3.18}$$

where the conditional PDF is found as a ratio of the joint PDF of vector $[\underline{Y}_i, Y_1]$ and PDF of Y_1: $f_{\underline{Y}_i|Y_1}(\underline{y}_i \mid z) = f_{\underline{Y}_i, Y_1}(\underline{y}_i, z) / f_{Y_1}(z)$. The joint PDFs for any subset of the state space variables $\underline{Y}$ can be found from the joint PDF of the whole set $f_{\underline{Y}}(\underline{y})$ as marginal PDFs

$$f_{\underline{Y}_i, Y_1}(\underline{y}_i, z) = \int_{-\infty}^{+\infty} f_{\underline{Y}}(z, \underline{y}_i, \underline{y}^R)\, d\underline{y}^R \tag{3.19}$$

$$f_{Y_1}(z) = \int_{-\infty}^{+\infty} f_{\underline{Y}}(z, \underline{y}^R)\, d\underline{y}^R$$

where, for each integral, $\underline{y}^R$ are the remaining variables of the vector $\underline{Y}$. The joint PDF of $\underline{Y}$ can be obtained from the joint PDF of $[\underline{X}, \underline{Q}]$ and transformation of variables (3.16) via a conventional mathematical technique (see for example Williams, 2001)

$$f_{\underline{Y}}\left(\underline{y}\right) = f_{\underline{X}^*}\left(\psi^{-1}\left(\underline{y}\right)\right)\left|J\left(\begin{matrix}\underline{x}^* \\ \underline{y}\end{matrix}\right)\right| \tag{3.20}$$

where $\underline{X}^* = [\underline{X}, \underline{Q}]$, $\psi^{-1}(.)$ is the inverse of the transformation (3.16) and $|J(.)|$ is Jacobian of the inverse transformation: $\det\left(dx_i^* / dy_j\right)$, $i, j = 1..n_p$.

In general, a fragility function calculated according to (3.18) does not necessarily equal the CDF of capacity (3.13). Therefore, using (3.13), although convenient, can lead to potential errors in estimation of the damage. Expression (3.18) provides the exact fragility function, but due to mathematical complexity it can only be evaluated for relatively simple cases. Some of such instances can still be of a practical value. For example, in Chapter 6, we consider in detail the shear fragility of a reinforced concrete column, which is evaluated according to both (3.13) and (3.18).

Now, consider a problem of structural damage evaluation using a structural model. This problem is relevant for a case when we want to evaluate seismic performance of an existing structure by developing its structural model and performing structural analysis with the model. It is also the case for a building that is planned for construction, where the seismic performance evaluation of the design is usually based on a structural model as well. We shall see that in this case we can perform a much better structural damage evaluation using additional information available from the model, other than known values of *EDP*s.

When seismic performance evaluation is conducted for a structural model, the value of an *EDP* is obtained as a result of the mathematical simulation rather than as a result of real-life observation. To perform this mathematical simulation, it is necessary to have some preliminary work completed: first, a structural model of the structure has to be

developed, and second, all the parameters of the model have to have known values. Therefore, some suset of the structural member properties ($\underline{X}_j$, j = 1…m) has to be specified before the *EDP* value is obtained. We denote the subset of the member properties that defines the structural behavior by $\underline{X}_i^S$ ($\underline{X}_i^S \subset \underline{X}_j$). In general, the properties of the element, which are used for the calculation of the *EDP,* do not coincide with the element properties controlling the occurrence of damage. For the chosen limit-state function, damage depends on capacity. We define a subset of $\underline{X}_i$ that defines the capacity of the element by $\underline{X}_i^C$. It general, the subsets $\underline{X}_i^S$ and $\underline{X}_i^C$ do not coincide, but it is typical that they overlap: $\underline{X}_i^C \cap \underline{X}_i^S \neq \varnothing$. The size of overlapping depends on the definition of damage states, on the choice of *EDP* and on how the structural model is built and how detailed the structural model is. Incorporating all the available information into the conditioning part of (3.15), we can obtain the probability of an element being in the n-th or higher damage state as follows

$$F_{SM}^n(z) = P(C(\underline{X}_i^C) < z \mid EDP(\underline{X}_1^S,\ldots,\underline{X}_i^S,\ldots,\underline{Q}) = z, \underline{X}_1^S = \underline{x}_1^S,\ldots \underline{X}_i^S = \underline{x}_i^S,\ldots) \quad (3.21)$$

where we denote a fragility function with the known structural model properties included in the conditioning part by $F_{SM}^n(z)$ and $\underline{x}_j$, j = 1…m are the specified values of member properties $\underline{X}_j$.

Let us assume that the intersection of the sets $\underline{X}_i^S$ and $\underline{X}_i^C$ is not a null set. Then we denote by $\underline{X}_i^{CO}$ the part of parameters that affect only the capacity and are not important for the structural model, by $\underline{X}_i^{CS}$ the parameters that enter both structural model and capacity function ($\underline{X}_i^{CS} = \underline{X}_i^C \cap \underline{X}_i^S$) and by $\underline{X}_i^{SO}$ the parameters that are input into

structural model but do not affect the capacity of the element. Then vector $\underline{X}_i$ can be rewritten in terms of these sub-vectors: $\underline{X}_i = [\underline{X}_i^{CO}, \underline{X}_i^{CS}, \underline{X}_i^{SO}]$, and (3.21) takes the form

$$F_{SM}^{n}(z) = P(C(\underline{X}_i^{CO}, \underline{X}_i^{CS}) < z \mid EDP(..., \underline{X}_i^{S}, ..., \underline{Q}) = z, ..., \underline{X}_i^{CS} = \underline{x}_i^{CS}, \underline{X}_i^{SO} = \underline{x}_i^{SO}, ...) \quad (3.22)$$

Now, beside $EDP = z$, the conditioning part contains another piece of information, which is relevant to the event $C(\underline{X}_i^{C}) < z$. This piece is $\underline{X}_i^{CS} = \underline{x}_i^{CS}$. Taking this additional information into account, we can find a probability of the n-th or higher damage state as

$$F_{SM}^{n}(z) = P(C(\underline{X}_i^{CO}, \underline{x}_i^{CS}) < z \mid EDP(..., \underline{X}_i^{S}, ..., \underline{Q}) = z, ..., \underline{X}_i^{CS} = \underline{x}_i^{CS}, \underline{X}_i^{SO} = \underline{x}_i^{SO}, ...) \quad (3.23)$$

$$= P(C(\underline{X}_i^{CO}, \underline{x}_i^{CS}) < z)$$

The fragility function with conditioning on structural properties becomes a CDF of the capacity of the element where some part of the elements properties is known and the other part is uncertain (random). Therefore, the uncertainty in the damage estimation is reduced by the knowledge of some parameters. In the limit it is possible to have a case where we have the complete knowledge about damage. To see this, consider an element for which the following condition holds

$$\underline{X}_i^{C} \subset \underline{X}_i^{S} \quad (3.24)$$

The condition (3.24) states that all the properties that define the element's capacity are also needed for development of the structural model, meaning that knowledge of structural properties implies a full knowledge of "capacity" properties. Then, a probability of being in the n-th or higher damage state can be found in a way similar to (3.23) as follows

$$F_{SM}^{n}(z) = P(C(\underline{X}_i^C) < z \mid EDP(\underline{X}_1^S, \ldots, \underline{X}_i^S, \ldots, \underline{Q}) = z, \underline{X}_1^S = \underline{x}_1^S, \ldots \underline{X}_i^S = \underline{x}_i^S, \ldots) \quad (3.25)$$

$$= P(C(\underline{x}_i^C) < z)$$

$$= \begin{cases} 1 & C(\underline{x}_i^C) < z \\ 0 & C(\underline{x}_i^C) > z \end{cases}$$

Because of the known value of $C(\underline{x}_i^C)$, such a structural model based fragility function becomes deterministic, providing full knowledge about occurrence of damage. Depending on $C(\underline{x}_i^C)$, the fragility function takes on the value of 0 or 1. In practice, the knowledge of the element properties is usually neglected for the purpose of the damage analysis by fragility functions. Ignoring this information can lead to a less accurate damage estimation. We shall investigate this in detail in Chapter 4 by considering damage of the sample model: a reinforced-concrete moment frame.

For the case study in Chapter 4, we shall explore the situation where subset $\underline{X}_i^C$ belongs to $\underline{X}_i^S$, providing complete information about $\underline{X}_i^C$ once $\underline{X}_i^S$ is known (condition 3.24 holds). This case requires the use of (3.25) for damage estimation. It also should provide an upper bound on the error arising from neglecting information about element structural properties.

From the theoretical consideration presented above, it can be seen that difference between a classic fragility function ($F^n(z)$) and a structural model based fragility function ($F_{SM}^n(z)$) depends on the size of overlapping of the two sets of element properties: $\underline{X}_i^{CS} = \underline{X}_i^C \cap \underline{X}_i^S$. If the two sets do not overlap then there is no difference between $F^n(z)$ and $F_{SM}^n(z)$, implying that the standard fragility function provides the

best accuracy possible. This case is normally applicable to nonstructural building components and building contents because it is usually assumed that they do not affect the response behavior (*EDP*s) of the structure.

For structural members, the situation is different. It is almost always the case that there is an overlapping between structural model properties and capacity properties: $\underline{X}_i^C \cap \underline{X}_i^S \neq \varnothing$. In that case we can always achieve better accuracy by using a structural model based fragility function $F_{SM}^n(z)$ rather than a standard fragility function $F^n(z)$.

3.2 Multiple damage states

In practice, it is often desirable to consider more than one damage state for some damageable component. Multiple damage states can be used to represent different levels of damage (for example, a window can have three levels of damage: intact, cracked or broken), or to represent different modes of failure. An example of the latter could be a heavy and valuable piece of equipment for which the following three damage states can be considered: sliding more than some threshold value, overturning and loss of functionality (breaking). In this section, we shall consider the theoretical implications of the multiple damage states case.

Suppose that we want to consider several damage states for a damageable component. Let us assume that there are $N+1$ damage states: DS=0,..., N, where DS = 0 corresponds to the undamaged state. For any given level of response $EDP = z$, there exists a set of possible outcomes (damage levels)

$$(\Omega \mid z) = \{DS = 0,\ DS = 1,\ DS = 2, \ldots,\ DS = N\} \tag{3.26}$$

The obvious goal is to find the probability distribution associated with this set, so that we can determine the probability of occurrence of all possible outcomes including individual events (DS = i) and unions and intersections of events. First, we assume the most general relation between damage states, meaning that all unions and intersections of events and subsets of the events of the state space have non-zero probability associated with them. We will use fragility functions for the analysis. Assume that we have found N fragility functions

$$F^1(z) = P(DS \geq 1 \mid EDP = z) = P(DS = 1 \cup DS = 2 \cup \ldots \cup DS = N \mid EDP = z) \quad (3.27)$$
$$F^2(z) = P(DS \geq 2 \mid EDP = z) = P(DS = 2 \cup DS = 3 \cup \ldots \cup DS = N \mid EDP = z)$$
$$\ldots$$
$$F^N(z) = P(DS \geq N \mid EDP = z) = P(DS = N \mid EDP = z)$$

Now, consider the union of two events

$$\{DS \geq 1\} \cup \{DS = 0\} = \Omega \quad (3.28)$$

then it follows

$$P(DS \geq 1) + P(DS = 0) - P(DS \geq 1 \cap DS = 0) = 1$$

regrouping the terms we have

$$P(DS = 0) = 1 - P(DS \geq 1) + P(DS \geq 1 \cap DS = 0)$$

where we have skipped the conditioning on EDP for convenience. It is always true that $P(DS \geq 1 \cap DS = 0) = 0$, because DS = 0 means that the element is undamaged and the event DS ≥ 1 means that some damage has occurred and so, the event DS=0 ∩ DS ≥ 1 can not happen. Then, the probability of an element being undamaged is

$$P(DS = 0 \mid EDP = z) = 1 - P(DS \geq 1 \mid EDP = z) = 1 - F^1(z) \quad (3.29)$$

Similarly for $DS = 1$

$$\{DS \geq 2\} \cup \{DS = 1\} = \{DS \geq 1\} \tag{3.30}$$
$$P(DS \geq 2) + P(DS = 1) - P(DS \geq 2 \cap DS = 1) = P(DS \geq 1)$$
$$P(DS = 1) = P(DS \geq 1) - P(DS \geq 2) + P(DS \geq 2 \cap DS = 1)$$

Assuming that events $DS \geq 2$ and $DS = 1$ are also mutually exclusive, then

$$P(DS = 1 \mid EDP = z) = F^1(z) - F^2(z) \tag{3.31}$$

Applying the same procedure to the remaining damage states, we can obtain

$$P(DS = 0 \mid EDP = z) = 1 - F^1(z) \tag{3.32}$$
$$P(DS = i \mid EDP = z) = F^i(z) - F^{i+1}(z), \quad i = 1 \ldots N-1$$
$$P(DS = N \mid EDP = z) = F^N(z)$$

providing that the following holds

$$DS = i,\ i = 0 \ldots N \text{ are mutually exclusive} \tag{3.33}$$

The assumption (3.33) is usually satisfied if the damage states are defined to represent increasing severity of damage. However, if the damage states represent different failure modes, then they are not necessarily mutually exclusive. In the aforementioned example of heavy piece of equipment, all the damage states are not exclusive. For example, the equipment can just break, or it can break and overturn, or it can break and slide. Therefore, the damage states can happen in any combination, making the damage analysis more complicated. We shall discuss such a case in Section 3.2.1.

From (3.32), we can easily derive the following property of a set of fragility functions: for every value of the argument z, the fragility functions provide a decreasing

sequence of values as DS goes from 1 to N. Since $P(DS = i \mid EDP = z) \geq 0$ for any i, it follows

$$1 \geq F^1(z) \geq F^2(z) \geq \ldots \geq F^N(z) \qquad \forall z \tag{3.34}$$

The condition (3.34) holds even when the damage states are not mutually exclusive. We can show this as follows. Consider events $DS \geq i$ and $DS \geq i+1$. Clearly

$$\{DS = i+1 \cup DS = i+2 \cup \ldots \cup DS = N\} \subseteq \{DS = i \cup DS = i+1 \cup \ldots \cup DS = N\} \tag{3.35}$$

$$\{DS \geq i+1\} \subseteq \{DS \geq i\} \quad \forall i$$

so giving

$$P(DS \geq i+1 \mid EDP = z) \leq P(DS \geq i \mid EDP = z) \quad \forall i$$

Figure 3.1 shows a set of fragility functions for the case of five damage states and the corresponding probabilities of damage state occurrence. Figure 3.2 shows the probability space structure for different values of EDP: $EDP = z_1$, $EDP = z_2$. Probability space is presented in terms of sets A_i denoting the event $DS \geq i$.

It is important to remember that (3.32) can be used to find the probability distribution on damage states, conditioned on EDP, only if property (3.33) holds. In many cases, this can be assured by the appropriate definitions of the damage states. Otherwise, we can not use the simple and convenient relations (3.32), and we need to work out some other approaches that are discussed in Section 3.2.2.

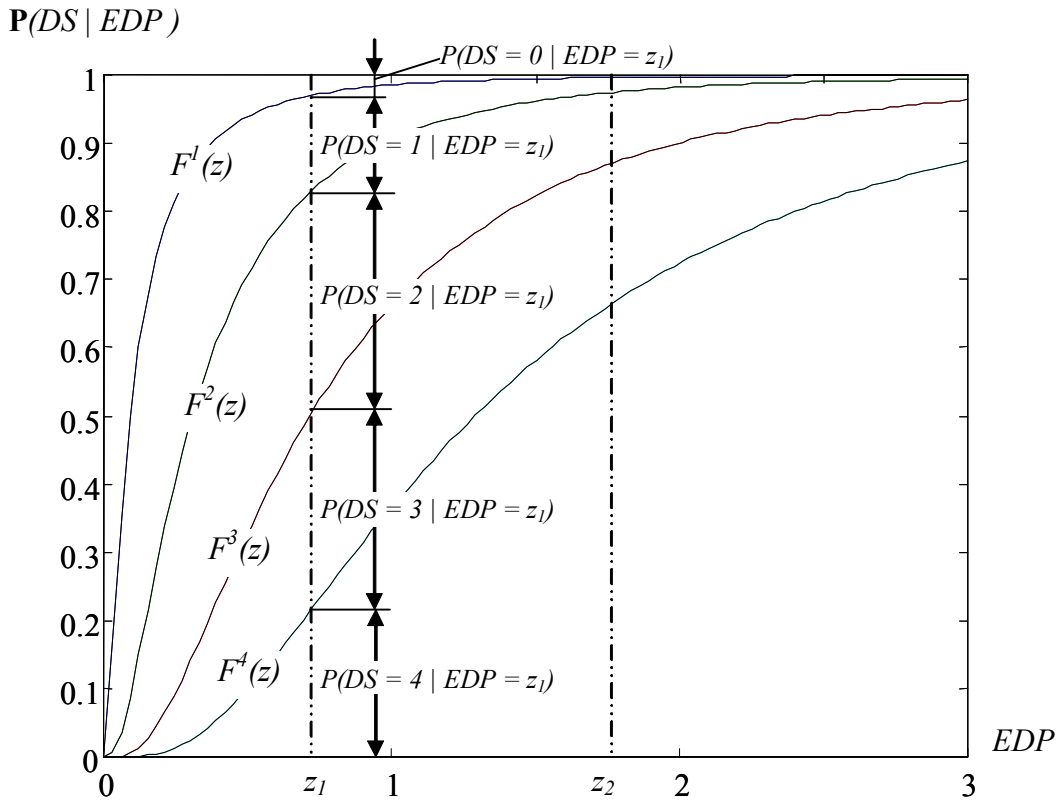

Figure 3.1 Fragility functions for multiple damage states

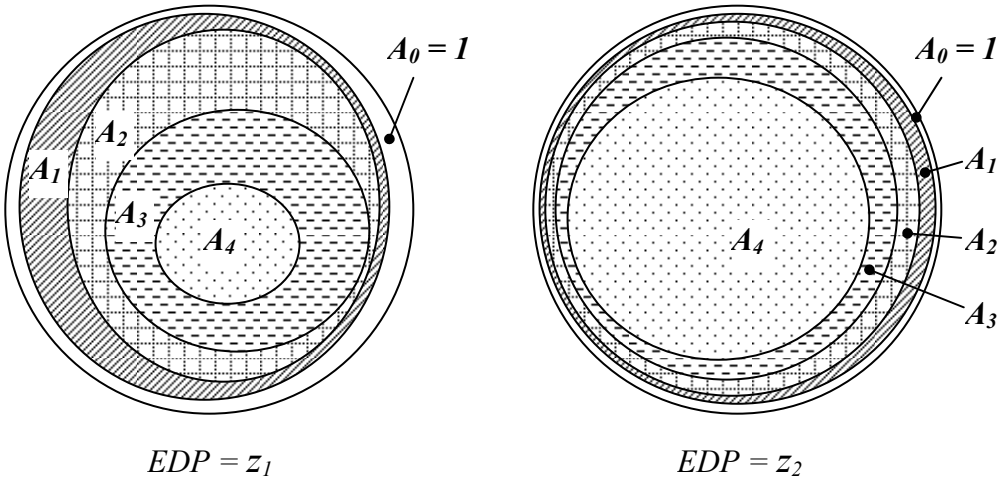

Figure 3.2 Damage states probability space for different values of EDP

3.2.1 Fragility functions (not mutually exclusive damage states)

Consider the case when the damage states are not mutually exclusive. First, we will investigate a nonstructural element that has three damage states. We assume, as before, that nonzero damage states exclude the zero damage state, but $DS = 1$ and $DS = 2$ are not mutually exclusive. Thus, probability of the event $DS = 1 \cap DS = 2$ is not zero.

In general, the event $DS = 1 \cap DS = 2$ represents an extra level of damage, that is equivalent to a damage state that is defined as the onset of both $DS = 1$ and $DS = 2$. In this case there are four distinct events corresponding to the four damage states: $DS = 0$, $DS = 1$, $DS = 2$, $DS = 1 \cap DS = 2$. Since the assumption (3.33) is not satisfied, the relations (3.32) take the following form

$$\begin{aligned} P(DS = 0 \mid EDP = z) &= 1 - F^1(z) \\ P(DS = 1 \mid EDP = z) &= F^1(z) - F^2(z) + P(DS = 2 \cap DS = 1 \mid EDP = z) \\ P(DS = 2 \mid EDP = z) &= F^2(z) \end{aligned} \tag{3.36}$$

Now we can not find the probabilities of all the damage states of interest from the standard set of fragility functions alone. From the second equation, we can only find the difference between the probability of $DS = 1$ and the probability of $DS = 1 \cap DS = 2$. Therefore, the set of two fragility functions does not have enough information to determine the probabilities of all events, if the damage states are not disjoint. For the case of two damage states, we need one more function that is defined as follows

$$F^{12}(z) = P(DS = 2 \cap DS = 1 \mid EDP = z) \tag{3.37}$$

then the probability of each damage state is given by

$$P(DS = 0 \mid EDP = z) = 1 - F^1(z) \tag{3.38}$$

$$P(DS = 1 \mid EDP = z) = F^{1}(z) - F^{2}(z) + F^{12}(z)$$

$$P(DS = 2 \mid EDP = z) = F^{2}(z)$$

$$P(DS = 2 \cap DS = 1 \mid EDP = z) = F^{12}(z)$$

For the general case of $N+1$ damage states (including undamaged), the number of all possible distinct events includes all combinations of the damage states and can be found as follows

$$N^{total} = \binom{N}{1} + \binom{N}{2} + \ldots + \binom{N}{N-1} + 1 \tag{3.39}$$

The first term is equal to N and represents the individual events. Note that this is exactly the number of distinct events if all the damage states are mutually exclusive. The second term represents the combination of two types of damage: $DS = i \cap DS = j$. The third term is the number of all possible combinations of three damage states and so on. The total number of all possible distinct events is given by

$$N^{total} = 2^{N} - 1 \tag{3.40}$$

In order to find the probability of all these events, we have to have exactly N^{total} fragility functions. This is achievable but quite cumbersome. In some cases, this situation can be avoided by a proper definition of the damage states or by taking into account additional considerations, as shown in the Section 3.2.2.

3.2.2 Selecting damage states

There are cases where it is possible to reduce the number of distinct events even if the damage states are not mutually exclusive. Consider an element with three damage states: $DS = 0$, $DS = 1$, $DS = 2$, and assume that $DS = 1$ and $DS = 2$ are not mutually

exclusive, implying that there is a nonzero probability of the event $DS = 1 \cap DS = 2$. In practice, if $DS = 2$ represents a more severe damage state, it can be true that damage states $DS = 2$ and $DS = 1 \cap DS = 2$ are equivalent in terms of their consequences. This can be written as a condition

$$C(DS = 2) = C(DS = 1 \cap DS = 2) \tag{3.41}$$

where $C(\ )$ is some function representing the consequences of the event. Some common consequence functions are cost of repair or downtime. Then we can combine these two damage states into one

$$\{DS = 2^*\} = \{DS = 2\} \cup \{DS = 2 \cap DS = 1\} \tag{3.42}$$

For this case, $DS = 2^*$ is equivalent to $DS = 2$. Furthermore, we introduce another new event

$$\{DS = 1^*\} = \{DS = 1\} \setminus \{DS = 2 \cap DS = 1\} \tag{3.43}$$

This means that $DS = 1^*$ is equivalent to $DS = 1$, without $DS = 2$ as shown on Figure 3.3. The redefined damage states $\{DS = 0, DS = 1^*, DS = 2^*\}$ are indeed mutually exclusive. Therefore, the theory developed for mutually exclusive events is applicable. Moreover, we do not even have to find the new fragility functions. Consider the second equation of the relations (3.36) for the events $DS = 0$, $DS = 1$, $DS = 2$

$$P(DS = 1 \mid EDP = z) - P(DS = 2 \cap DS = 1 \mid EDP = z) = F^1(z) - F^2(z) \tag{3.44}$$

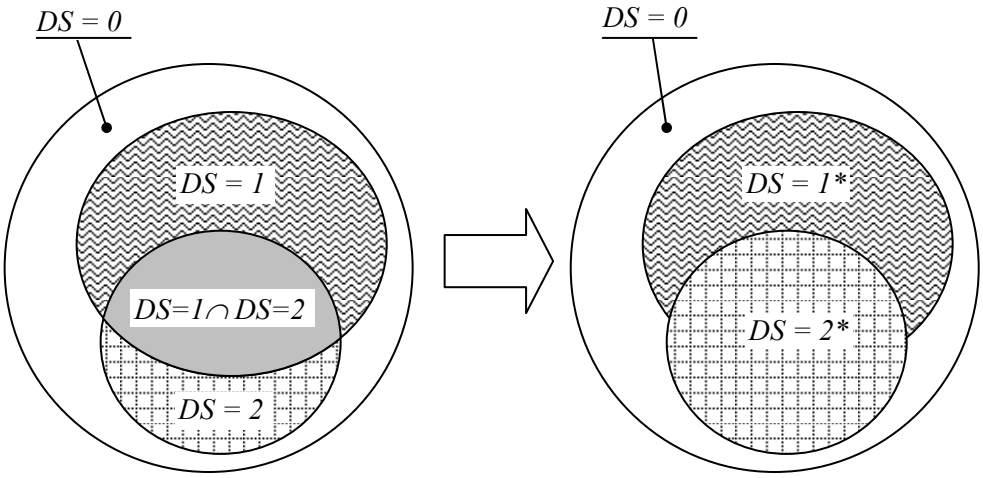

Figure 3.3 Original state space and redefined state space with corresponding probability measures

It can be seen that the left-hand side of this equation is just the probability of $DS = 1^*$. Using the fact that $DS = 2$ is equivalent to $DS = 2^*$, we can write

$$P(DS = 0 \mid EDP = z) = 1 - F^1(z) \tag{3.45}$$
$$P(DS = 1^* \mid EDP = z) = F^1(z) - F^2(z)$$
$$P(DS = 2^* \mid EDP = z) = F^2(z)$$

Fragility functions that have been obtained for damage states $DS = 1$, $DS = 2$ are applicable to the damage states $DS = 1^*$, $DS = 2^*$ in the most simple and effective form (3.32). Therefore, the rule for choosing the damage states might be as follows: the consequences of a higher damage state should include the consequences of a lower damage state, so that condition (3.41) will be satisfied. This is usually easy to accomplish for the case where damage states represent the severity of damage.

In case of different failure modes, distinct damage states may cause very different consequences. Take the example of a heavy piece of equipment with three damage states of interest: sliding more than some threshold value, overturning and breaking. The potential respective consequences for these damage states are: blocking egress, injuring a

human, and lost of functionality. Clearly, none of the outcomes can be encompassed by the other. Therefore, condition (3.41) can not be satisfied and we have to develop fragility functions for all intersections of events (3.39). In the case where developing the complete set of fragility functions is not possible, it may be reasonable to introduce the assumption of independence of damage states. Then the probabilities of all events can be found with the standard set of fragility functions (P($DS \geq i \mid EDP = z$), $i = 1..N$, where N is the number of damage states). In particular, for a component with two damage states, we have $P(DS = 2 \cap DS = 1 \mid EDP = z) = P(DS = 2 \mid EDP = z)P(DS = 1 \mid EDP = z)$, so substituting into (3.36), we have

$$P(DS = 0 \mid EDP = z) = 1 - F^1(z) \tag{3.46}$$

$$P(DS = 1 \mid EDP = z) = \left(F^1(z) - F^2(z)\right)/\left(1 - F^2(z)\right)$$

$$P(DS = 2 \mid EDP = z) = F^2(z)$$

Thus, probabilities of all events of interest are expressed in term of fragility functions. For a general case of N damage states, the assumption of mutual independence of all damage states allows one to obtain probabilities of each damage state in terms of N standard fragility functions. The accuracy of such a simplified model depends on whether the damage states are indeed independent. If the different damage states are only slightly correlated, the assumption of independence can be a reasonable practical option to exploit for damage analysis.

4 Damage estimation coupled with structural analysis (single damage state)

4.1 EDP dependent on damage

4.1.1 Methods of damage estimation

In structural reliability theory, the probability of damage is estimated by integration over the failure region in the corresponding state space (Section 2.2.1). Given the complexity of earthquake engineering applications, the integral is usually calculated by simulation. Figure 4.1 shows the structure of the state space and relation between different groups of variables in the space. Notations in this figure are consistent with those used previously: $\underline{Q}$ – properties of the earthquake, $\underline{X}^{SO}$ – properties of the structural members that are used for structural analysis only, $\underline{X}^{CS}$ – properties of the structural members that are used both for structural analysis and damage analysis, $\underline{X}^{CO}$ – properties that are used for damage analysis only, $\underline{EDP}$ – engineering demand parameters, $\underline{DM}$ – damage measure. Early

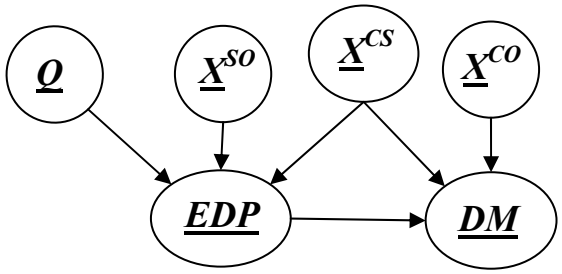

Figure 4.1 Relations between the variables in the state space.

In the case that the structural response defining properties overlap with damage defining properties ($\underline{X}_i^{CS} \neq \varnothing$), one should use care while disaggregating the analysis into two separate modules, one for structural analysis and one for damage analysis. A

disaggregated analysis assumes that only the vector of *EDP*s is transferred from the structural analysis to the damage analysis. Utilizing relation (3.13) instead of (3.23) or (3.25) assumes that there is no knowledge about $\underline{X}^{CS}$ when doing the damage analysis, contradicting the fact that these properties have already been defined during the structural analysis. Therefore, in the case of Monte Carlo simulation, two distinct samples of $\underline{X}^{CS}$ are used: one for structural analysis and another one for damage analysis, as shown in Figure 4.2. It is foreseeable that such approach could reduce the accuracy of damage estimation. If equations (3.23) or (3.25) are used for damage analysis, the integration does not have inconsistencies. But this approach requires that damage analysis is performed, in part, together with structural analysis as shown in Figure 4.3. We shall investigate the difference between a coupled damage analysis (Figure 4.3) and an uncoupled damage analysis (Figure 4.2) by studying three separate simulation methods for damage assessment.

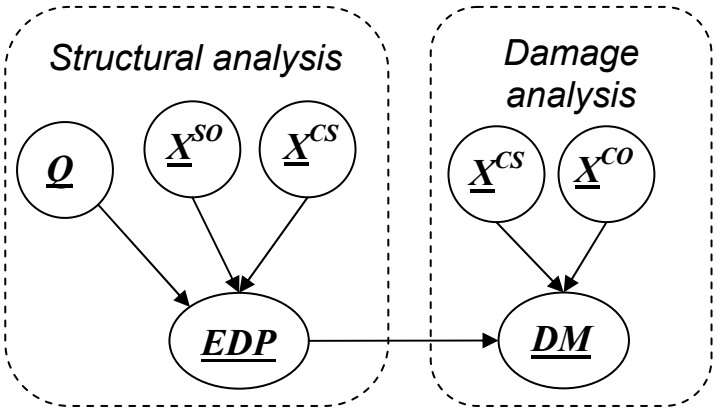

Figure 4.2 Uncoupled structural and damage analyses.

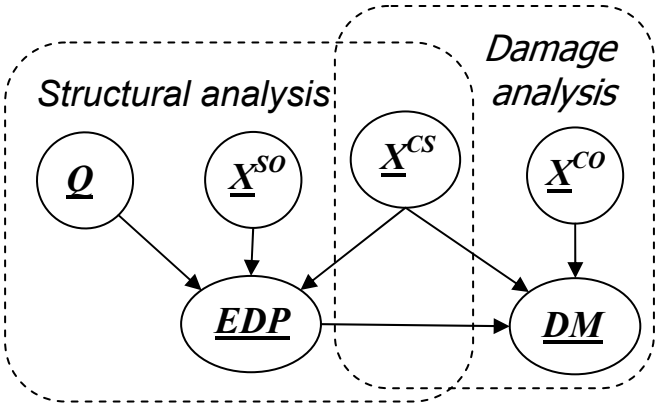

Figure 4.3 Coupled structural and damage analyses

Method 1. Vector $\underline{X} = [\underline{X}^{SO}, \underline{X}^{CS}, \underline{X}^{CO}]$ is randomly sampled according to its probability distribution at the start of each simulation. $\underline{EDP}$ is then calculated as a result of a nonlinear dynamic time history structural analysis, using these sampled structural properties $[\underline{X}^{SO}, \underline{X}^{CS}]$ Then $\underline{DM}$ is calculated according to (3.25) by using the obtained values of $\underline{EDP}$ and the sampled values of $\underline{X}^{CS}$ and $\underline{X}^{CO}$. For each damage calculation, only one sample of the structural properties, $\underline{X}^{CS}$, is used. To perform the integration over the state space of structural random variables, $\underline{X}$, they are generated a statistically significant number of times. In essence, the method performs a coupled damage analysis with a randomized structural model and a structural model based fragility function (3.23). It results in an implementation of the scheme presented by Figure 4.3.

Method 2. Vector $\underline{X}^{S} = [\underline{X}^{SO}, \underline{X}^{CS}]$ is randomly sampled according to its probability distribution. $\underline{EDP}$ is then calculated as a result of a nonlinear dynamic time history structural analysis using these sampled structural properties. Then $\underline{DM}$ is estimated from $\underline{EDP}$ by using (3.13). This is equivalent to ignoring the previous sample of $\underline{X}^{CS}$, used in the structural analysis, and estimating these damage properties from a new random

sample of $\underline{X}^{CS}$ and $\underline{X}^{CO}$. The two samples of $\underline{X}^{CS}$ are independent and identically distributed. Effectively, the method implements the structure shown by Figure 4.2, where a part of the structural model is randomized twice: one time for the purpose of structural analysis and the other time for the purpose of damage analysis. The method is inconsistent because of the "double-counting" of the structural properties $\underline{X}^{CS}$. However, it provides a desirable disaggregation of the problem and it is often used in to damage estimation.

Method 3. The uncertainty in the structural properties is ignored by taken them to be equal to their expected values $\underline{X}^{S} = E[\underline{X}^{S}]$, for the purpose of the structural analysis. Everything else is the same as in Method 2. The method is the easiest of all three methods to implement in practice, since in the case of fixed excitation ($\underline{Q}$), it uses the computationally intensive dynamic structural simulation only once. For this reason, it is often used and so it is included in the present study along with Methods 1 and 2.

In addition to the sampling of structural properties, there exist two ways to apply the earthquake load $\underline{Q}$. One way is to choose different ground motion time histories (by selecting a set of appropriate recorded time histories or by randomly generating the time histories from a stochastic ground motion model) and the other way is to use a single time history for all simulations. In the latter case, the particular properties of the chosen ground motion can be a factor in the final damage estimation. Therefore, three methods together with the two ways to apply the earthquake load constitute six different cases of analysis that will be studied further.

For the present study, we consider the case where the structural properties include all the damage-related properties, so (3.24) holds and $\underline{X}^{CO} = \varnothing$. Therefore, a structural

model based fragility function (3.23) becomes a step function (3.25). Also, we do not randomize the structural properties that are not used for damage analysis, $\underline{X}^{SO}$. Figure 4.4 illustrates all cases that are considered in the present study; *i.i.d.* in the figure stands for independent identically distributed random variables; $\underline{X}^{CO}$ is not shown since it is a null set and $\underline{X}^{SO}$ is a know deterministic value equal to its best estimate, $E[\underline{X}^{SO}]$.

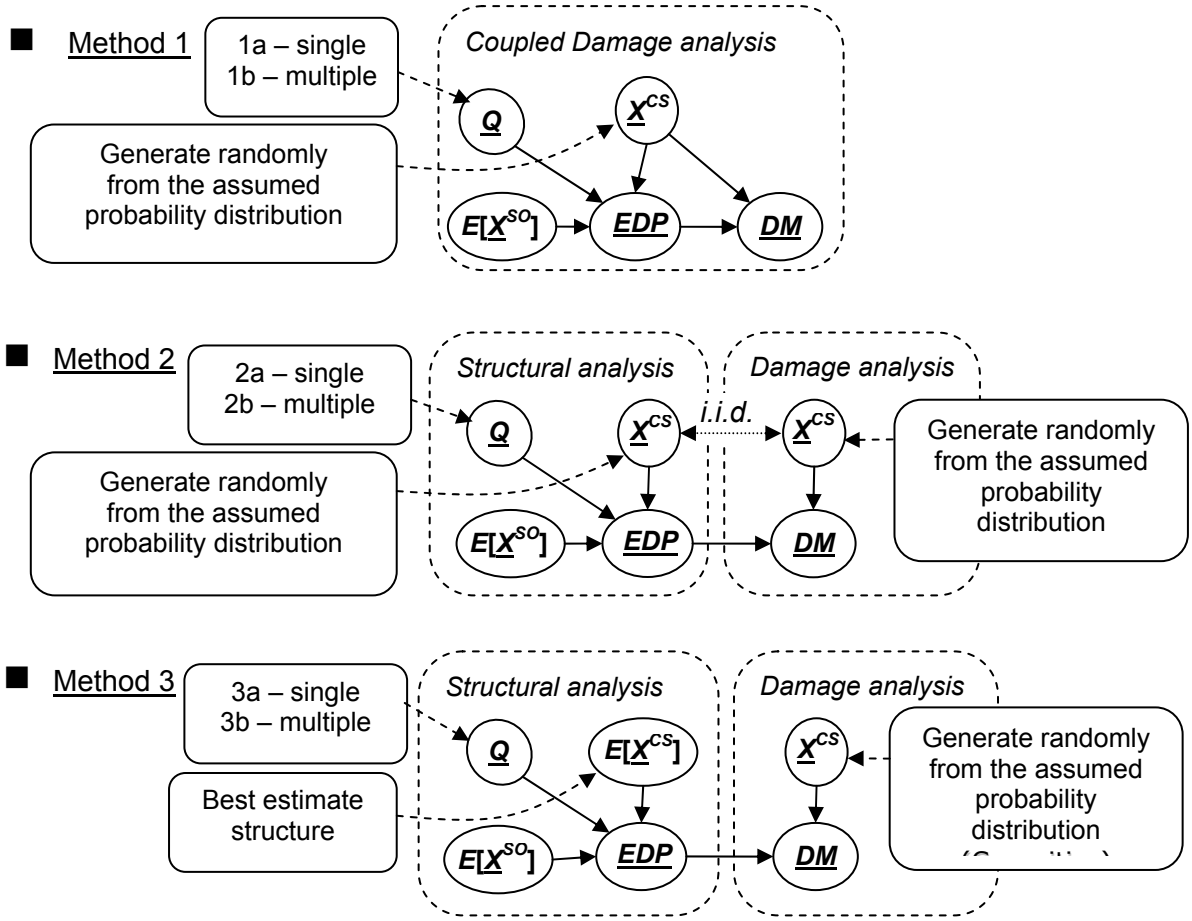

Figure 4.4 Methods used for the sample case study damage estimation.

It is noted that the idea of Method 1 can be expressed by the following: some damage to the structural elements is determined by the structural model and is derivable from the results of the structural analysis. In the examples in this chapter, we deal with the case when (3.24) holds, therefore damage to the structural elements is completely

defined by the structural model. Mathematically, Method 1 represents the correct integration performed according to (2.9). Method 2 ignores the damage information obtained from the structural analysis and introduces a separate module of damage analysis on top of the structural simulation that uses the fragility functions. Mathematically, it is equivalent to double integration over the subset of the structural properties $\underline{X}^{CS}$ in (2.9). Method 3 is a variation of the semi-deterministic approach in damage estimation: for the sake of computational convenience, the uncertainty of the structural properties is ignored while performing the structural analysis. Then at the last step, the uncertainty is introduced by fragility functions for the damage estimation. This "late" introduction of the structural uncertainty, although convenient, is mathematically inconsistent with rigorous damage estimation.

4.1.2 Structural model description

The reinforced concrete moment frame shown in Figure 4.5 is chosen as a case study. The frame represents the south frame of a 7-story hotel building located in Van Nuys, California. For a detailed building and structural model description see Beck et al. (2002) and Li and Jirsa (1998). The 2-D model of the frame is developed for the present study. The model is a simplified version of the model that was used in Beck et al. (2002). The flexural behavior of the beams and columns is represented by one-component Giberson beams with plastic hinges at the ends (Sharpe, 1974). Shear deformation for the beams and columns is assumed to be elastic and is incorporated in the flexural elements. The Q-HYST bi-linear hysteresis (Saiidi and Sozen, 1979) is used to model the stiffness degradation of reinforced concrete members in flexure as shown in Figure 4.6.

Properties of the reinforced concrete members are taken from the original structural drawings (Rissman and Rissman Associates, 1965). The software program for cross-section analysis of reinforced concrete members, UCFyber (ZEvent, 2000), is used to calculate parameters of the Q-HYST hysteretic rule of the force-deformation curves for each flexural member. Interactions of axial load and flexure and also shear and flexure are not considered in the model. The inelastic dynamic analysis program, Ruaumoko (Carr, 2001), is used to perform the structural analyses.

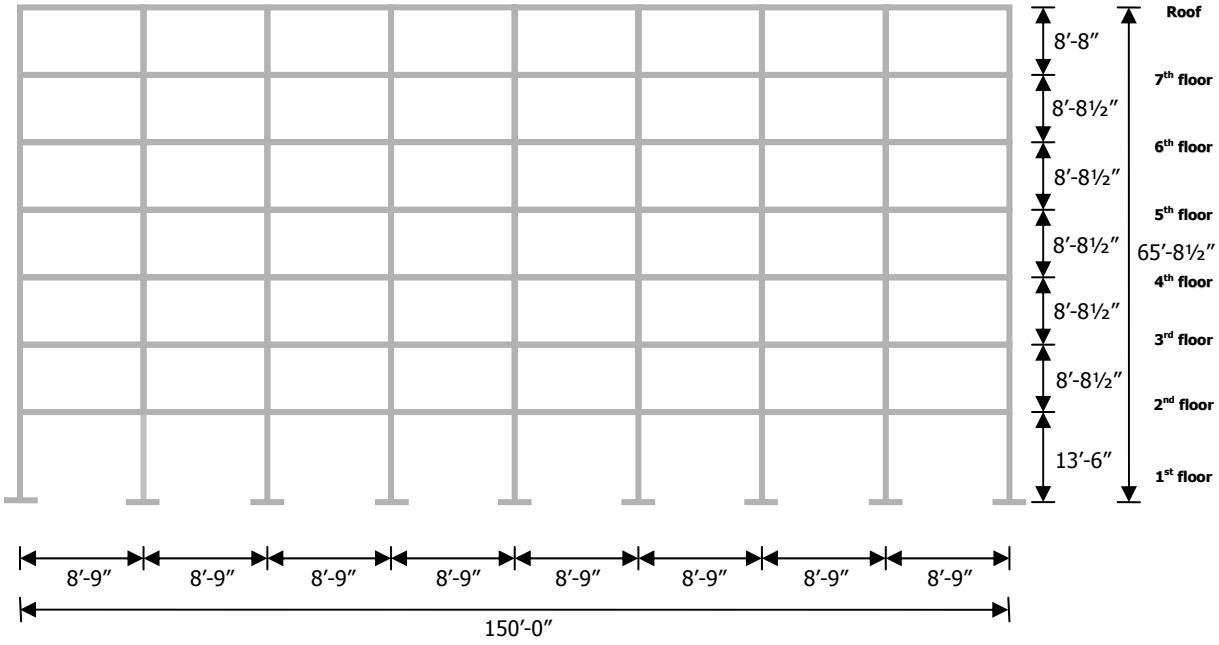

Figure 4.5. Reinforced concrete moment-resisting frame chosen for the case study.

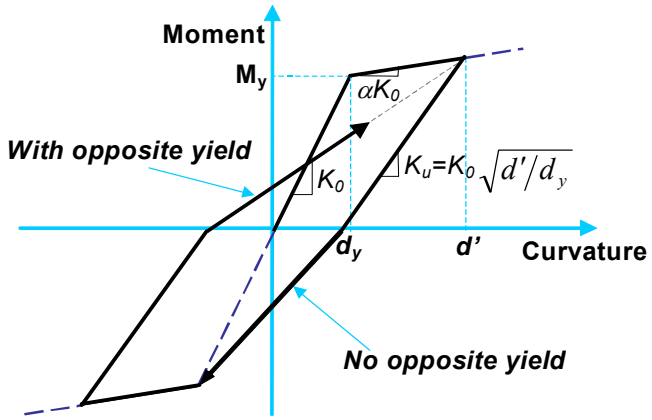

Figure 4.6. Flexural members hysteretic rule: Q-HYST.

4.1.3 Damage model

For the present study, only structural damage is considered. It is assumed that each structural member has only two damage states: "undamaged" (DS = 0) and "yield" (DS =1). A member is considered to be in damage state "yield" if the yielding point in the moment-curvature relations has been reached. Alternatively, the damage state can be defined as a reduction of the minimal stiffness from the original value K_0 to the post-yield value αK_0.

The "yield" damage state of the i-th flexural member can be described by the following damage model

$$DS = \text{"yield"} \Leftrightarrow d_y(\underline{X}_i) < d^i_{\max}(\underline{X},\underline{Q}) \tag{4.1}$$

where $d_y(\underline{X}_i)$ is the yield curvature of the reinforced concrete member, $d^i_{\max}(\underline{X},\underline{Q})$ is the maximum curvature attained by the element during the simulation. For each member, d_y is calculated by UCFyber assuming zero axial load. Since there is no interaction of axial load and flexure or shear and flexure in the model, the flexural properties of the

member do not depend on the other member properties or load characteristics. Therefore, the yield curvature d_y of each member depends only on the properties of the member $\underline{X}_i$, implying that the form ($C(\underline{X}_i)$) used in (4.1) is valid. It can be seen that (4.1) is satisfied for the damage state and structural model as we have defined them.

Note that (4.1) is the problem-specific version of (3.10), where the limit-state function has been formulated according to the particular features of the element under consideration. Therefore, the validity of (4.1) is essential for further analysis because the effects of violation of (3.10) can appear in the results of the analysis and disturb the whole picture. For example, if we were to use a structural model with axial load – flexure interaction, the yield curvature d_y would depend on the axial force, meaning that there is a dependence on the overall structural properties and earthquake excitation: d_y ($\underline{X}$, $\underline{Q}$). In this case (4.1) would not be satisfied regardless of the choice of the member yield model $d_y(\underline{X}_i)$.

Comparing the limit state model (4.1) with the one used in (3.11) – (3.13), it can be noted that $d_y(\underline{X}_i)$ is, by definition, the capacity of the structural member with respect to the "yield" damage state, formulated in terms of maximum curvature $d^i_{\max}$. Therefore, the maximum curvature $d^i_{\max}$ is the *EDP* chosen for the damage analysis. According to (3.13), the fragility function for this case is a CDF of capacity

$$F^1(z) = (d_y(\underline{X}_i) < z) \tag{4.2}$$

This is the fragility function to be used for the damage estimation in Method 2 and Method 3.

Consider the chosen *EDP* – maximum curvature of the element $d^i_{\max}$. In order to obtain its value, it is necessary to perform a dynamic structural analysis. To do this, we need to specify the parameters of the structural model. From the flexural hysteresis rule (Figure 4.6), it can be observed that two of the needed parameters are yield moment, M_y, and initial stiffness, K_0. From these two parameters, the yield curvature can always be derived: $d_y = M_y / K_0$. Therefore, as a result of the dynamic simulation, the value of maximum curvature $d^i_{\max}$ for each element and the value of yield curvature are obtained. Substituting this information into the conditioning part of (3.21) for the *i*-th element

$$F^n_{SM}(z) = P(d^i_y(\underline{X}_i) < z \mid d^i_{\max}(\underline{X},\underline{Q}) = z, d^i_y(\underline{X}_i) = \tilde{d}^i_y, \ldots) \tag{4.3}$$

$$= P(\tilde{d}^i_y < z \mid d^i_{\max}(\underline{X},\underline{Q}) = z, d^i_y(\underline{X}_i) = \tilde{d}^i_y, \ldots)$$

$$= \begin{cases} 1 & \tilde{d}^i_y < z \\ 0 & \tilde{d}^i_y > z \end{cases}$$

where $\tilde{d}^i_y$ is the numeric value of the yield curvature of the *i*-th element and is drawn from the probability distribution defined by (4.2), which has been used during the dynamic simulation. Thus, whenever the maximum curvature attained during the dynamic simulation exceeds the sampled yield curvature of the element, the element is considered to be in damage state "yield." This is the structural model based fragility function that is used for damage estimation by Method 1.

Note that $\tilde{d}^i_y$ is one of the properties of the element, which is known from the input structural data and which is also relevant to the "capacity" of the element with respect to the "yield" damage state in terms of the maximum curvature. In fact, for the

chosen model, this parameter actually is the abovementioned capacity, meaning that knowledge of the structural properties provides complete information about the element's capacity. Therefore, the presented model also satisfies (3.24) as intended for the present study.

Once the damage state of each element is determined, the global damage is estimated as the number (N_t) of the elements in the "yield" damage state. Since each structural member (beam or column) can yield at each of its ends, the number of damaged elements is equal to the number of plastic hinges formed. Therefore, the number of damageable elements (beam or column ends) is twice of the number of flexural members in the frame. For the chosen frame, the total number of flexural members is 119, hence there are 238 damageable elements in the frame. For each dynamic structural simulation, the number of damaged elements N_t is calculated by afore-described three different methods. The results are presented in Section 4.1.6.

Note that the final goal of the building evaluation is the decision variable. In the present study, N_t is chosen to be a performance criteria primarily for demonstration purposes and because of the easiness of its calculation. However, this parameter is closely related to some important decision variables, such as repair cost. The relation between N_t and repair cost can be estimated as follows: if the cost to repair each yielded beam or column end is denoted by C_{ph}, then the total cost of repair is $C_{ph}N_t$. Therefore, the conclusions that are made for N_t are also valid for a decision variable such as building repair cost, making the results viable for practical purposes.

4.1.4 Interpretation of the chosen damage model

In earthquake engineering, damage states are used to quantify structural damage inflicted by an earthquake. There are different ways to choose damage states. In this chapter, we used a damage state that is formulated in terms of a structural state – "yielding."

In a more conventional approach, damage states are formulated in terms of visible signs of deterioration. For example, typical damage states of reinforced concrete members can be defined as cracking, concrete crushing, concrete spalling, buckling of longitudinal reinforcement and breakage of longitudinal reinforcement.

It is generally accepted within the earthquake engineering community that the structural states of reinforced concrete members (such as "yielding") are related to the visible degradation of the members. There are experimental studies that support this relation. For example, Tanaka and Park (1990) conducted a test program that demonstrates a very close relation between yielding of longitudinal reinforcement and a damage state that they described as "first visible crushing of cover concrete." Figure 4.7 shows the test results for one of the eight specimens they tested. It can be seen that crushing of cover concrete occurs shortly after the onset of tensile yielding of the longitudinal reinforcement. This picture is typical for all eight tested specimens. Crushing of cover concrete occurs in close proximity to yielding. In six cases, crushing happened shortly after yielding and in two cases just before yielding.

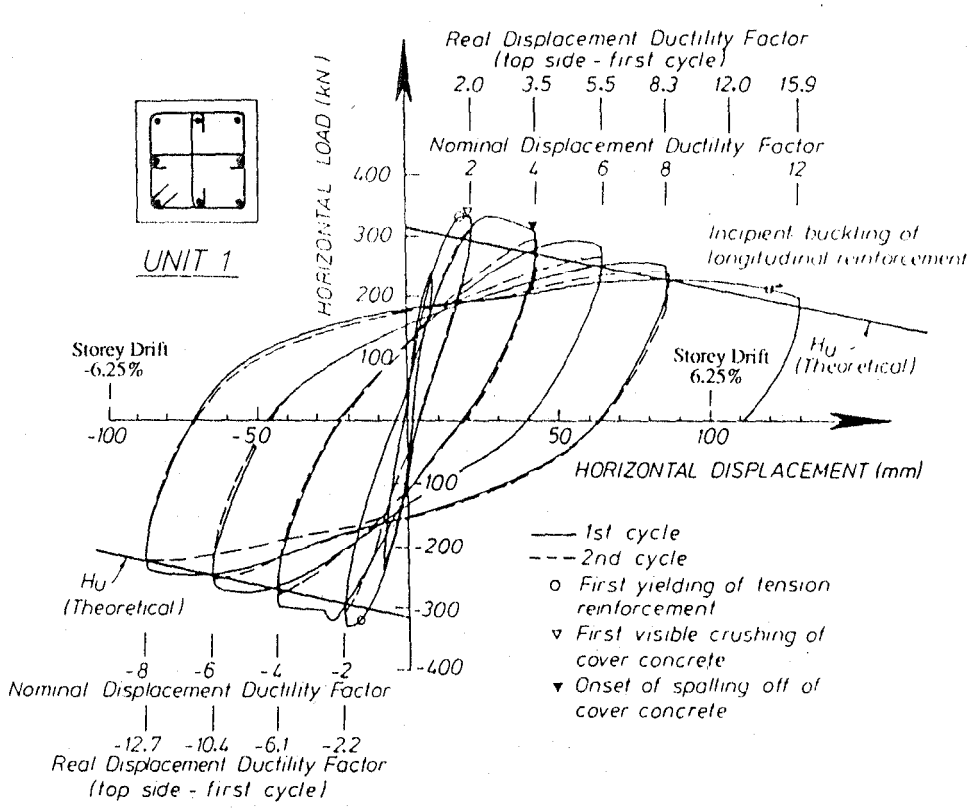

Figure 4.7 Relation between force-displacement history and observed damage states of a reinforced concrete column (Tanaka and Park, 1990)

Based on these results, we can interpret a damage state used in this chapter ("yielding") as "first visible crushing of cover concrete," making the chosen damage model fully meaningful in terms of an intuitive (descriptive) understanding of damage.

4.1.5 Parameters of the damage model and ground motions

Before the damage analysis by either of three methods can be performed, we need to define the probability distribution of the parameters that are important for damage analysis. In the present case, the only parameter that is relevant to the damage analysis is yield curvature. Therefore, for each element we define its probability distribution by specifying the cumulative distribution function of the yield curvature. For the present

study, we adopt a lognormal probability distribution. For each element, the parameters of the probability distribution are found as follows. The yield moment is assumed to be equal to

$$M_y^i = \hat{M}_y^i x \tag{4.4}$$

where $\hat{M}_y^i$ is the best estimate of the yield moment of the *i*-th element, as calculated by UCFyber (ZEvent, 2000) and x is a lognormally distributed random variable with expectation $E[x] = 1$ and the coefficient of variation $\delta[x] = 0.08$, making the yield moment a lognormal random variable with expectation $E[M_y^i] = \hat{M}_y^i$ and coefficient of variation $\delta[M_y^i] = 0.08$. The study by Ellingwood *et al.* (1980) suggests that coefficient of variation 0.08 is a reasonable estimate of uncertainty of the flexural strength of reinforced concrete members. The stiffness K_0^i is assumed to be known and equal to the value calculated by UCFyber (ZEvent, 2000). Therefore, yield curvature is a lognormal random variable with the following CDF

$$F_{d_y^i}(z) \sim LN\left(\mu_x + \ln\left(\overline{M}_y^i / K_0^i\right), \sigma_x\right) \tag{4.5}$$

where μ_x = - 0.0032 and σ_x = 0.08 are mean and standard variation of $ln(x)$ that has normal distribution. These values of μ_x and σ_x provide the required expectation and coefficient of variation of x. Formula (4.5) is used for generating a randomized structural model and as a fragility function (4.2).

Note that for the present study we are not concerned with effects of the uncertainty of the model parameters on the damage estimation. The focus is on an investigation of how different ways to implement the uncertainty in the model influence

the damage estimation. Therefore, the choice of capacity probability distribution is not of high importance here.

The mass properties and stiffness properties (K_0^i) of the structural model are assumed to be known. Therefore, the natural frequencies of the original (undamaged) structural model are the same for all randomly generated samples of the structural model. The first natural frequency of the present model is T_1 = 1.5 sec., which agrees with the value exhibited by the Van Nuys 7-story hotel in the longitudinal direction during the 1994 Northridge earthquake, as reported by Islam (1996). As the intensity measure of the input acceleration time histories, we use linear spectral acceleration S_a calculated for the first natural frequency of the model. The software program Bispec (Hachem, 2003) is used to determine S_a. Ground motions for the analysis are taken from the set of the ground motions developed for the SAC Steel Project (Woodward-Clyde Federal Services, 1997). We refer to this set as the SAC database.

4.1.6 Results and conclusions

In this section, we present the results of damage estimation performed by the three afore-described methods in terms of the calculated number N_t of yielded elements. Out of all three methods, only Method 1 is strictly correct. Therefore, we treat the results obtained by Method 1 as exact and results obtained by the other methods as approximate.

To compare the damage evaluation techniques, it is reasonable to isolate any other factors affecting the damage, such as the uncertainty of the ground motion. Thus, for the first analysis, we collect the statistics of total damage N_t calculated by three different methods for the same ground motion. For each acceleration time history, we perform 40 dynamic simulations with the structural model where yield curvature d_y^i is randomly

generated for every element. These simulations are used to calculate N_t by Method 1 and Method 2. For each acceleration time history, one dynamic simulation is performed with the structural model where the yield curvature d_y^i is set equal to its expected value: $E[\, d_y^i \,]$, then the total damage N_t is estimated by Method 3.

Table 4.1 gives the results of damage estimation for the ground motion time history LA15 from the SAC database at the level of intensity S_a = 0.5g. It can be seen that for this particular ground motion, Method 2 overestimates the damage on average by (102.1 – 96.3)/ 96.3 = 6.0% and Method 3 overestimates the damage on average by (103.7 – 96.3)/ 96.3 = 7.7%. It can be seen from the data that Method 2 gives a the variance for N_t that is 42% of that of Method 1. The variance is underestimated by (76.7 – 32.2)/ 76.7 = 58%. It is also observed that Method 3 produces a damage estimate with a variance that is 6.7% of the variance of the Method 1 estimation.

The effects that have been observed for this one particular ground motion might be occasioned by some particular features of this ground motion. To ensure that similar phenomena take place in general, independently of the individual characteristics of the

Table 4.1. Results of damage estimation for LA15 ground motion at 0.5g.

Simulation number	N_t Method 1	N_t Method 2	N_t Method 3
1	81	97	106
2	94	97	104
3	95	97	103
4	89	103	104
5	97	104	103
6	106	104	97
7	94	102	103
8	91	96	108
9	98	105	105
10	88	103	102
11	103	101	104
12	85	92	108
13	105	104	103
14	82	105	101
15	115	112	106
16	80	91	104
17	96	95	106
18	86	95	104
19	103	103	101
20	85	104	106
21	102	110	106
22	88	102	104
23	103	106	103
24	101	103	103
25	101	98	101
26	90	102	103
27	81	89	102
28	100	96	105
29	109	112	105
30	105	105	102
31	95	105	106
32	95	97	103
33	89	103	104
34	97	104	103
35	106	104	97
36	94	102	103
37	91	96	108
38	98	105	105
39	88	103	102
40	103	101	104
Mean	96.3	102.1	103.7
Variance	76.7	32.2	4.9

Table 4.2 Statistical properties of the damage estimation for different ground motion time histories.

Ground motion file	E[N_t] Method 1	E[N_t] Method 2	E[N_t] Method 3	Var[N_t] Method 1	Var[N_t] Method 2	Var[N_t] Method 3
LA01	111.2	115.8	115.9	127.7	62.6	6.5
LA02	120.1	123.3	118.4	46.0	20.7	3.5
LA03	106.9	112.9	112.7	125.7	56.7	5.5
LA05	108.6	112.3	110.4	75.1	32.8	4.5
LA07	113.1	117.5	118.9	68.3	26.9	6.3
LA08	103.1	108.6	107.9	157.2	41.6	4.6
LA10	61.7	65.5	64.9	77.1	74.8	8.4
LA11	92.6	97.8	97.9	92.9	48.1	6.9
LA12	147.0	151.5	151.6	157.3	44.6	9.3
LA13	68.8	72.4	72.0	38.4	27.5	6.1
LA14	89.3	93.4	94.6	71.7	38.9	4.7
LA15	96.3	102.1	103.8	76.7	32.2	4.9
LA16	83.0	87.9	86.8	72.8	41.1	8.0
LA17	86.9	90.8	91.0	79.1	29.3	3.2
LA18	96.3	100.4	101.2	96.1	36.5	6.9
LA19	124.9	129.1	127.0	85.6	44.9	7.3
LA20	101.6	106.8	106.3	112.2	54.7	7.1
LA22	109.8	113.0	112.2	45.0	24.3	5.4
LA23	97.3	99.7	95.4	57.8	30.1	5.3
LA27	87.4	91.7	93.5	75.6	35.3	2.6
LA29	98.3	101.0	96.5	105.9	56.8	9.5
LA30	104.6	111.3	108.6	109.2	49.7	10.3
LA33	71.4	76.6	74.1	52.2	44.0	8.0
LA39	91.9	96.8	95.5	63.7	36.5	7.4
LA41	90.2	93.9	90.8	66.5	39.0	5.7
LA42	85.0	88.8	86.0	82.0	50.5	7.9
LA55	77.6	80.9	81.8	71.5	37.0	4.5
LA56	46.8	49.7	42.2	109.2	59.7	5.1
LA58	68.2	72.2	71.2	103.7	71.7	7.8
LA59	132.7	137.5	137.7	47.4	23.9	4.5
LA60	111.9	115.5	112.0	60.9	36.3	6.9
Average values	**96.3**	**100.5**	**99.3**	**84.2**	**42.2**	**6.3**

input excitation, we conduct an analogous analysis for 30 other acceleration time histories from the SAC database. The chosen records and corresponding results are

shown in Table 4.2 together with the LA15 time history. All time histories in Table 4.2 are scaled to provide S_a = 0.5g. The scaling factor does not exceed 2 for all time histories. Statistical properties (mean and variance) of the global damage N_t are based on 40 dynamic simulations for each ground motion.

For the chosen set of earthquake ground motions, the damage estimated by Method 2 is on average (100.5 – 96.3)/96.3 = 4.4% greater than the exact solution (Method 1). This seems to be a reasonably good agreement for practical purposes. Method 3 exhibits slightly better results for average values: $E[N_t]$ has been overestimated by (99.3 – 96.3)/96.3 = 3.1%, providing essentially the same accuracy for the expected damage as Method 2. As far as the dispersion of the damage estimates is concerned, it can be noted that Method 2 gives the variance of N_t on average 50% less than the exact solution. The variance estimated by Method 3 on average is 7.5% that calculated by Method 1.

For a comprehensive evaluation of the seismic performance of a facility, it is usually necessary to estimate the decision variable of interest for different levels of seismic excitation. The accuracy of damage estimation may be different for different excitation intensities, affecting the reliability of the decision variable estimate. Therefore, we examine how the damage estimation changes depending on the intensity level. First, we perform damage estimation at different intensity levels by scaling one ground motion time history. We choose the ground motion that provides the values of damage that are the closest to the average values. The ground motion LA15 satisfies this criterion best of all. We scale LA15 to provide values of S_a from 0.1g to 1.0g at a 0.1g step. The results are shown in Figures 4.8 - 4.11. Figure 4.8 depicts the average values of N_t as a function

of S_a. As before, N_t is calculated by the three different methods. Assuming that Method 1 provides the exact result, the relative error of N_t estimation performed by Methods 2 and 3 is plotted in Figure 4.9. For Method 2, the error decreases from 40.5% to 3.2% over the range from 0.1g to 1.0g. For the range between 0.4g and 1.0g the error does not exceed 6.8%, averaging at 4.6%. Figure 4.10 displays the variance of N_t as a function of S_a. We can see that Method 2 underestimates the variance by approximately 50% for the lower end and provides roughly the same results as Method 1 for the high values of spectral acceleration (S_a > 0.5g). Method 3 underestimates the variance quite significantly: the variance of the damage estimate is on average about 10% of the variance obtained by Method 1 for the chosen range of ground motion intensity.

Figure 4.11 shows the coefficient of variation of the damage estimate. The average value of the coefficient of variation for Method 1 is 14.6%. For this example, the uncertainty of the damage estimate is caused by the uncertainty of building properties only (the ground motion is deterministic). More specifically, it is caused by the uncertainty of the capacity of the flexural members with respect to the yield damage state. Therefore, we can see how the one isolated factor of uncertain capacity affects the uncertainty of the damage estimate. The coefficient of variation of the flexural members' capacity is 8%. That has resulted in a coefficient of variation of the damage estimate of 14.6%. Thus, uncertainty in building structural properties approximately doubles when it gets to the damage estimate. Figure 4.11 also reveals that at the lower end, the uncertainty of the damage estimate is much higher than the average value. In the range of S_a < 0.5g the coefficient of variation is on average 30%. For the high end it is 6.8%, which is lower than the coefficient of variation of the source of uncertainty, the uncertain capacity. The

other two methods give much lower estimates of the coefficient of variation, essentially repeating the behavior shown by the variances: Method 2 – 8.6%, Method 3 – 4.3% on average over the whole range of S_a.

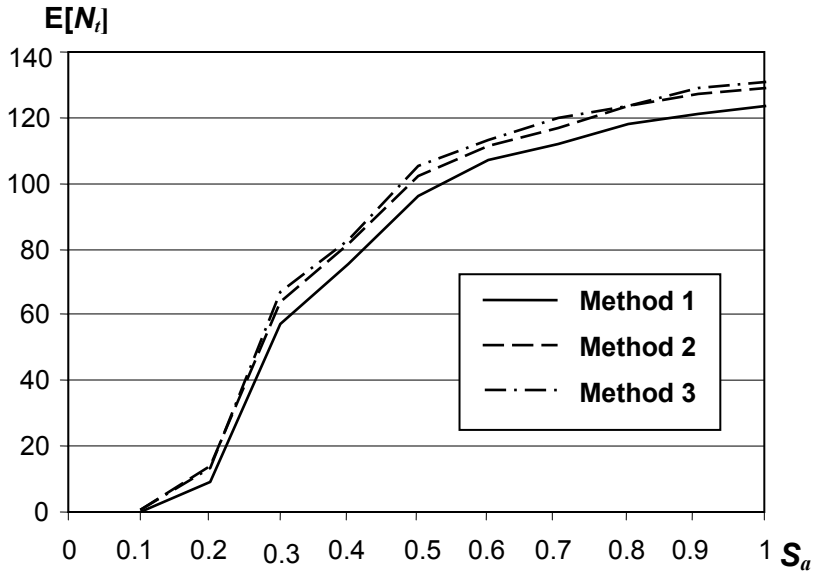

Figure 4.8. Expectation of damage E[N_t] as a function of spectral acceleration, ground motion LA15.

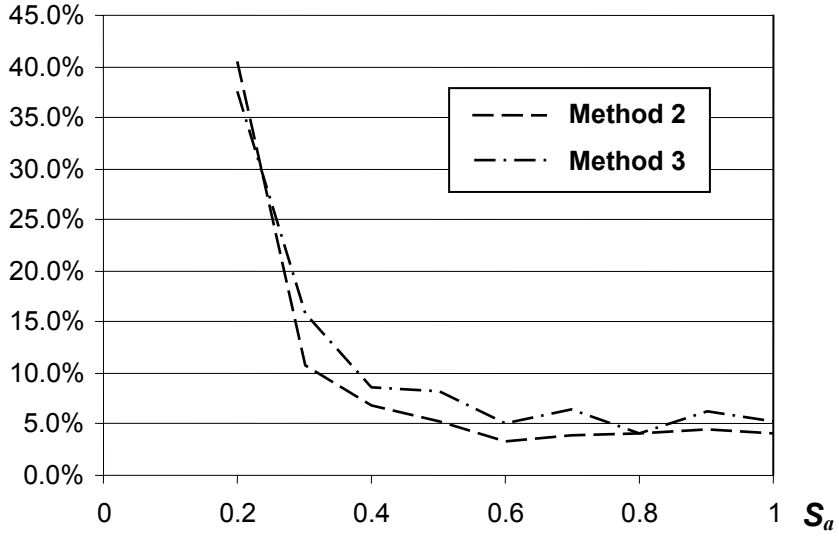

Figure 4.9. Relative errors of estimation of E[N_t] by different methods as a function of spectral acceleration, ground motion LA15.

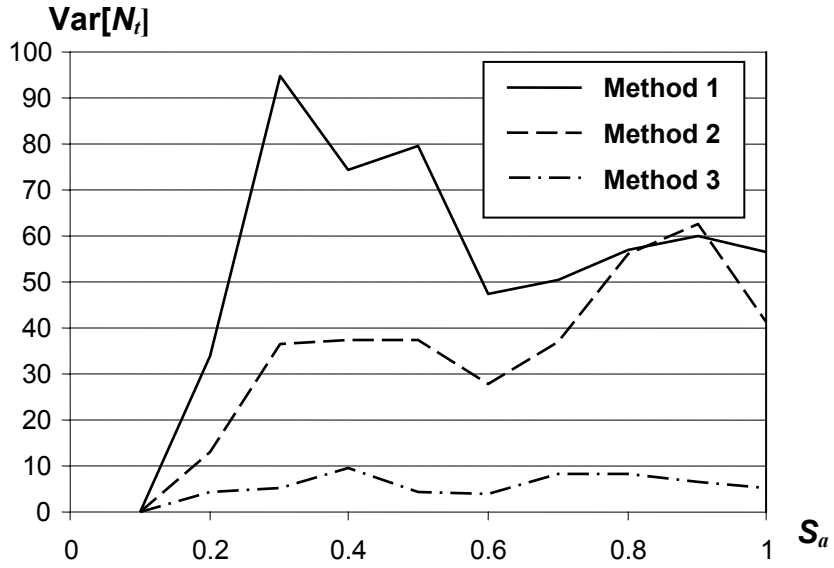

Figure 4.10. Variance of the damage estimate as a function of spectral acceleration, ground motion LA15.

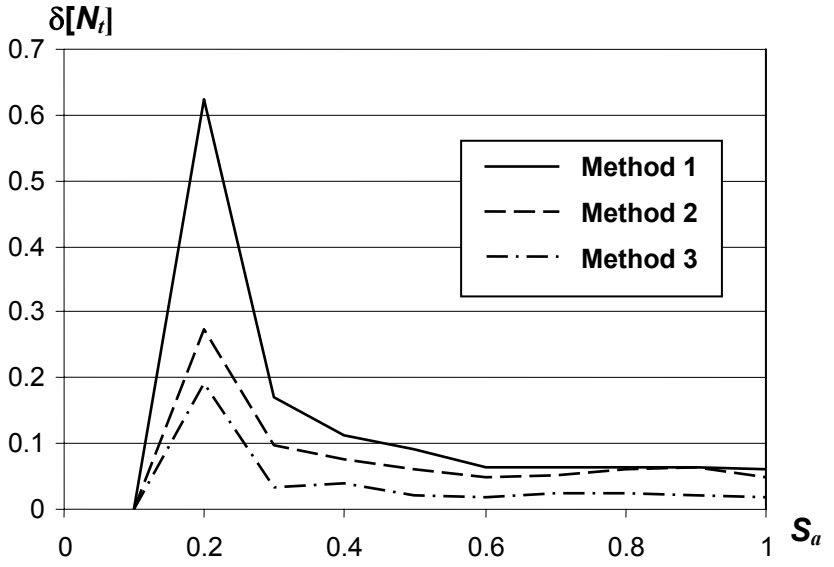

Figure 4.11. Coefficient of variation of the damage estimate as a function of spectral acceleration, ground motion LA15.

In order to isolate the possible influence of the particular characteristics of the ground motion, we repeat the analysis at each level of the spectral acceleration S_a with 40 different ground motions. All ground motion is taken from SAC database. The selection

process is conducted as follows. For a given intensity level, we pre-select at least 40 ground motion time histories that do not require excessive scaling (no more than 2.0 no less than 0.5), and then we scale all of them to that intensity level. This way we avoid over-scaling of ground motion time histories and a possible use of ground motions that are not typical for the given intensity. Then if there are 40 pre-selected time histories than we use all of them, if there are more than 40 time histories we arbitrary select 40 of them. These 40 selected ground motions are used for all structural analyses performed at the given intensity level, meaning that the same set of 40 ground motions is used for all three methods of damage analysis. At each value of S_a, we performed 40 (one for each of the selected 40 ground motion time history) dynamic simulations using 40 randomly generated structural models (Method 1 and Method 2 used for damage estimation, the same set of 40 generated structural models is used for both methods) and 40 dynamic simulations with the best estimate structure (Method 3 used for damage estimation). The results are presented in Figures 4.12 – 4.15. Note that for this case, Method 3 does not have any computational advantage over Method 1 and 2. For each of the 40 ground motion records, for each S_a value, we need to perform a dynamic simulation. Therefore, using the best estimate structural model instead of the randomized one does not reduce the number of dynamic analyses. Method 2 overestimates the expected value of damage with the relative error in the range 3% to 21%, with the maximum error at 0.2g. The average error for higher end (between 0.4g and 1.0g) is 4.1%. Method 3 provides damage estimates closer to the results of Method 1. The estimation error is less than 9.8%, the maximum occurring at 0.2g. The average error at the high end (0.4g –1.0g) is very low: 0.8%.

Figure 4.14 shows the variances of the damage estimates produced by the three methods for the set of ground motion time histories. There is no statistically significant difference between the variance estimates provided by the different methods. Therefore, the case of a set of ground motion records is appreciably different from the case of a single record (LA15) where the discrepancy between the variance estimates is apparent. Figure 4.15 shows the coefficient of variation of the damage estimate for the three methods. The results are practically identical for all three methods. The value of the coefficient of variation is considerably higher than for the case of the single excitation (Figure 4.11), reflecting the uncertainty introduced by the multiple ground motion time histories.

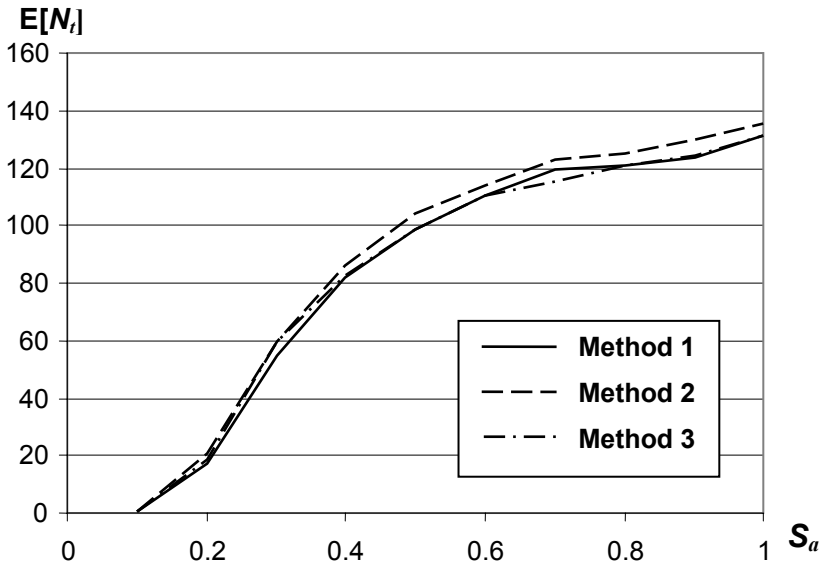

Figure 4.12. Expectation of damage E[Nt] as a function of spectral acceleration, set of ground motion records.

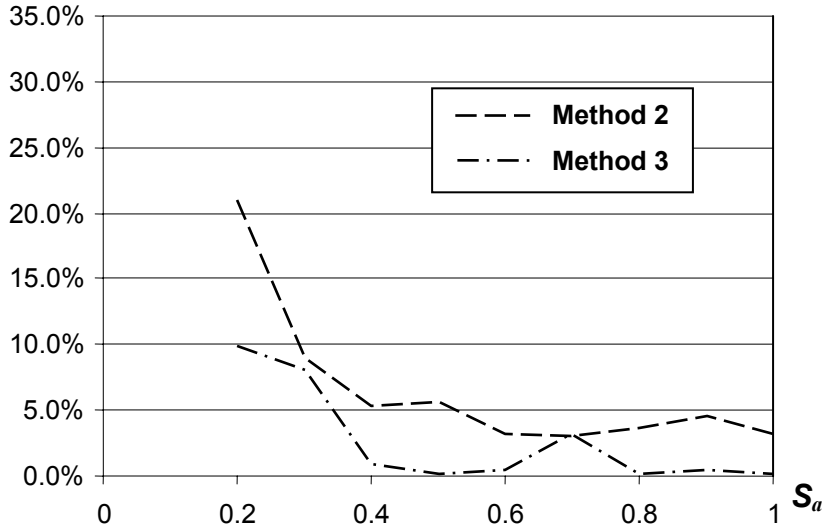

Figure 4.13. Relative errors of estimation of E[Nt] by different methods as a function of spectral acceleration, set of ground motion records.

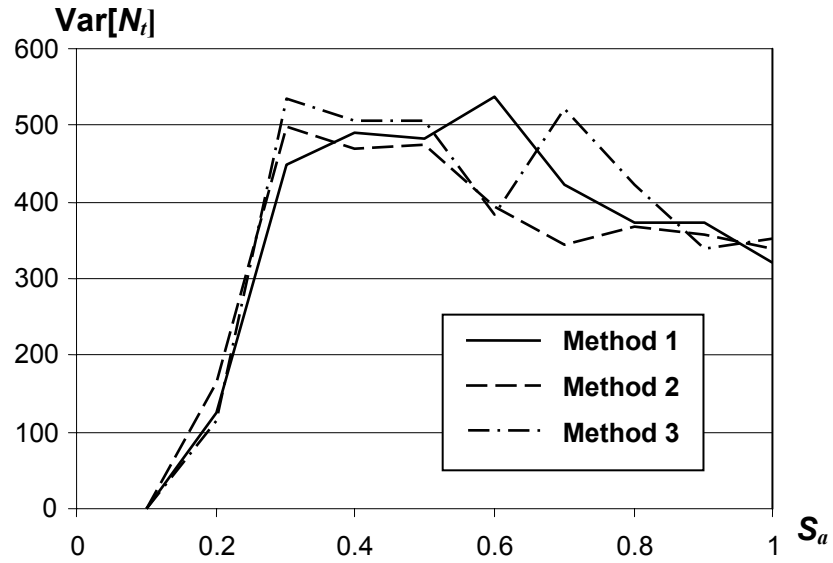

Figure 4.14. Variance of damage estimation as a function of spectral acceleration, set of ground motion records.

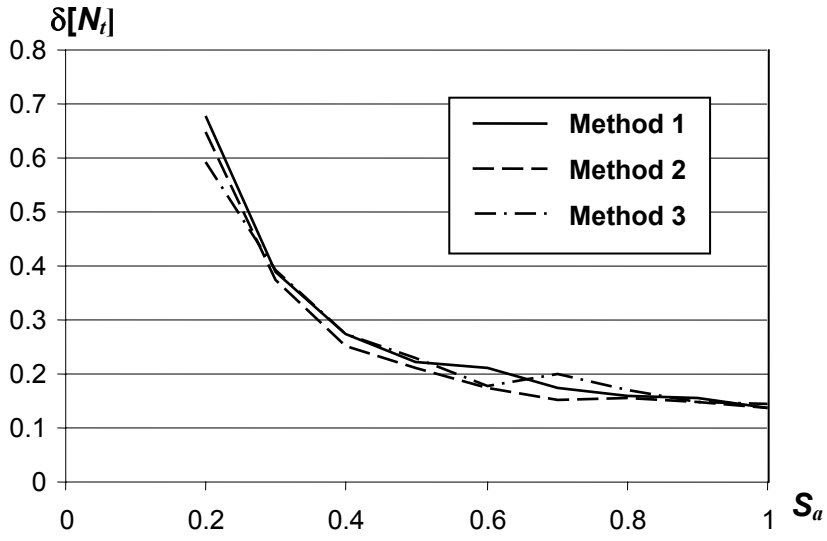

Figure 4.15. Coefficient of variation of the damage estimate as a function of spectral acceleration, set of ground motion records.

The purpose of this chapter is to compare two different approaches to the structural damage estimation: the damage analysis uncoupled from structural analysis, which performs damage evaluation based on the knowledge of *EDP* alone, and a proposed, coupled damage analysis approach, which predicts damage using both knowledge of EDP and knowledge of structural properties. In particular, we want to study the flaw of the fragility functions as applied to structural damage. This flaw is present whenever there exist such properties that are used for both structural damage (capacity) and structural response ($\underline{X}_i^C \cap \underline{X}_i^S = \underline{X}_i^{CS} \neq \varnothing$). The usage of fragility functions in this case results in using two samples of such properties $\underline{X}_i^{CS}$ instead of one. To explore this flaw, we have developed a damage model (damage state, EDP and limit-state function) that maximizes the possible discrepancy between the two approaches by maximizing the set of overlapping properties ($\underline{X}_i^C \subset \underline{X}_i^S$, thus $\underline{X}_i^{CS} = \underline{X}_i^C$) and excludes any other possible sources of error such as an imperfect limit-state function (see Chapter

4.2 for details). Then we have used three different methods of damage estimation. The approach based on coupled structural and damage analysis is implemented through Method 1. This method uses one set of randomly generated structural properties to conduct structural analysis and consecutive damage analysis. Method 2 and Method 3 are based on uncoupled structural and damage analyses. Both of them make use of two sets of structural properties. The difference is that Method 2 uses two randomly generated sets of structural properties, but Method 3 uses the best-estimate structural properties for the structural analysis and randomly generated properties for damage analysis.

The results have shown that all three methods provide fairly close estimates of the expected damage, providing some justification of the uncoupled damage and structural analyses. However, it still needs to be determined if this holds for other problems encountered in reality. The effects of possibly important factors, such as the level of uncertainty in the structural properties, the form of the probability distribution of the structural properties or redundancy of the structural model, have not been studied. These factors might be an interesting subject of future research. More importantly, the acceptable performance of the uncoupled analyses is shown for the case where the double sampling of structural properties is the only cause of the discrepancy between the results obtained by the uncoupled analyses and the results obtained by the coupled structural and damage analyses. As we shall see in Section 4.2, this is hardly the case with fragility functions for practical applications, since there is also usually an error caused by an inexact limit-state function.

The variance estimates exhibited a more diverse pattern of behavior than the mean estimates. While the estimates from Methods 1 and 2 in general agree, the variance

estimated by Method 3 is significantly lower for deterministic excitation. Therefore, performance of the uncoupled structural and damage analyses is adequate for this problem only if the randomized structure or multiple ground motion time histories are used. When the deterministic, best-estimate structure is employed together with a single ground motion record, the dispersion of the damage estimate is significantly underestimated. It means that the application of the Method 3 is not justified for the purpose of the analysis beyond mean values. Whenever one wishes to estimate variance of the damage or the probability of exceeding (or not exceeding) some damage threshold value, Method 3 should not be used. This is an important result because Method 3 can be viewed as a particular implementation of a general family of methods that can be defined in the following way: deterministic load – deterministic structure – probabilistic damage model. For example, deterministic load can be a monotonic lateral force used in push-over analysis. Therefore, it might be possible to extend the present results to a common damage estimation technique where a deterministic push-over analysis is complemented with a damage analysis using fragility curves, implying that the results obtained by such techniques should be treated with caution.

4.2 Inexact damage state description (imperfect limit-state function)

In this section, we deal with limit-state functions that define the damage state imprecisely. In terms of the theory outlined in Chapter 3, a limit function is imprecise if the condition (3.2) is violated. The violation of this condition is a common case in damage analysis. In practice, a perfect limit-state function is rarely used. The reason for this is that a perfect limit-state function is usually impossible to determine or it is very complex and unsuitable for practical applications. In order to handle the problem,

assumptions and simplification are introduced to make the function usable. These simplifications always introduce some errors, as a result, when the limit-state function is sufficiently simple for practical use, the condition (3.2) is violated to some extent. Indeed, the most common form of limit-state function is the one exemplified by (3.11). The underlying idea of such limit-state function formulation is quite intuitive: a particular damage state is achieved once "capacity" is less than "demand," leading to limit-state function of the kind: "capacity" – "demand" < 0. In the terminology adopted for the present study, "demand" is referred to as EDP – engineering demand parameter. This simplistic approach, although convenient, does not always adequately represent the onset of the damage state. This follows from the fact that only one damaging factor is taken into consideration, while there may be a combination of independent factors that lead to a particular damage state.

The error arising from the discrepancy between the failure region and limit-state function (condition 3.2 violated) can be handled in different ways. In the case that a perfect limit-state function is unattainable, the conventional approach involves introduction of a set of parameters into the limit-state function, which are treated as uncertain. The probability distributions of the parameters are estimated by some statistical method from experimental observations of real damage (see for example Kiureghian 1999, Gardoni et al. 2001).

In cases when the exact limit-state function is available, we have a choice between using the exact (possibly complicated) and inexact (but simple) limit-state functions. The choice can be made based on some sort of a cost-benefit analysis, where cost is the error of estimation introduced by the simpler model and the benefits are the

computational effort and time savings associated with it. In the present section, we perform a damage analysis based on two limit-state functions: one exact and the other inexact. Then we compare the results and perform a cost-benefit analysis to find out if the usage of the simplified limit-state function is justified. We do this as part of the case study that is described next.

4.2.1 Structural model

The structural model is similar to the one described in Section 4.1.2. The reinforced concrete moment-resisting frame depicted in Figure 4.5 is used. The moment-curvature relation for the flexural members is shown in Figure 4.6. All members are linear in shear. For the analysis in this section, we modify the moment-curvature behavior to account for the axial load-flexure interaction; that is, we introduce a yield surface into the model. The yield surface for each member is evaluated by the cross-section analysis program UCFyber (ZEvent, 2000) based on the member properties. The properties are taken from the structural drawings. For each member, the analysis has been performed to provide the calculated yield surface in moment vs. axial force coordinates. An example of the analysis result is shown in Figure 4.16. The calculated yield surface is used as an input for the structural model. Therefore, the yielding curvature in the hysteretic rule (Figure 4.6) is modeled as depending on the current axial force, making the structural model closer to reality.

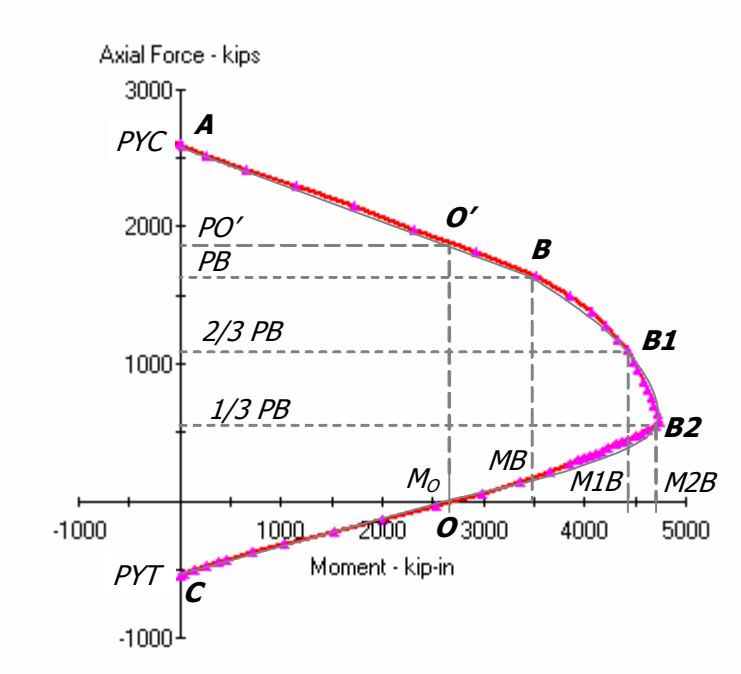

Figure 4.16 Example of the yield surface of the flexural members (axial force - moment interaction).

4.2.2 Damage model

For the present study, we choose a damage model that is based on the model described in Section 4.1.3. We modify it to reflect the changes made to the structural model. The damage states are preserved unchanged: "undamaged" (DS = 0) and "yield" (DS =1). A flexural member is considered to be in damage state "yield" if the yielding point in the moment-curvature relations has been reached. The exact limit-state function for this damage state can be written as follows

$$DS = \text{“yield”} \Leftrightarrow \exists t \ni d_y\left[X_i, P_a(t)\right] < d_i(t) \tag{4.6}$$

where t represents time during the dynamic structural simulation, $P_i(t)$ is the axial force in the i-th flexural member at time t, $d_y\left[X_i, P_i(t)\right]$ is the yield curvature of the i-th member at time t, $d_i(t)$ is the current curvature of the i-th member at time t. Statement (4.6) is equivalent to stating that the i-th flexural member is in damage state "yield" if

and only if at some point during the seismic event the curvature in the element has exceeded the yield curvature.

The limit-state function defined in (4.6) is perfect, meaning that we can not observe the "yield" damage state without satisfying the right-hand inequality in (4.6). In the following analysis, the damage estimate based on this limit-state function is considered to be accurate and is used as a reference when compared to the damage estimation based on an approximate limit-state function.

We can see that using the structural model with axial load-flexure interaction leads to a more complex limit-state function for the "yield" damage state. The simpler limit-state function defined in (4.1) fails to accurately describe the damage state of interest, meaning that condition (4.1) for the present system is not satisfied. Therefore, exploiting the limit-state function (4.1) for the estimation of damage will introduce some error. Evaluation of this error is one of the goals of the present case study. We use the inexact limit-state function defined in (4.1) for uncoupled damage estimation. The result obtained from this analysis is compared with the results based on the exact limit-state function (4.6). From a comparison, the error associated with the imperfect limit-state function can be evaluated.

4.2.3 Model parameters for the methods of damage estimation

In order to isolate the error introduced by the imperfect limit-state function, one would need to use estimation methods that do not bring in any additional errors. The exact method of damage estimation has been presented in Section 4.1.1 (Method 1). Therefore, to perform the comparison of the exact and inexact limit-state functions, one would need to use this method for both of them. However, the goal of this study is not to

study the errors arising just from a particular limit-state function, but rather studying the errors that can emerge as a result of using the uncoupled structural and damage analyses as applied to structural damage. Therefore, we use Method 1 in conjunction with the exact limit-state function (4.6) to obtain the mathematically correct damage estimate. This estimate is then used as a reference point for comparison with the damage estimates obtained by Methods 2 and 3.

Method 1 needs to be adjusted to accommodate the present structural model and damage model. First, we need to properly randomize the structural model. Previously, we used the lognormally distributed yield curvature (4.5). The parameters of this distribution correspond to the yield curvature of the flexural member not subjected to axial force. In order to be consistent with the structural properties utilized before, we assume that yield curvature defined by (4.5) corresponds to the zero axial force point at the yield surface (point O in Figure 4.16), meaning that the zero axial point is defined exactly as in (4.4)

$$M_o^i = \overline{M}_O^i x \tag{4.7}$$

where M_o^i is the yield moment of the i-th element at zero axial force, $\overline{M}_O^i$ is the best estimate of the yield moment of the i-th element at zero axial force, as calculated by UCFyber (ZEvent, 2000) and x is a lognormally distributed random variable with expectation $E[x] = 1$ and a coefficient of variation $\delta[x] = 0.08$. Then the randomization of the whole yield surface is performed by multiplying by x in such a way that it provides a uniform radial expansion or contraction of the whole yield surface.

Second, in order to assess the damage for each element, we need to define how the limit-state function (4.6) is to be evaluated. It is conveniently done by keeping track

of the current ductility ratio during the dynamic simulation: $d_i(t)/d_y[X_i, P_a(t)]$. It easy to see that for this ratio, the following is true

$$\max_t \left(d_i(t)/d_y[X_i, P_a(t)]\right) > 1 \Leftrightarrow \exists t \ni d_y[X_i, P_a(t)] < d_i(t) \tag{4.8}$$

The maximum ductility demand is the output provided by many standard dynamic structural simulation programs, including the one that is used in the present study (Ruaumoko by Carr, 2001). Whenever the structural analysis provides a maximum ductility ratio for a particular element greater than 1, the element is considered to be in the "yield" damage state. Therefore, Method 1 easily accommodates the exact limit-state function (4.6), despite its complexity. Moreover, to perform damage estimation with Method 1, one does not need to exert any additional effort besides those that have been taken for building the structural model and conducting structural simulations. The damage estimate obtained via this procedure is considered to be exact and is used as a reference point for the approximate methods that we define next.

Method 2 represents the uncoupled analyses approach to damage estimation. As shown in Chapter 3 and Section 4.1 this approach has an inherent deficiency if applied to structural members. This deficiency is occasioned by interdependency between properties of the structural members and practically all *EDP*s that are encountered in practice. It results in using two sets of structural properties for the same analysis instead of the single set. The effects of this discrepancy have been studied in Chapter 4.1. This is the first source of error associated with the fragility functions of structural members. Also, this source is characteristic only for structural members analyzed by uncoupled methods.

The second source of error, inexact limit-state functions, can appear in many damage estimation techniques. We want to know how the effects of an inexact limit-state

function manifest themselves if uncoupled analyses are used. To study the isolated effects of the inexact limit-state function (avoid double sampling), one would need to use such inexact limit-state function, where arguments of this limit-state function are not used for calculation of the *EDP*, and estimate damage by Method 2. However, for structural elements it is usually the case that the damage, at least partially, is defined by the same parameters that are used for calculation of *EDP*. It is also true for the damage state model ("yield") and *EDP* (curvature) used in this study, since yield curvature (defines capacity with respect to "yield" damage state) is used in the structural model to calculate curvature. Therefore, the effects of the inexact limit-state function can not be studied separately, if the chosen damage model is used.

Since we want to study the performance of the uncoupled analyses approach (Method 2), there is a logical question to ask: is it possible, within such approach, to use the exact limit-state function? If it were, a damage estimate obtained by Method 2 would be off by the error caused by double sampling of element properties that define both damage state and structural response (and this error has already been studied), and we would not need any further research. Let us investigate if Method 2 can be used with the exact limit-state function (4.6). Method 2 is based on standard fragility functions (3.13). The fragility function has to be generally applicable to the element of interest, meaning that it has to be independent of the particular design and location (see Section 3.1). The most general expression of the limit-state function that can possess such a property is given by (3.7). Comparing the exact limit-state function ($d_y\left[X_i, P_a(t)\right] < d_i(t)$), and general form ($g_n(EDP(\underline{X}, \underline{Q}), \underline{X}_i) < 0$) it can be seen that the former can not be written in the form of latter since the crucial (damage defining) element property – yield curvature,

can not be separated from the site specific building properties and earthquake excitation $\underline{Q}$, meaning that yield curvature of the element can not be written as a function of element properties only. The yield curvature of the element depends also on the current axial force that is the function of the site specific seismic loading ($\underline{Q}$) and the specific building properties ($\underline{X}$), that is, dead and live load distribution and force paths in the load-bearing structure. Therefore, the general (independent of site conditions) form of the limit-state function is incompatible with the exact limit-state function (4.6), implying that Method 2 can not be used with the exact limit-state function because of the generality requirement for the fragility functions. Some ways to reduce the error caused by inexactness of the limit-state function are explored in Section 4.2.5. In particular, it is shown that by selecting an appropriate fragility function for the uncoupled damage estimation, the discrepancy between a safety region defined by the exact limit-state function and a safety region defined by the inexact one can be reduced.

Since Method 2 can not be used with the exact limit-state function, we use the approximate limit-state function defined by (4.1). In this case, the fragility function is the CDF of capacity given by (4.5), where the parameters of this CDF of capacity are the same as the ones used for the structural model without axial force-flexure interaction. Therefore, the damage estimate will bear the error introduced by inexactness of the limit-state function. Since the results of Method 2 are not exact because of using two sets of structural properties, the error of estimation obtained by Method 2 will include the errors originating from two different sources: double sampling the set of structural properties (a result of dependent damage and EDP) and inexact limit-state function (a result of the universal applicability requirement for fragility functions). Since both error sources are

inherent for any problem of this kind (site-specific structural damage estimation), we evaluate here the combined error resulting from both factors.

Method 3 is used for damage evaluation to explore the benefits and cost of simplification of Method 2. The method is identical to the Method 3 used before: the best estimate structural model (with axial force-flexure interaction) is used for all dynamic simulations, and then the CDF of capacity (4.5) is applied as the fragility function.

4.2.4 Results and conclusions

The results of damage estimation for the LA15 ground motion record are presented in Figures 4.17 - 4.20. The damage estimates have been obtained for the range of S_a between 0.1g and 1.0g. The mean values of damage estimate for this excitation are shown in Figure 4.17. The relative error of estimation for Method 2 and Method 3 is given in Figure 4.18. It can be noted that inexact limit-state function introduces a significant error into the damage estimate. Method 2 consistently overestimates the damage by 40 – 60% with the average 50%. Method 3 overestimates the damage by 50 – 70% with average 61%. This is significantly worse than for the case of the exact limit-state function (see Chapter 4.1).

Note that if a compressive axial force is not excessive (less than *PO'* in Figure 4.16), then the yield moment at this force is greater than in a zero axial force case. Therefore, if moderate compressive axial loads are present, the model with axial force-flexure interaction is stronger than the model without such interaction. In the present model, the compressive axial forces due to the dead load are low enough to provide some increase of the yield moment for all columns. Therefore, the model with axial force-flexure interaction is, on average, stronger with respect to "yield" damage state, than the

model without the interaction. Comparing Figures 4.8 and 4.18, we can see that Method 1 reflects this increase of strength by providing considerably lower values of N_t than for the case without axial force-flexure interaction. No significant increase of strength can be deduced from estimates provided by Methods 2 and Method 3. The opposite trend can be observed: the Method 2 and 3 damage estimates for the stronger (with axial force-flexure interaction) structure are slightly higher than for the weaker (without axial force-flexure interaction) one, which contradicts the actual physical behavior.

Figures 4.19 and 4.20 show the variance of damage estimates and coefficient of variation, respectively, for the LA15 ground motion record. Differences between the variances estimated by the different methods are less significant than for the structure without axial force-flexure interaction. However, as far as the coefficient of variation is concerned, the picture is similar with the one we had before: the coefficient of variation for Method 2 is slightly lower than for Method 1 at the low end and approximately equal to it at the high end, Method 3 provides a coefficient of variation that is approximately 30% of that of Method 1 similar to that for the structure without axial force-flexure interaction (Figure 4.11).

The results of damage estimation for the previously described set of SAC ground motion records (40 at each S_a level) are presented in Figures 4.21 - 4.24. The mean values and the relative error of the damage estimates of Methods 2 and 3 are given in Figures 4.21 and 4.22, respectively. The expected values of the damage estimates obtained by Methods 2 and 3 are practically identical. All the trends that have been observed for the LA15 record are also manifested for the set of ground motion records. Methods 2 and 3 are insensitive to the increase of the structural strength, providing the same (or slightly

higher) values of expected damage than for the structure without axial force – flexure interaction (Figure 4.12). The overestimation of damage by both Methods 2 and 3 is in the range 30% – 50% with average 42%.

Figure 4.23 and 4.24 present the variance and coefficient of variation of the damage estimates, respectively. The behavior of both parameters is distinctly different from the single (LA15) excitation case (Figures 4.14 and 4.15). The estimates for Methods 2 and 3 are quite close and both overestimate the variance by approximately 100% over most of the S_a range, only converging with the Method 1 estimate at S_a = 1g. For the coefficient of variation, the picture is the opposite. Because of the higher values of the expected damage, the coefficient of variation is approximately 50% lower for Methods 2 and 3 than for Method 1. This ratio holds for S_a between 0.2g and 0.7g, while for higher values of S_a, all the coefficients of variation of the estimates converge. The surprising observation is that the overall uncertainty of the damage estimation, measured by the variance and coefficient of variation, is much lower than for the LA15 excitation case, independently of the method used for estimation. Such a result is counter intuitive. The expected behavior would be an increase in the dispersion of the damage estimates, since using multiple ground motion records introduces additional variability compared to the single excitation case.

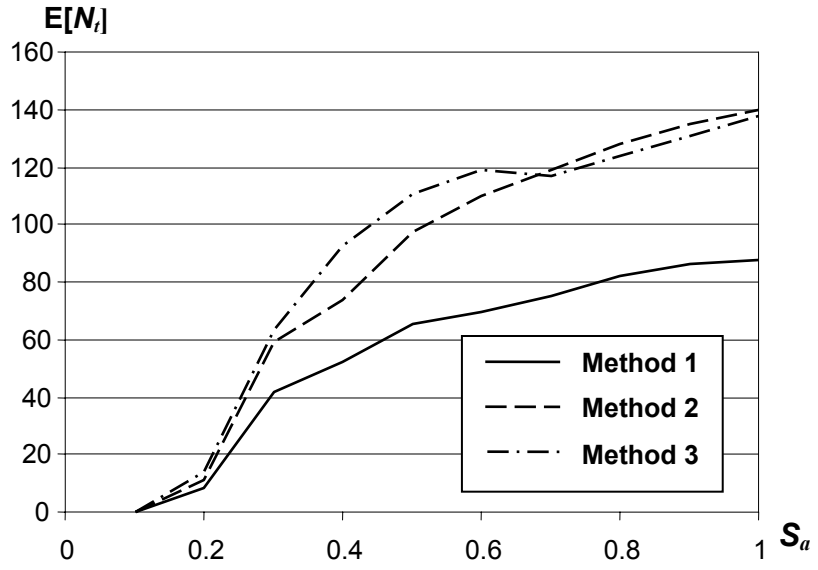

Figure 4.17. Expectation of damage E[N_t] as a function of spectral acceleration for the axial force-flexure interaction model, ground motion LA15.

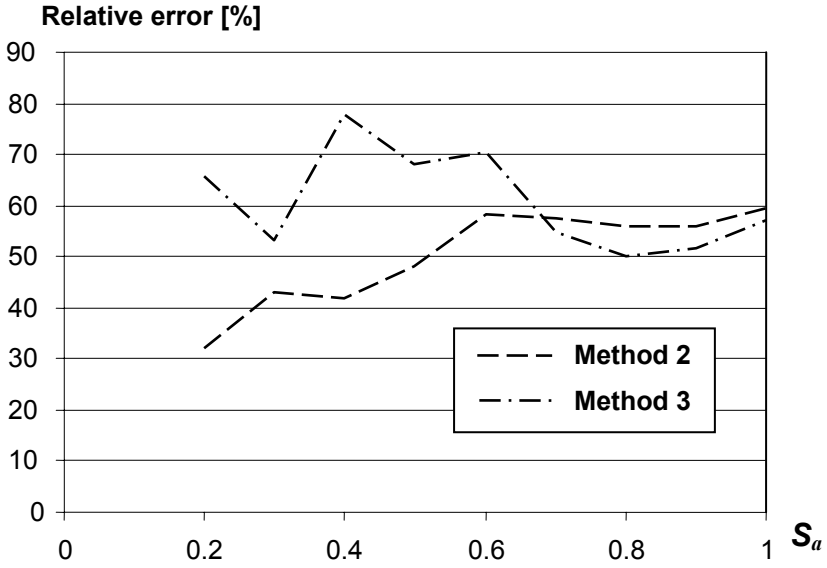

Figure 4.18. Relative errors of estimation of E[N_t] by different methods as a function of spectral acceleration for the axial force-flexure interaction model, ground motion LA15.

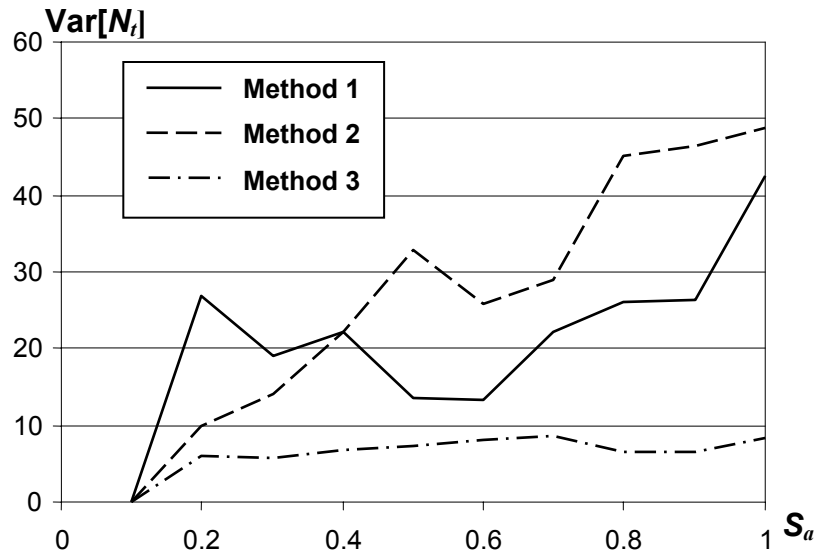

Figure 4.19. Variance of damage estimation as a function of spectral acceleration for the axial force-flexure interaction model, ground motion LA15.

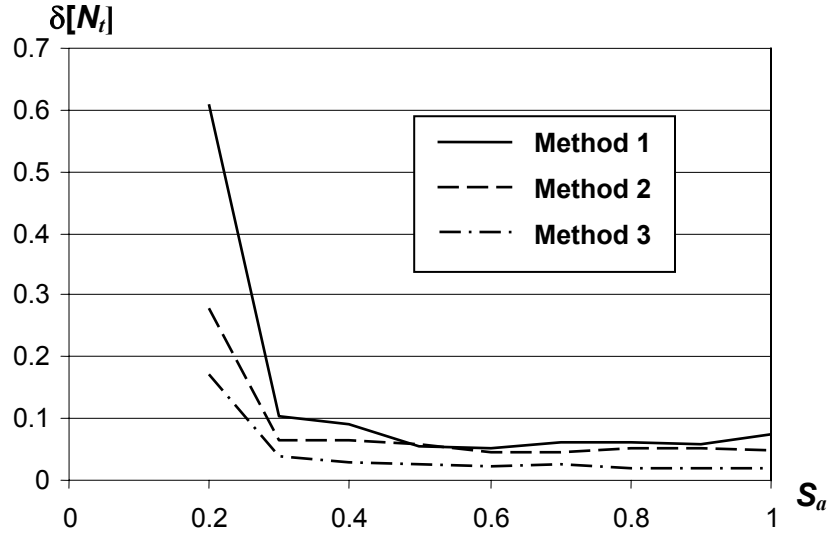

Figure 4.20. Coefficient of variation of the damage estimate as a function of spectral acceleration for the axial force-flexure interaction model, ground motion LA15.

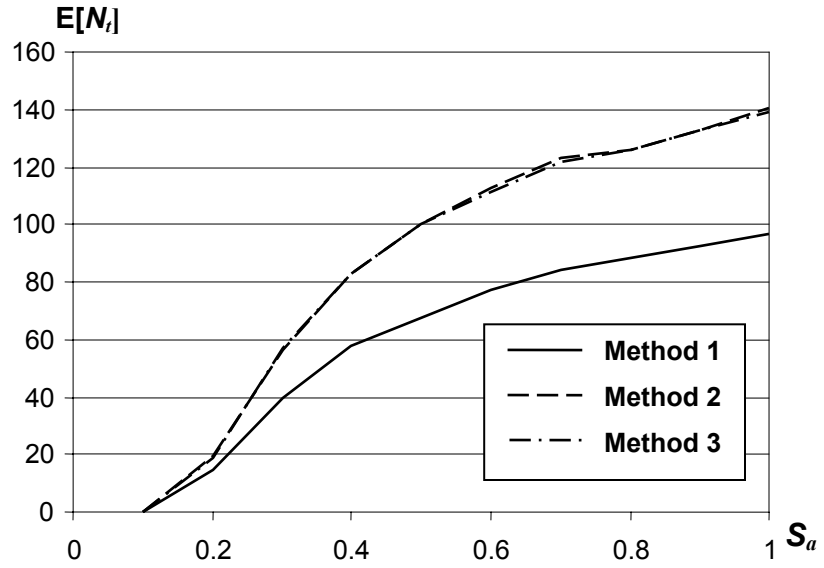

Figure 4.21. Expectation of damage E[Nt] as a function of spectral acceleration for the axial force-flexure interaction model, set of ground motion records.

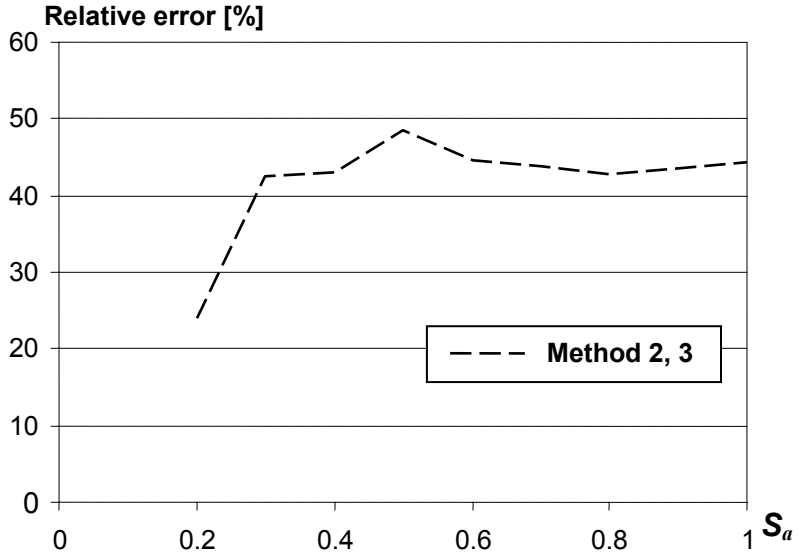

Figure 4.22. Relative errors of estimation of E[Nt] by different methods as a function of spectral acceleration for the axial force-flexure interaction model, set of ground motion records.

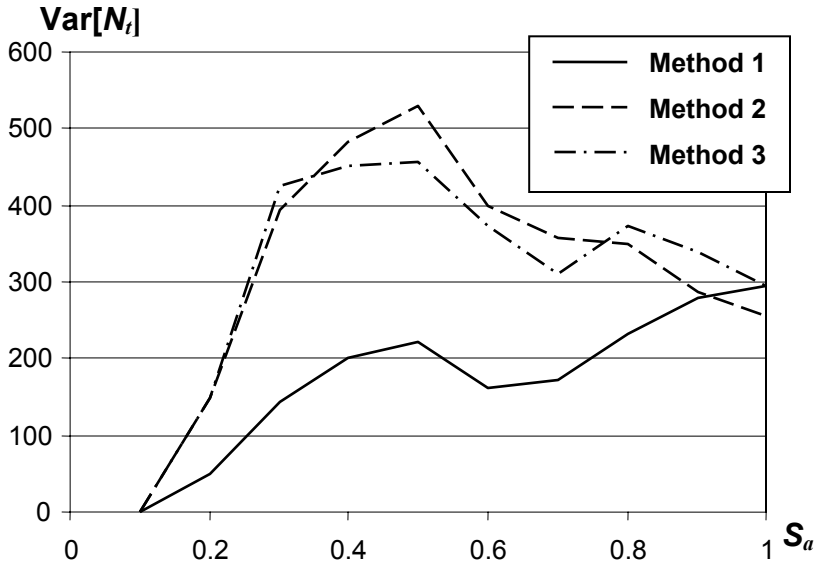

Figure 4.23. Variance of damage estimation as a function of spectral acceleration for the axial force-flexure interaction model, set of ground motion records.

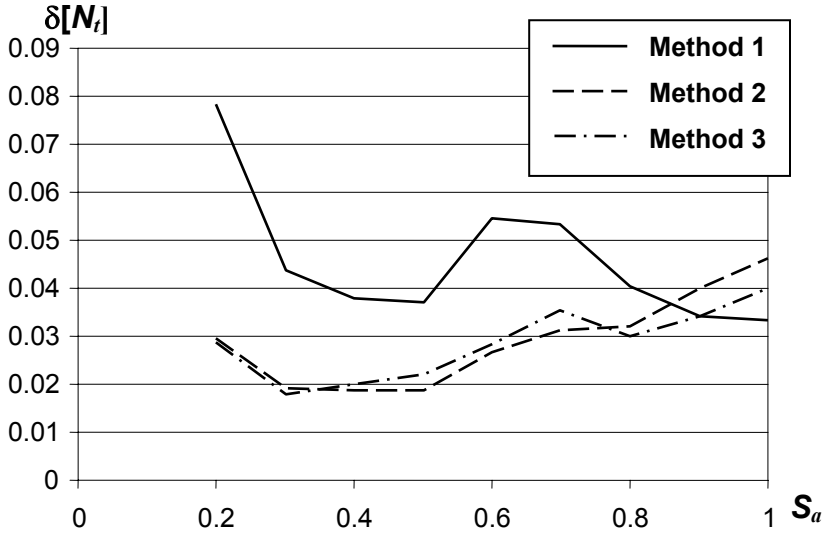

Figure 4.24. Coefficient of variation of the damage estimate as a function of spectral acceleration for the axial force-flexure interaction model, set of ground motion records.

Evaluating in general the performance of the three different methods of damage estimation, it can be seen that the inexact limit-state function can lead to a significant error for the mean values of the damage estimates. The error of estimation for Method 2

is on average 50%-60%. This error partially comes from using two samples of the structural properties (yield curvatures) in the analysis. But comparing the results from Section 4.1.6 and this section it is apparent that the contribution of double sampling of structural properties is insignificant. As far as expected damage is concerned ($E(N_t)$), the major part of the error arises from the inexact limit-state function. The magnitude of the error caused by the inexact limit function is particularly notable because of the simplicity of incorporating the exact limit-state function when Method 1 is utilized.

The exact limit-state function can be easily implemented if the structural analysis based damage estimation technique (Method 1) is used. It is remarkable that despite the increased complexity of the limit-state function for the model with axial force-flexure interaction, Method 1 can include this limit-state function into the analysis without any additional effort. This reduced computational effort is ensured by the existence of the built-in indicator of "yielding," the ductility. Ductility indicates the onset of yielding independently of how exactly the yielding moment (curvature) is specified. Therefore, switching to a more complicated structural model (more complicated limit-state function) does not cause any difficulties with pinpointing the "yield" damage state: we just have to pick up members with ductility demand greater than 1. Ductility output is provided by the majority of modern structural analysis programs, and so to correctly estimate the "yield" damage state, one does not need to modify standard software: once the structural model is established, the damage and the damage gauge are "built-in" there.

We can see that for the present problem there is no trade-off between accuracy and cost since the better accuracy can be achieved for no additional effort. This can be

done by switching from uncoupled structural and damage analyses to coupled structural and damage analyses.

Discussing the result from a more general perspective, it can be noted that Method 2 fails to capture the effects of a very common feature of modern structural models: axial force-flexure interaction. It does not reflect the increase of the strength of the model resulted from such interaction. It is a special example of an intrinsic shortcoming of fragility functions: it is unable to capture enhancement of structural models. It might be seen as the down side of the fragility functions generality: universal fragility functions can not account for many of the details of the structural model exactly because they are designed to fit them all. Therefore, they are bound to bring in the errors that can be quite significant, as demonstrated in this chapter, and these errors can not be generally estimated for each problem beforehand.

On the other hand, advances in structural modeling can be easily accommodated by a Method 1 type analysis. For example, the yield model can be improved by various features, like shear-flexure interaction or interaction between different directions in 3D models, and the hysteretic rule can change or fiber-based elements can be used. No matter how the yielding is implemented, its onset can always be monitored using the ductility ratio. This ratio is calculated by all modern structural simulation software packages, implying no additional effort for evaluating the “yield” damage state. Similar advances can be made in the modeling of post-yielding behavior, like predicting the point of maximum strength or the pattern of strength degradation. Once a model of post-yield behavior is developed, it is easy to define parameters that can be a marker of any point of interest on the force-deformation curve, such as maximum strength or the point of

strength decrease to 80% of the maximum. The latter are often used to define member collapse. Such parameters can be easily implemented in existing and future structural analysis software, and can be used for evaluating the corresponding damage states in a way similar to how the ductility ratio is used for evaluating the "yield" damage state.

Summarizing the results of this chapter, it can be concluded that the proposed damage analysis that is coupled with structural analysis (Method 1) proves to be advantageous compared with the approach using uncoupled damage and structural analyses with respect to both accuracy of damage estimates and required computational effort. This makes it a valuable contribution to the coming performance-based earthquake engineering era.

4.2.5 Alternative damage models for uncoupled damage analysis.

Although in the present case, only an inexact limit-state function can be used for an uncoupled damage analysis, there are ways to improve this function, making it closer to the exact one. One of them is to use more information about a component. The other is to use more information about the structural analysis results, that is, considering more parameters of structural response (*EDP*s) and using multidimensional fragility functions. Both of these approaches can provide better damage estimation but both of them require additional efforts, and are expected to perform worse than a coupled damage analysis.

4.2.5.1 Utilizing additional information about components

First, consider the discrepancy between the limit-state functions used for the different methods of damage estimation. Figure 4.25 gives a subset of the safety region for the exact-state function and both failure and safety regions for the approximate limit-state function given the maximum curvature obtained during the analysis. The horizontal

axis represents the yield moment of the element under consideration. In the present case, the yield moment is taken at the zero axial force and is a random variable given by (4.7). Therefore, Figure 4.25 depicts the regions in the state space for the case where the CDF of yield curvature at zero axial force is taken as a fragility function. These regions are determined as follows.

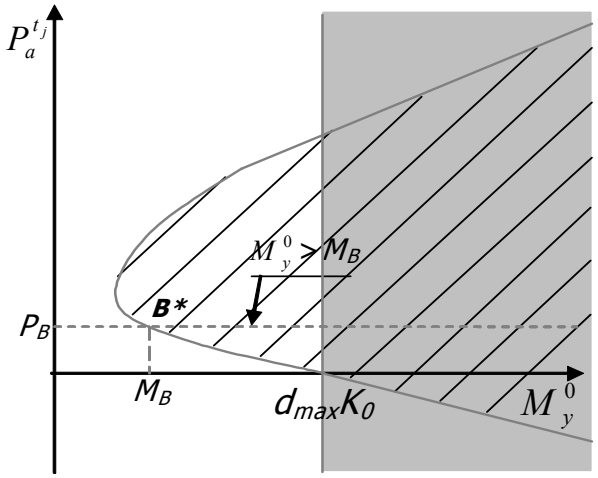

Figure 4.25 Safety regions for exact (hatched) and approximate (shaded) limit-state functions, fragility function is CDF of capacity at zero axial force

Given the maximum curvature, Methods 2 and 3 use the limit-state function (4.1) that can be rewritten in terms of yield moment

$$DS = \text{“yield”} \Leftrightarrow M_y^0 < d_{\max} K_0 \tag{4.9}$$

where M_y^0 is the yield moment at zero axial force, $d_{\max}$ is the maximum curvature attained during the analysis, K_0 is the initial flexural stiffness of the element under consideration. For this approximate damage model, given the maximum curvature, the occurrence of damage depends only on the value of yield curvature and does not depend on anything else. Therefore, the failure region is given by the inequality in (4.9) and the safety region is given by $M_y^0 > d_{\max} K_0$ (shaded area in Figure 4.25).

Consider now the exact limit-state function (4.6) used in Method 1. This function describes the failure region in a multivariate state space that includes the current yield moments (corresponding to the current axial force) at every time step, as well as the current applied moment at every time step during the dynamic structural analysis. It is impossible to portray the limit-state function in this multivariate state space, since it can have thousands of variables. However, we can partially depict the exact limit-state function (4.6) in a 2-D space that includes the axial load at an arbitrary point in time $P_a^{t_j}$ and some parameter defining the yield surface ("defining" means that this parameter defines a particular sample of yield surface, e.g., known value of yield moment at some level of axial force). The exact failure region can not be found in this 2-D space, but the safety region can be determined and is shown as a hatched area in Figure 4.25. The algorithm for finding the safety region for the exact limit-state function is illustrated by Figure 4.26.

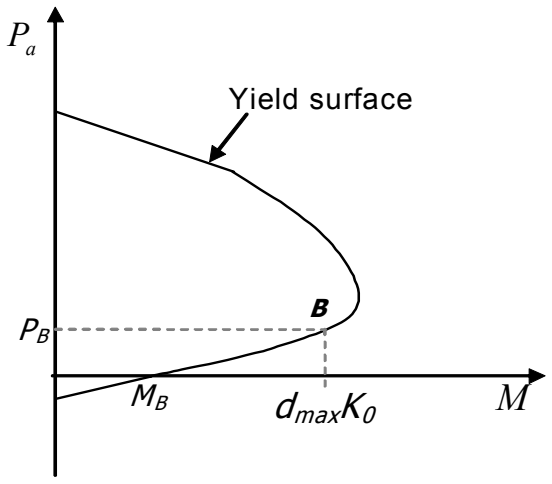

Figure 4.26 Using flexural member's yield surface for determining safety region in terms of yield moment at zero axial force

According to (4.6), the "yield" damage state occurs whenever the current yield moment is less than the current applied moment. In the chosen 2-D coordinate system, it is impossible to consider the current applied moment. However, it can be seen that if the current yield moment is greater than the product $d_{\max} K_0$ then there is no yielding at this time step. In this case, $d_{\max} K_0$ can be interpreted as the maximum applied moment observed during the analysis, providing that there is no yielding at the time step when the observation of $d_{\max}$ is made. Clearly, if the current yield moment is greater than the maximum applied moment then it must be greater then the applied moment at each time step. Therefore, we can find the lower bound (sufficient condition) on the safety region as the following inequality

$$M_y^{t_j} > d_{\max} K_0 \tag{4.10}$$

where $M_y^{t_j}$ is the yield moment at the current time step, t_i. The lower bound means that we know for sure that if at time t_i the current axial force and the yield moment at zero axial force correspond to a yield moment satisfying the inequality (4.10) then no damage can occur; if (4.10) is violated, we do not know if the "yield" damage state takes place or not at this particular time, because $M_y^{t_j}$ may be either greater or less than the current applied moment.

We determine the area corresponding to (4.10) as follows. If the current axial force is zero, then $M_y^{t_j} = M_y^0$ and (4.10) becomes $M_y^0 > d_{\max} K_0$. Therefore, at $P_a^{t_j} = 0$, the safety region for the exact limit-state function coincides with the safety region for the approximate limit-state function (4.9). Next, consider the case where the axial force is

non-zero and compressive, $P_a^{t_j} = P_B$. In the axial force-moment plane, take the point B with the coordinates: $d_{\max} K_0$ and P_B, as shown in Figure 4.26. Then we choose a value M_B of the yield moment at zero axial force that insures that the yield surface goes through this point. Clearly, if $M_y^0 > M_B$ then $M_y^{P_B} > d_{\max} K_0$, where $M_y^{P_B}$ is the yield moment at axial force P_B. Since we consider the case where $P_a^{t_j} = P_B$, it is also true that $M_y^{t_j} = M_y^{P_B}$, therefore, $M_y^{t_j} > d_{\max} K_0$, meaning that the condition of the safety region is satisfied. Thus, at $P_a^{t_j} = P_B$, the safety region is defined by $M_y^0 > M_B$ as shown in Figure 4.25. In a similar way, all points can be found to define the safety region for the exact limit-state function, which is shown as a hatched area in Figure 4.25.

Figure 4.27 compares two limit-state functions for a typical distribution of the axial force (moderate compressive load is prevailing). Clearly, in the range of values where the axial force is most likely to be, the safety region is smaller for the approximate limit-state function than for the exact one. Figure 4.27 shows the lines corresponding to 10^{th} and 90^{th} percentiles for the assumed probability distribution of $P_a^{t_j}$. In this range, the approximate limit-state function assumes no damage for the area inside the infinite strip *CBED*, while the exact function indicates no damage for at least the area inside the infinite strip *CAGFD* and the latter can be noticeably larger. Therefore, the approximate limit-state function is conservative for this case. One can expect that damage estimates for the uncoupled damage analysis that uses the CDF of yield curvature at zero axial force as the fragility function will be higher than for the uncoupled damage analysis. This is confirmed by the results presented in Section 4.2.4.

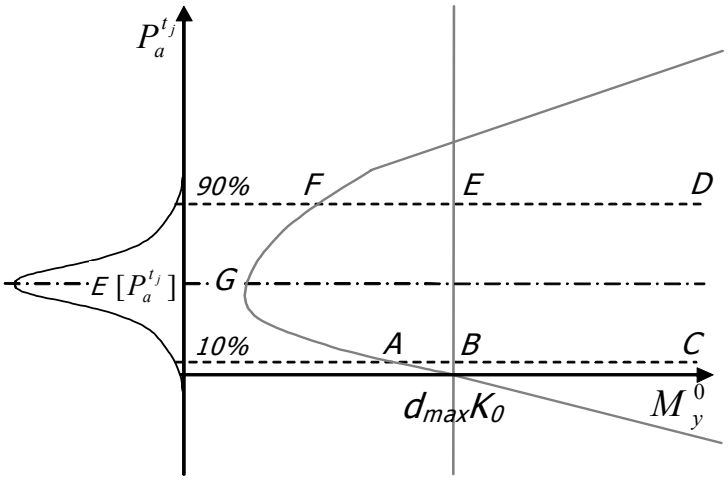

Figure 4.27 Comparison of the safety regions defined by exact and approximate limit-state functions for the assumed probability distribution of current axial force.

The framework presented so far in this section framework can be used for analyzing possible improvements to the uncoupled damage analysis. For example, consider a case where the CDF of yield curvature at the expected value of axial force, $E[P_a^{t_j}]$, is used as a fragility function. Denote the corresponding yield moment at $E[P_a^{t_j}]$ by $M_y^{E[P_a]}$. Then we can compare the exact and approximate limit-state functions by drawing the corresponding safety regions in 2-D space where the coordinates are $M_y^{E[P_a]}$ and current axial force $P_a^{t_j}$. Utilizing the same procedure that was used for plotting Figure 4.25, we obtain Figure 4.28. It is noted that for the most probable values of the current axial force (between the 10^{th} and 90^{th} percentiles), the discrepancy between the two safety regions is smaller than in the previous case. However, the approximate limit-state function may become non-conservative, since the safety region may be larger than that

defined by the exact limit-state function (Recall that the hatched area in Figure 4.28, as in Figure 4.25, is a subset of the actual safety region).

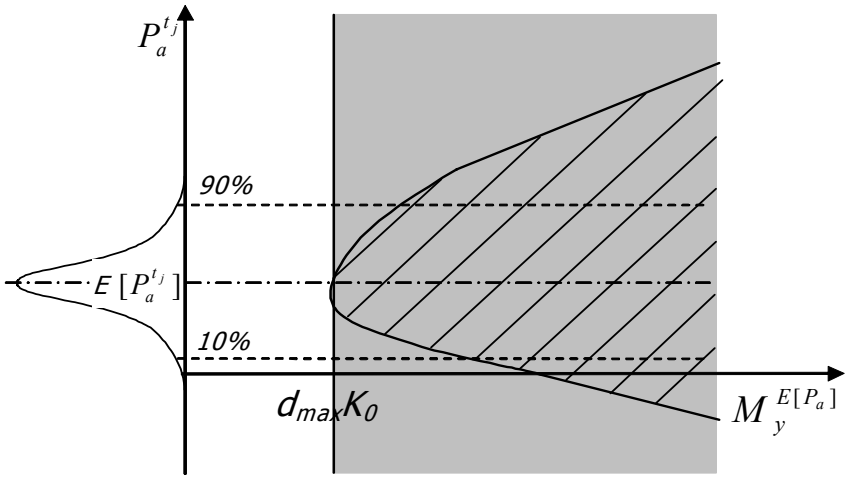

Figure 4.28 Safety regions for exact (hatched) and approximate (shaded) limit-state functions, fragility function is CDF of capacity at expected axial force

Depending on the location of the expected axial force relative to the yield surface of the flexural member under consideration and on the dispersion of the axial force, the difference between the exact and inexact limit-state functions can change. For example, Figure 4.29 compares the safety regions for the case where both the expected value and standard deviation of the axial force are significantly lower than in the previous case (Figure 4.28). It can be seen, that in this case, the approximate limit-state function should provide results that are the closest to the exact one. The areas of the important parts of the safety regions agree most closely out of all previously considered cases. Although the safety regions are still far from coinciding, the triangles OAB and ODC partially offset

each other, providing approximate equality of the safety regions' areas, but not necessarily equality of the probabilities of being in the safety regions in the two cases.

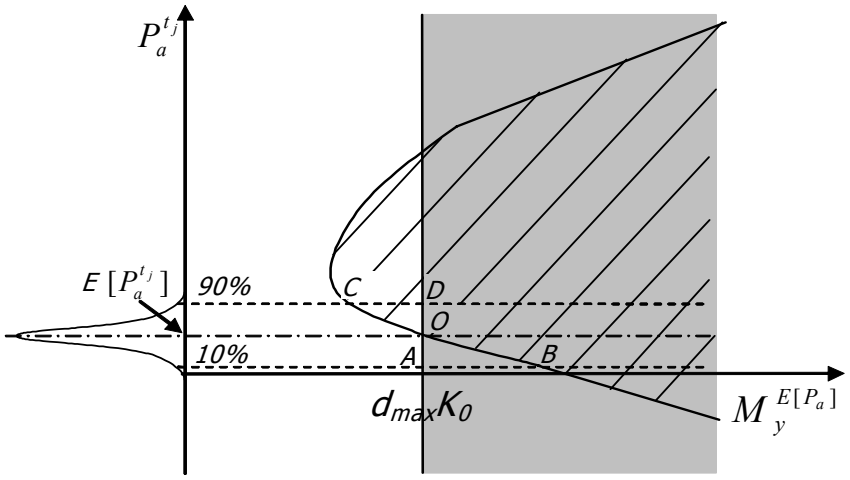

Figure 4.29 Safety regions for exact and approximate limit-state functions, lower values of axial force expected value and standard deviation are used

In summary, the use of the CDF of yield curvature at the expected axial load as the fragility function should provide better performance then the CDF of yield curvature at zero axial force. Therefore, this is a viable way of improving the performance of the uncoupled damage analysis. A good practical approximation to the expected values of axial force may be the dead load applied to the structural components. In this way, we are improving the uncoupled damage analysis by using additional information about the component (dead load axial force). However, it requires first, estimation of the dead load for each appropriate component and this may not be necessarily the input information for the structural model and, therefore, this will involve additional efforts to perform this estimation and second, increase of the number of different fragility functions used in the

analysis, since the components that are otherwise equal may have different dead load, necessitating usage of several fragility functions (each for each dead load value) instead of one. Therefore, the improvement of the uncoupled damage analysis here comes at some cost, and it still does not match the performance of the coupled damage analysis.

4.2.5.2 Utilizing multidimensional fragility functions

The other way of advancing uncoupled damage analysis is using additional information about the structural analysis, that is, multiple *EDP*s. For the present model, a logical approach would be to use the information about the axial force, that is, besides maximum curvature we can also use maximum axial force observed during the structural analysis. Then a two dimensional fragility function is needed: $P(DS = "yield" \mid d_{\max} = z, P_{\max} = u)$, where $P_{\max}$ is the maximum compressive axial force. We shall analyze how this function can be developed and what are the benefits of using it.

First, the limit-state function must be developed. Now, the function can be developed in terms of maximum curvature, maximum compressive axial force and any relevant member property or a set of properties, e.g., yield curvature at zero axial force or yield curvature at expected axial force, as used previously. There is an infinite number of ways to formulate this limit-state function. Depending on what particular form is chosen, the function may be closer or further from the exact one. For demonstration purposes, we define a simple limit-state function as follows

$$DS = \text{“}yield\text{”} \Leftrightarrow d_y^0 < d_{\max} \; or \; P_a^0 < P_{\max} \tag{4.11}$$

where d_y^0 is the yield curvature at zero axial force and P_a^0 is the yield compressive axial force at zero moment (marked as PYC in Figure 4.16). Thus, the "yield" damage state is assumed to be caused by either excessive moment or excessive axial force. We shall see how this function compares to the exact one by considering a 2-D space in the same coordinates as before, M_y^0 and $P_a^{t_j}$.

There exist two different cases with respect to relative magnitudes of the maximum curvature and the maximum compressive axial force. In a case where the maximum axial force is relatively small, the safety region for the inexact limit-state function does not change and is found exactly as in the case of one-dimensional fragility function. For the exact limit-state function, the knowledge of the maximum axial force observed during the analysis does not directly affect the shape of the safety region either. However, it puts an upper bound on the value of $P_a^{t_j}$, effectively changing its distribution. It also excludes a part of the 2-D space (i.e., the part corresponding to inequality $P_a^{t_j} > P_{\max}$) out of consideration. Figure 4.30 shows how the knowledge of maximum force affects the analysis in this case. Note that the conditional PDF of $P_a^{t_j}$ is not a cut and inflated part of the unconditional PDF, since the conditioning here is on the event $P_a^{t_i} \le P_{max}$, $i = 0 \ldots N_{ts}$ where N_{ts} is the number of time steps in the dynamic structural analysis rather than on the event $P_a^{t_j} \le P_{max}$, also axial forces at different time steps are correlated and, therefore, can not be discarded in the conditioning. It can be seen that introduction of the axial force as a second *EDP* improves the uncoupled damage analysis performance. The improvement is achieved primarily due to the down-shift of the range of most likely

values of $P_a^{t_j}$, which makes the situation similar to one presented in Figure 4.29 where the non-overlapping areas of the two safety regions partially offset each other.

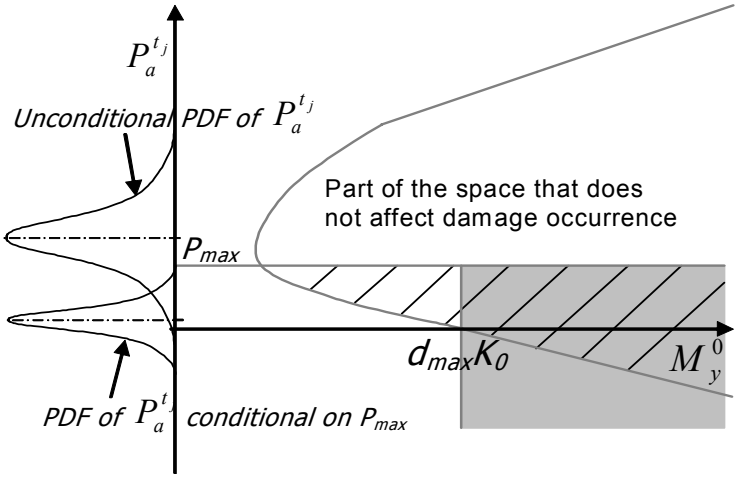

Figure 4.30 Safety regions for exact (hatched) limit-state function and two-dimensional approximate (shaded) limit-state function, axial force is relatively small

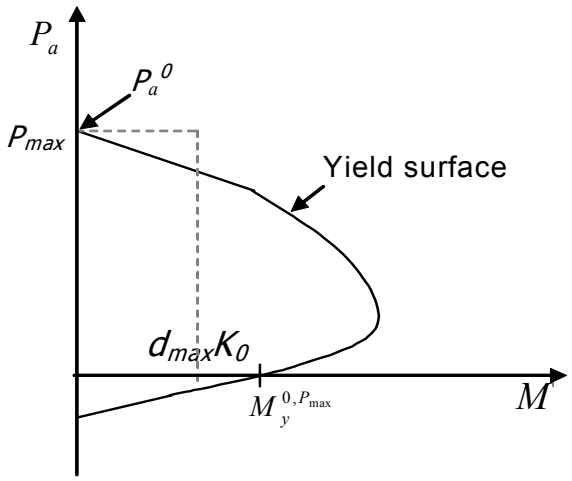

Figure 4.31 Procedure of finding safety region for two dimensional fragility function, axial force is relatively high

Next, consider a case where the maximum axial force is relatively large. Figure 4.31 shows how the safety region is found in this case. It can be seen that whether damage occurs or not is controlled by the maximum axial force, that is, if $P_{max} < P_a^0$, the yield moment at zero axial force is high enough to ensure that the inequality $M_y^0 > d_{\max} K_0$ is satisfied also, so according to (4.11), no damage is assumed. Therefore, the safety zone is given by $M_y^0 > M_y^{0,P_{\max}}$, where $M_y^{0,P_{\max}}$ is the yield moment at zero axial force that makes the yield force at zero moment equal the maximum observed axial force, $P_a^0 = P_{max}$. Note that this safety region is smaller than for the case of the one-dimensional fragility function, since $M_y^{0,P_{\max}}$ is greater than $d_{\max} K_0$.

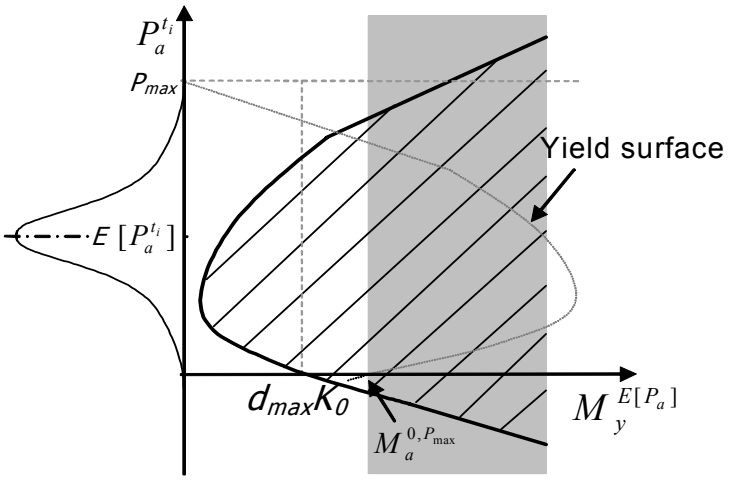

Figure 4.32 Safety regions for exact (hatched) limit-state function and two-dimensional approximate (shaded) limit-state function, axial force relatively large

Figure 4.32 pictures the two safety zones for this case. As before, the shaded area marks the safety region for the approximate limit-state function and the hatched area depicts the safety region for the exact limit-state function. It can be seen from the figure

that discrepancy between the two safety regions is greater than in the case of one-dimensional fragility function, since the safety zone for the approximate function is moved to the right as compared to Figure 4.25 and the safety zone for the exact limit-state function is approximately the same.

This analysis shows that it is unclear whether using the two-dimensional fragility function reduces the discrepancy between exact and inexact limit-state functions. For the particular form of 2-D limit-state function considered in this section, the overall effect depends on the distribution of maximum axial forces and maximum curvatures throughout the whole structure. If the case with relatively low maximum axial force is prevailing, the damage estimates for the uncoupled damage analysis will be closer to the exact solution; for the other case they will probably be less accurate than the ones obtained through the original one-dimensional fragility. Note that developing and using two-dimensional fragility functions is much more complicated than one-dimensional ones, therefore, one have to be careful when implementing such functions, since the benefits might be questionable.

In summary, we can see that there are ways to improve the uncoupled damage analysis, but they require additional efforts that have to be measured against the benefits they provide. The merits of different ways to implement the uncoupled damage analysis have to be considered on a case by case basis. For the present study, we select the implementation that requires approximately the same effort as the coupled damage analysis. Therefore, in this way, the comparison of the two approaches is valid, since it is made on the “apple to apple” basis.

5 Damage estimation coupled with structural analysis (multiple damage states)

In this chapter, we shall compare the results obtained by the three methods of damage estimation for the case of multiple damage states. For all three methods, we use the exact limit state. Therefore, only the error caused by the double sampling of structural properties is present. As before, we use a reinforced-concrete moment frame shown in Figure 4.5 as a case study. A more advanced structural model of the frame is used. We shall describe the modifications of the structural model next.

5.1 Structural model

The structural model used in this chapter is based on the structural model described in Chapter 4.1.2. We assume the same properties for all of the structural members, including no axial force-flexure interaction. The difference is in post-yield behavior of the flexural members. The present model accounts for strength degradation of the reinforced concrete members. The hysteretic behavior of the flexural members is shown in Figure 5.1. All parameters unrelated to strength degradation are identical to the parameters of the hysteretic rule presented in Figure 4.6. Strength loss begins at the curvature of maximum strength (d_m). The best estimate of maximum strength curvature ($\hat{d}_m$) is found for each flexural member by UCFyber (ZEvent, 2000). After d_m, the strength is assumed to degrade linearly to the value of $0.3M_y$. The slope of the declining backbone curve is defined by specifying the location of the point of 20% strength decrease from the maximum value ($0.8M_m$). We call this point the "ultimate" curvature: d_u. The best estimate of the ultimate curvature ($\hat{d}_u$) is assumed to be: $\hat{d}_u = 1.65\,\hat{d}_m$.

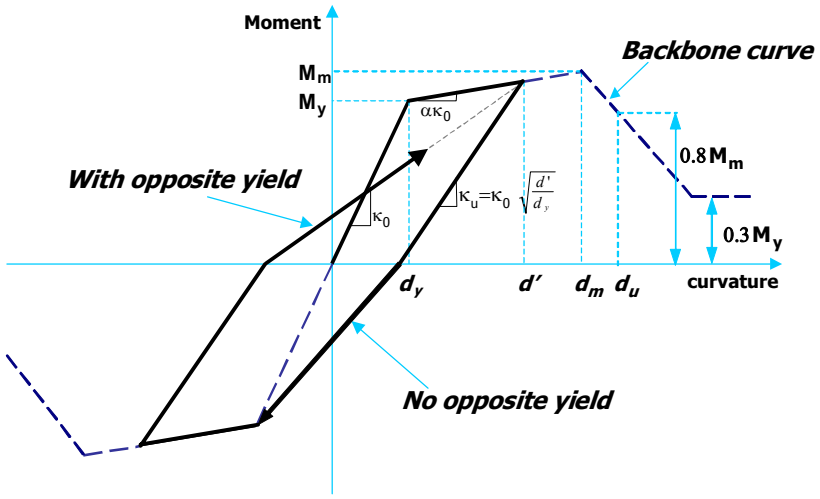

Figure 5.1 Hysteretic rule for flexural members (Q-HYST with strength degradation).

5.2 Damage model

We consider three damage states. The first one ($DS = 1$) is "yield"; we modify its definition to account for the presence of multiple damage states: a flexural member is in the "yield" damage state if the maximum curvature attained during the structural analysis has exceeded the yield curvature (d_y) but has not yet reached maximum strength curvature (d_m). The second damage state ($DS = 2$) is the "maximum strength," which is defined by the following: a flexural member is in "maximum strength" damage state if the maximum curvature has exceeded d_m but has not yet reached the curvature (d_u) corresponding to a strength decrease to 80% of the maximum strength. The third damage state ($DS = 3$) is "ultimate," which is defined as follows: a flexural member is in "ultimate" damage state if the maximum curvature has exceeded d_u. Thus, all three damage states are defined in terms of structural behavior. This approach is not uncommon in the earthquake engineering community (see for example Stone and Taylor, 1993), and also, as we have shown in Section 4.1.4, damage states defined in terms of structural behavior can be related to damage states defined in terms of detectable (visible)

deterioration. It is easy to see that all three damage states are mutually exclusive. Therefore, as shown in Section 3.2, it is sufficient to have three fragility functions in order to obtain the probabilities of all damage states.

In order to find the fragility functions, it is necessary to specify the limit-state functions for the events $DS \geq 1$, $DS \geq 2$, $DS = 3$. From the damage state definitions, we can derive limit-state functions for the i-th flexural member

$$\begin{aligned} DS \geq 1 \;\Leftrightarrow\; & d_y(\underline{X}_i) - d^i_{\max}(\underline{X}, \underline{Q}) < 0 \\ DS \geq 2 \;\Leftrightarrow\; & d_m(\underline{X}_i) - d^i_{\max}(\underline{X}, \underline{Q}) < 0 \\ DS = 3 \;\Leftrightarrow\; & d_u(\underline{X}_i) - d^i_{\max}(\underline{X}, \underline{Q}) < 0 \end{aligned} \tag{5.1}$$

All limit-state functions are written in the form (3.11) where maximum curvature ($d^i_{\max}$) represents a demand parameter (*EDP*) and characteristic curvatures: d_y, d_m, d_u represent the capacities with respect to "yield," "maximum strength" and "ultimate" damage states, respectively. Therefore, neglecting the dependence of maximum curvature on the capacities, the fragility functions can be found according to (3.13)

$$\begin{aligned} F^1(z) &= P(\, d_y(\underline{X}_i) < z \,) \\ F^2(z) &= P(\, d_m(\underline{X}_i) < z \,) \\ F^3(z) &= P(\, d_u(\underline{X}_i) < z \,) \end{aligned} \tag{5.2}$$

Thus, fragility functions for damage states $DS \geq 1$, $DS \geq 2$ and $DS = 3$ are the CDF of d_y, d_m and d_u, respectively. We shall use these fragility functions for damage analysis by Methods 2 and 3, where the probabilities of separate events ($DS = 1$, $DS = 2$ and $DS = 3$) given *EDP* (maximum curvature $d^i_{\max}$) are found according to (3.32).

Since the critical curvatures d_y, d_m and d_u are necessary input data for the structural analysis (they define the backbone curve for the flexural hysteretic rule in Figure 5.1), the capacities in limit-state functions (5.1) are fully defined by the parameters of the structural model, implying that (3.24) holds. Therefore, damage analysis performed by Method 1 is based on the binary (step-function) expression (3.25), meaning that a flexural member is considered to be in $DS = 1$, $DS = 2$ or $DS = 3$ if the maximum curvature attained during the structural analysis falls in the ranges $[d_y, d_m]$, $[d_m, d_u]$ or $[d_u, \infty)$, respectively.

The uncertainty in the critical curvatures (d_y, d_m, d_u) for each flexural member is modeled as follows

$$d_y = \hat{d}_y \, x_1 \qquad (5.3)$$

$$d_m = \hat{d}_m \, x_2$$

$$d_u = \hat{d}_u \, x_3$$

where $\hat{d}_y = \hat{M}_y / K_0$, $\hat{M}_y$ is yield strength, K_0 is the pre-yield stiffness as given in Section 4.1.5; $\hat{d}_m$, $\hat{d}_u$ are the best estimates of "maximum strength" curvature and "ultimate" curvature respectively, which are obtained as described in Section 5.1; x_1, x_2, x_3 are lognormally distributed random variables with unit expected values ($E[x_k] = 1$, $k = 1..3$) and with coefficients of variation equal to 0.08, 0.16, 0.24, respectively. The coefficient of variation (COV) of x_1 is assumed to be 0.08 to provide the same COV of d_y as before (see Section 4.1.5). The COV of $\hat{d}_m$ is twice of the COV of $\hat{d}_y$ and the COV of $\hat{d}_u$ is three times of the COV of $\hat{d}_y$. Such an increase in the variability of d_m and d_u is

assumed to account for the higher uncertainty in post-yield behavior of reinforced concrete members in comparison with pre-yield behavior.

The other significant difference between the uncoupled damage analysis used in Methods 2 and 3 and the coupled damage analysis used in Method 1 is that the former ignores correlation between capacities with respect to different damage states. Fragility functions used in Methods 2 and 3 are marginal CDFs of capacities with respect to the three damage states ("yield," "maximum strength," "ultimate") but the marginal probability distributions do not contain any information about the correlation between different capacities. Therefore, the uncoupled analysis does not take into account correlations between capacities.

Correlations between the capacities can be incorporated into the coupled structural and damage analyses by using correlated random variables x_1, x_2 and x_3, while generating the structural properties by (5.3). In general, one might expect quite strong correlation between some structural properties, such as yield strength and maximum strength. Therefore, we have considered two cases: one with relatively low correlation where the coefficients of correlation between x_1, x_2 and x_3 are all equal to 0.6 and a case of highly correlated capacities where all coefficients of variation between x_1, x_2 and x_3 are equal to 0.9.

5.3 Repair cost

Damage analysis is one step in the seismic performance analysis of real estate. It provides estimates of damage inflicted on the facility but the final goal of performance analysis is estimation of decision variables. Therefore, it is important to compare the results obtained by different damage estimation methods when they are expressed in

terms of the decision variables rather than in terms of the damage measure. This can be done through a relation between damage measure and decision variables.

One decision variable that can be used by decision makers is repair cost. Therefore, we use repair cost as a decision variable for the multiple damage state case study presented in this chapter. The relation between damage states and repair cost is assumed to be as follows

$$\begin{aligned} DS = 1 &\Rightarrow Cost = \$20{,}000 \\ DS = 2 &\Rightarrow Cost = \$30{,}000 \\ DS = 3 &\Rightarrow Cost = \$40{,}000 \end{aligned} \tag{5.4}$$

The uncertainty of repair cost for each damage state is neglected. The expected values of the repair cost of reinforced concrete members are based on the estimates given by Beck et al. (2002). We have obtained repair cost estimates for all four cases under consideration: single and multiple ground motion excitations, with low and high correlation between the capacities. The results are presented in the next section.

5.4 Results

Figures 5.2 – 5.31 presents the results of damage analysis and loss analysis for the sample structure with low (0.6) coefficient of correlation between structural properties of reinforced concrete members (yield curvature, curvature at maximum strength and curvature at 80% of maximum strength). Figures 5.2 – 5.7 compare the expected number of members in the three different damage states for a fixed (LA15) excitation. Methods 2 and 3 provide similar results, slightly underestimating the overall number of damaged assemblies and significantly underestimating the severe damage states: “maximum strength” and “ultimate.” This shows that the uncoupled damage analysis may be non-

conservative with respect to severe damage characterized by the post-yield damage states, "maximum moment" and "ultimate." In reality, the presence of these damage states can lead to very serious consequences for the whole structure, such as partial or total collapse, which is a life safety threat. Even without a collapse, severely damaged members can compromise the structural integrity of the whole facility, leading to a high probability of it being "red-tagged" and shut down for some period of time. Therefore, underestimation of severe damage states may significantly reduce the accuracy of some decision variables, such as down time and life safety, and it may lead to making erroneous decisions with respect to seismic risk. Finding the exact reason for such difference between estimates of severe damage obtained by different damage analysis methods is an important subject of future research.

It is interesting to note that all three methods show a decrease in the total number of damaged members for high excitation levels (S_a > 0.6g). This phenomenon can be explained by the existence of a weak spot in the structure. For the more intense load, this weak spot acts like a fuse, experiencing quick yielding and consecutively more severe damage states. As a result the loads transferred through this damaged segment are reduced, which reduces the load on other structural members.

The uncertainty in the damage estimation is illustrated by Figures 5.8 – 5.13. The variances differ considerably for Method 1 and Methods 2 and 3, however, the absolute values of variance do not reflect the real level of uncertainty because of the significant difference in the expectations. For this purpose it is better to use the coefficients of variation, which for the "yield" damage state (DS = 1) resembles the picture for the single damage state case: Methods 1 and 2 exhibit convergent results while Method 3 greatly

underestimates the uncertainty in the damage prediction. For both of the more severe damage states, all three methods demonstrate very similar coefficients of variations. Results of the repair cost estimation are presented in Figures 5.14 – 5.16. In terms of expected cost, there is no significant difference in cost estimates obtained by different methods for the low intensity excitation (S_a less than 0.7g). For high levels of spectral acceleration, cost estimates obtained by Methods 2 and 3 are lower than Method 1 estimates due to underestimation of the severe damage states.

Figures 5.17 – 5.31 show the results of damage analysis for a set of 40 ground motion records selected for each S_a level. The expected number of members in three different damage states is shown in Figures 5.17 – 5.22. In general, the conclusions drawn from the results obtained for LA15 excitation are also valid for the set of ground motions. Estimates for DS = 1 are close for all three methods, while for DS = 2 and DS = 3, they are significantly underestimated by Methods 2 and 3. Uncertainty in the estimation is presented in Figures 5.23 – 5.28. The absolute values of variance differ significantly for different methods, but the coefficients of variation are quite close for all damage states. Figures 5.29 – 5.31 present results of the repair cost estimation for the set of ground motions. The results show that, for this case, Methods 2 and 3 underestimate the expected repair cost more than in the case of the fixed (LA15) excitation. At the same time, the uncertainty in the repair cost estimate (measured by the variance and coefficient of variation) is very similar for all three methods.

These results confirm the result of the single damage state analysis that Method 3 significantly underestimates the uncertainty in the damage estimates in the case of a single ground motion. It is also found for the case of multiple damage states that Methods

2 and 3 do not adequately estimate the more severe damage states (2 and 3) in terms of expected values. At the same time, the uncertainty estimates, as measured by the coefficients of variation, are quite similar regardless of the method used.

Figures 5.32 – 5.63 present the results of damage analysis for different levels of correlation between structural properties. We consider two cases: the correlation coefficients between yield curvature, curvature at maximum strength and curvature at 80% of maximum strength are 0.6 in the first case (low correlation) and 0.9 in the second case (high correlation). Figures 5.32 – 5.47 deal with the LA15 ground motion. Figures 5.32 – 5.37 demonstrate the effect of correlation on the estimated number of damaged members. Estimates are obtained by Method 1 and Method 2. Method 3 does not require randomization of structural properties and, therefore, is insensitive to correlation changes. Method 1 shows that the expected number of members in DS = 1 (yield) is slightly lower for the case with high correlation. Method 2 does not show any consistent variation in estimates for different correlation levels. Figures 5.38 – 5.43 present the variance of the damage estimates for the two levels of correlation. No consistent difference can be inferred between the high and low correlation cases. Figures 5.44 – 5.47 compare repair cost estimates for the two given correlation levels. Method 1 shows that repair cost tends to be lower for the higher correlation case, implying a more robust structure. In contrast, Method 2 does not indicate a definite difference between two cases, slightly favoring the higher costs for higher correlated curvatures. No significant trends can be observed in the uncertainty (variance) of the cost estimates for both methods.

Figures 5.48 – 5.63 present the results of damage and repair cost estimation for the set of ground motion records. In general, conclusions drawn from the results of the

LA15 ground motion are also valid for the set of ground motions. For Method 1, we can see that the decrease in the average number of members in the "yield" (DS = 1) damage state for high correlation is more pronounced in the case of multiple ground motions. The same can be noted for repair costs. Method 1 shows that first, repair costs for the high correlation case are lower than repair costs for the low correlation case, and second, the difference between these two cases is more significant for set of ground motions than for the LA15 record. These results show that modeling a structure with high correlation of structural properties should predict less damage than a model with low correlation. Note that Method 2 does not reveal any significant influence of the correlation of structural properties on the seismic performance.

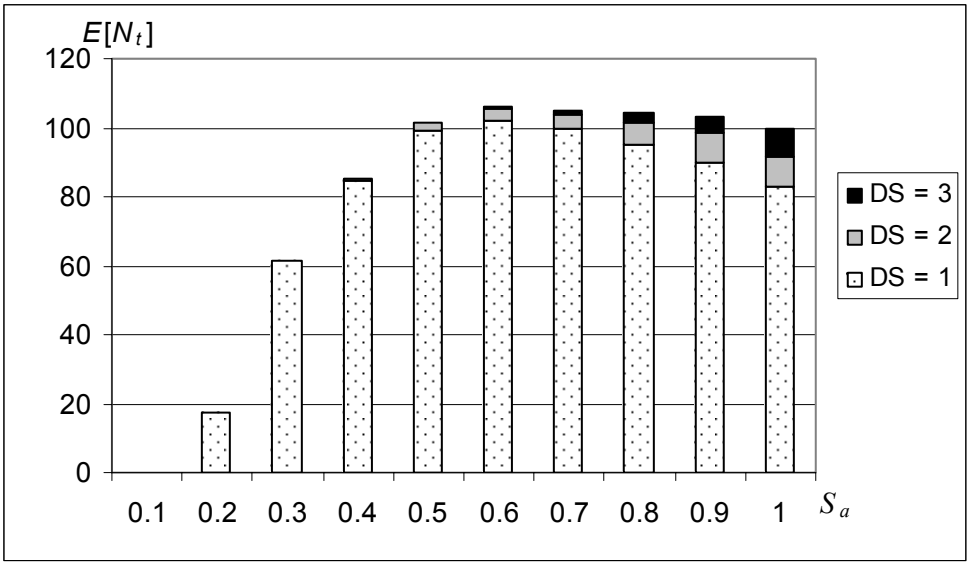

Figure 5.2 Expected number of flexural members in three damage states of interest, obtained by Method 1, correlation of capacities 0.6, ground motion LA15.

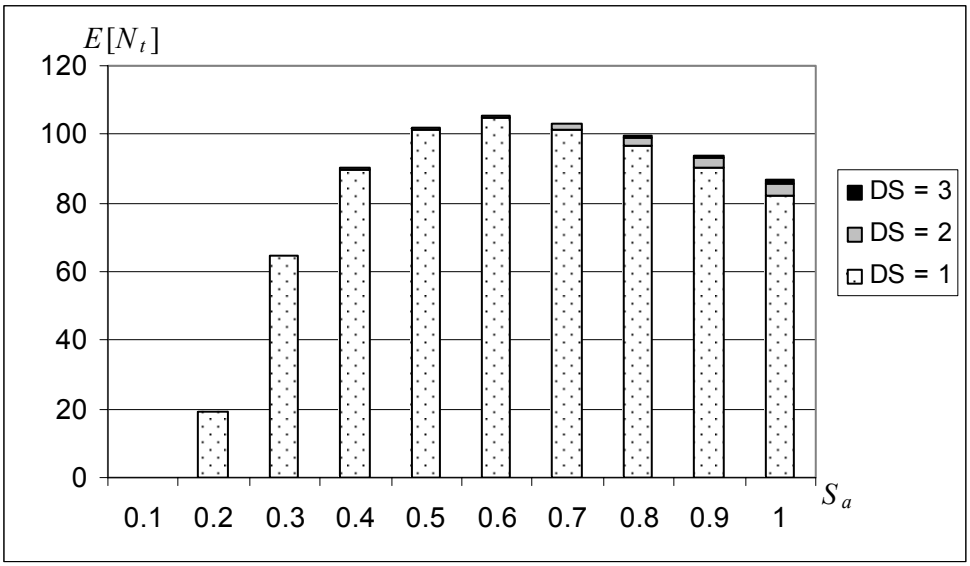

Figure 5.3 Expected number of flexural members in three damage states of interest, obtained by Method 2, correlation of capacities 0.6, ground motion LA15.

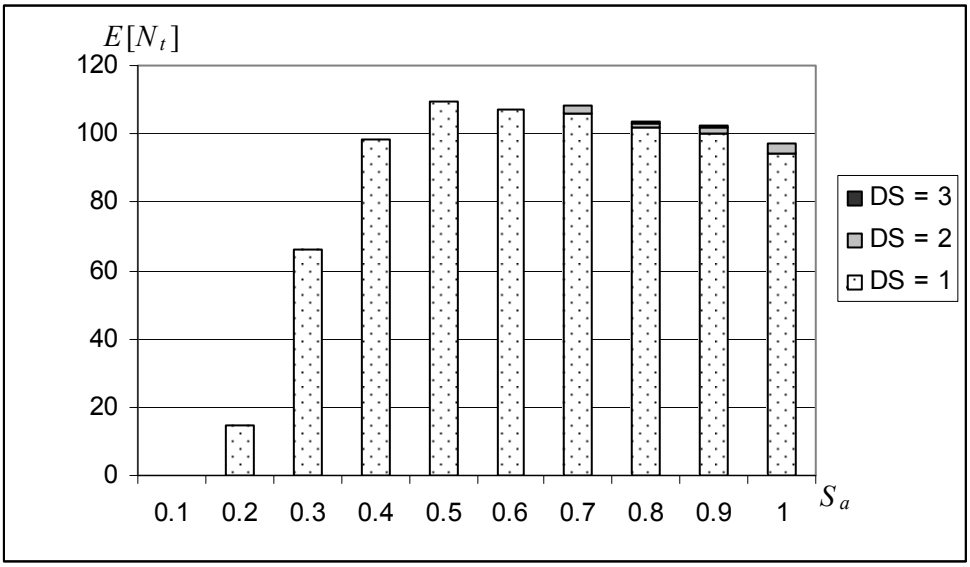

Figure 5.4 Expected number of flexural members in three damage states of interest, obtained by Method 3, correlation of capacities 0.6, ground motion LA15.

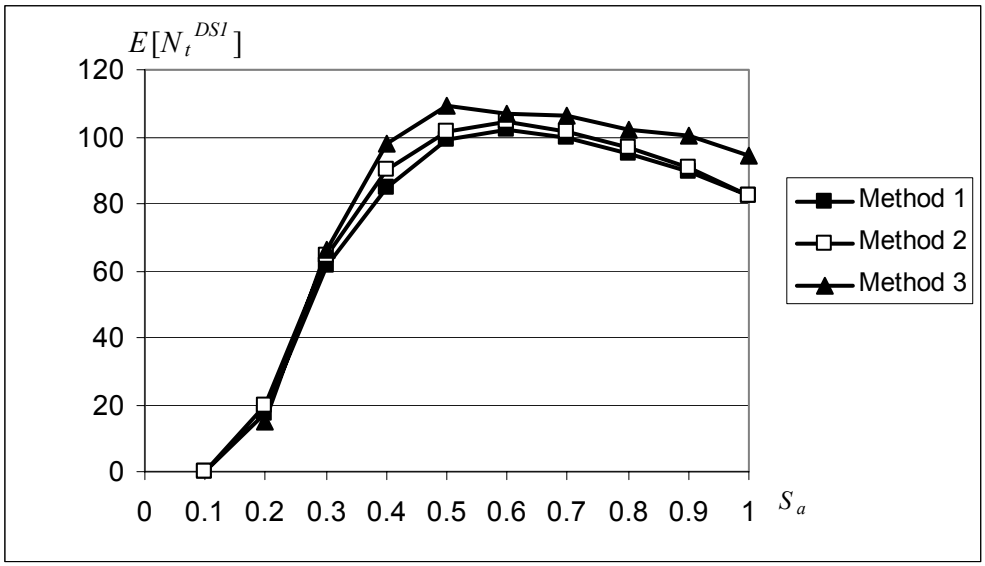

Figure 5.5 Expected number of flexural members in *DS* = 1 for multiple damage states model with correlation of capacities 0.6, ground motion LA15.

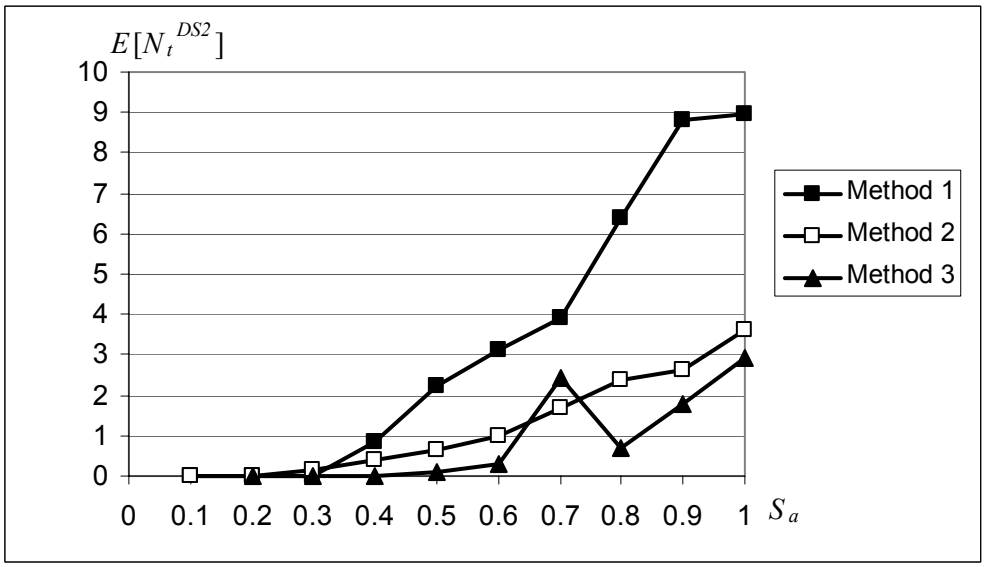

Figure 5.6 Expected number of flexural members in *DS* = 2 for multiple damage states model with correlation of capacities 0.6, ground motion LA15.

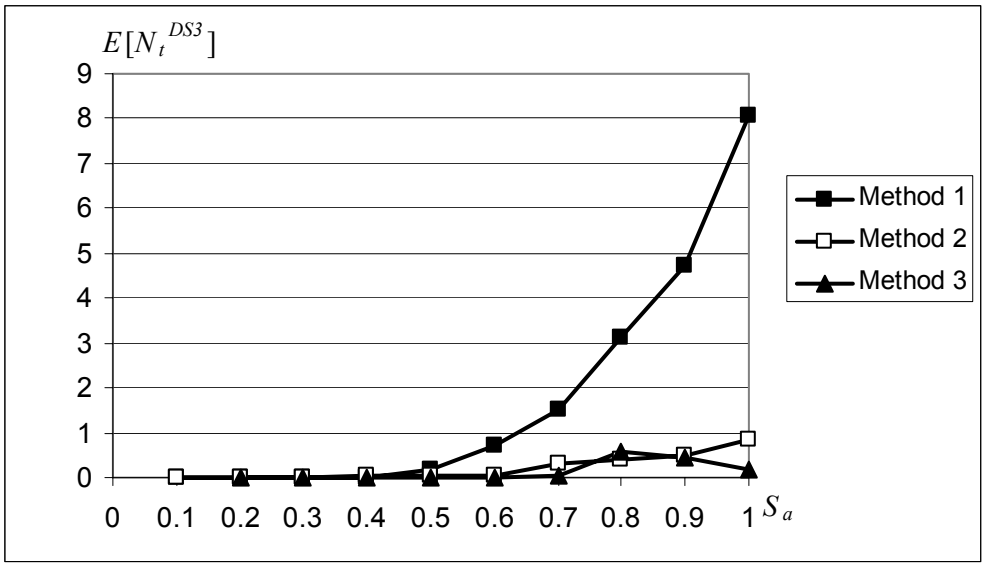

Figure 5.7 Expected number of flexural members in *DS* = 3 for multiple damage states model with correlation of capacities 0.6, ground motion LA15.

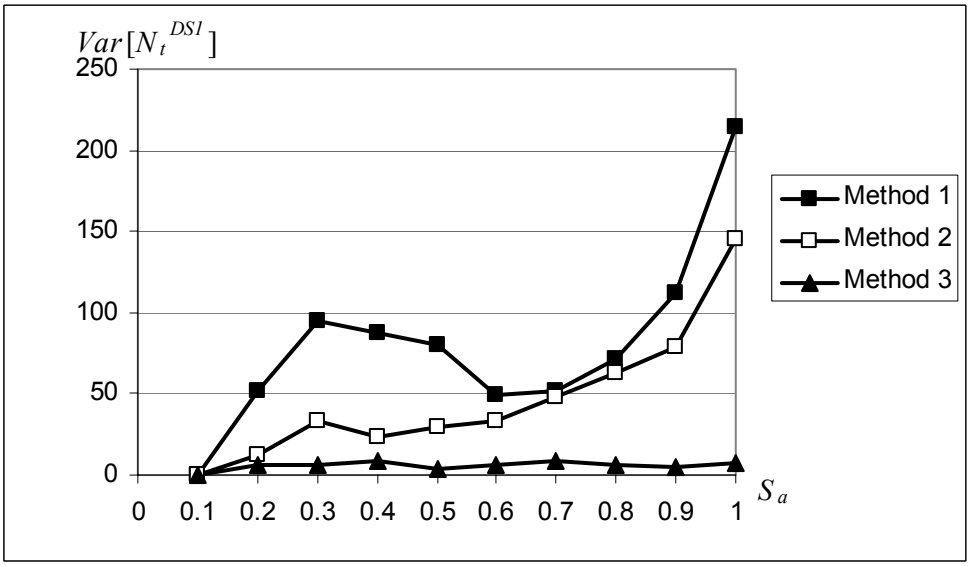

Figure 5.8 Variance of number of flexural members in *DS* = 1 for multiple damage states model with correlation of capacities 0.6, ground motion LA15.

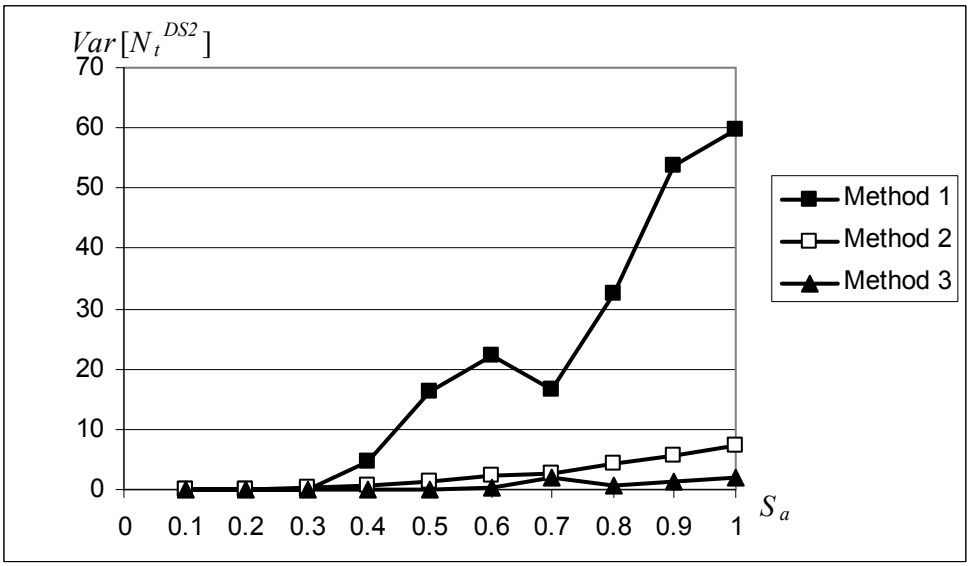

Figure 5.9 Variance of number of flexural members in *DS* = 2 for multiple damage states model with correlation of capacities 0.6, ground motion LA15.

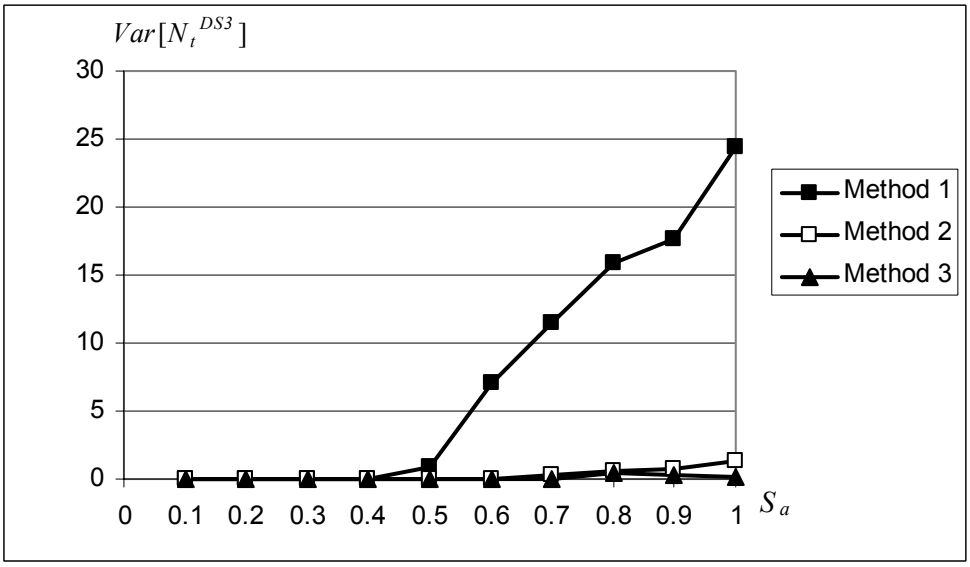

Figure 5.10 Variance of number of flexural members in *DS* = 3 for multiple damage states model with correlation of capacities 0.6, ground motion LA15.

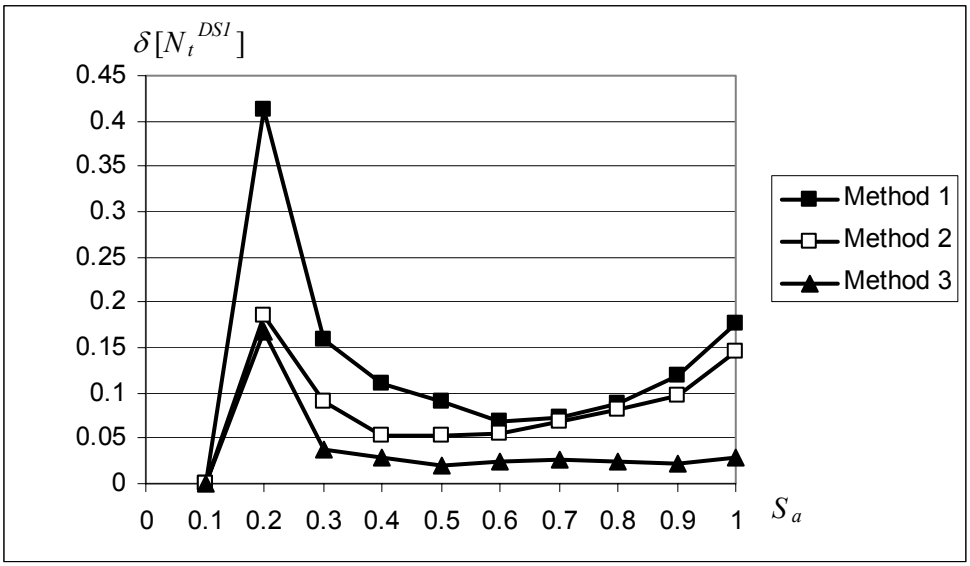

Figure 5.11 Coefficient of variation of number of flexural members in *DS* = 1 for multiple damage states model with correlation of capacities 0.6, ground motion LA15.

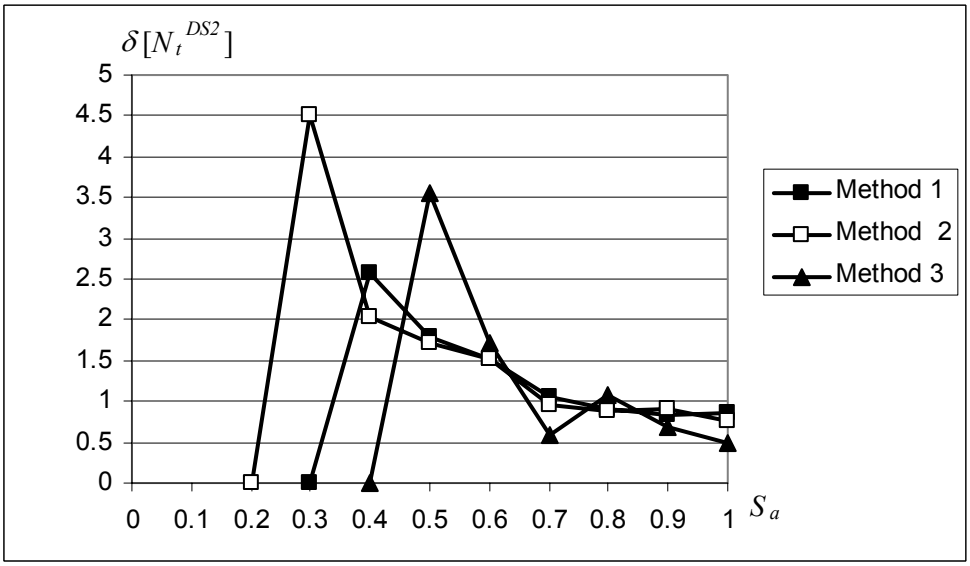

Figure 5.12 Coefficient of variation of number of flexural members in *DS* = 2 for multiple damage states model with correlation of capacities 0.6, ground motion LA15.

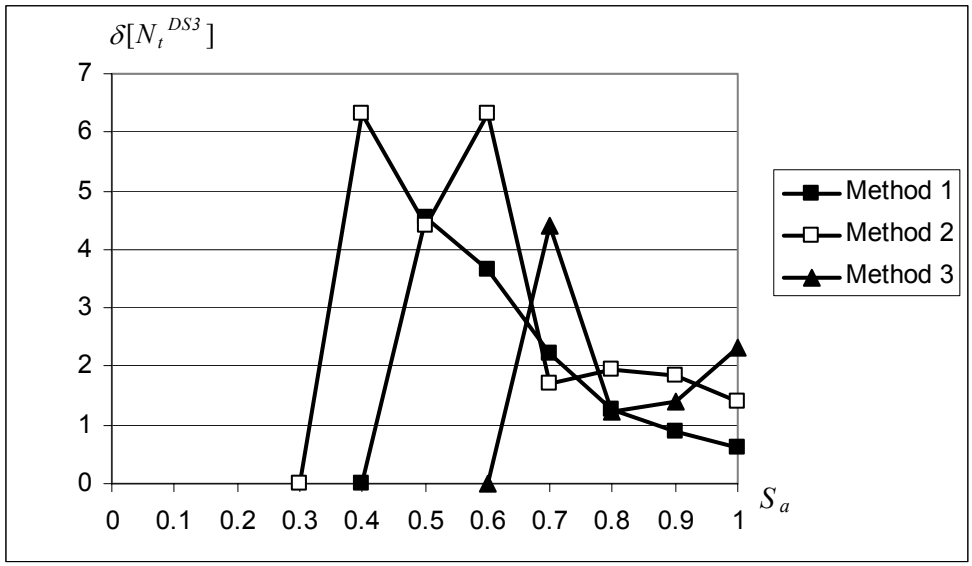

Figure 5.13 Coefficient of variation of number of flexural members in *DS* = 3 for multiple damage states model with correlation of capacities 0.6, ground motion LA15.

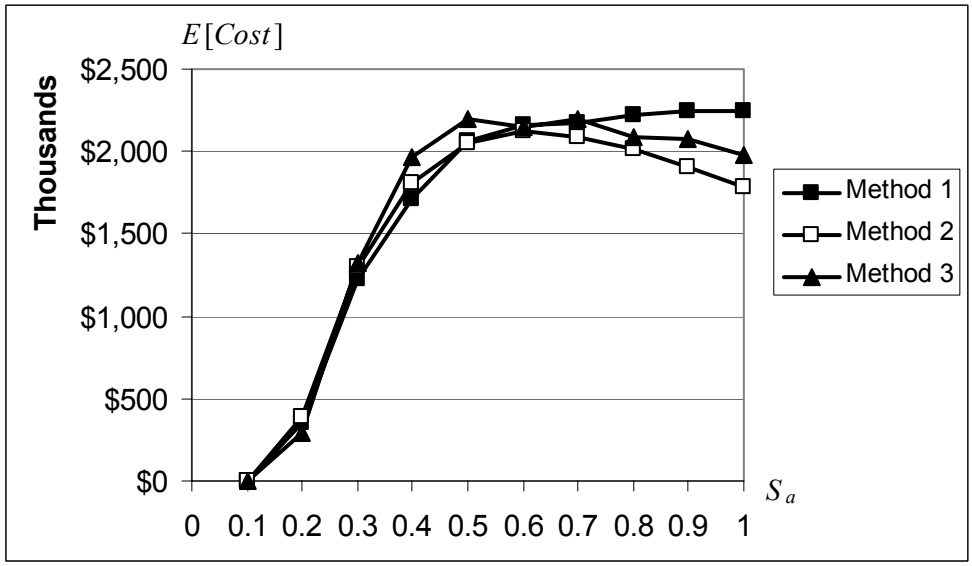

Figure 5.14 Expected repair cost estimate for multiple damage states model with correlation of capacities 0.6, ground motion LA15.

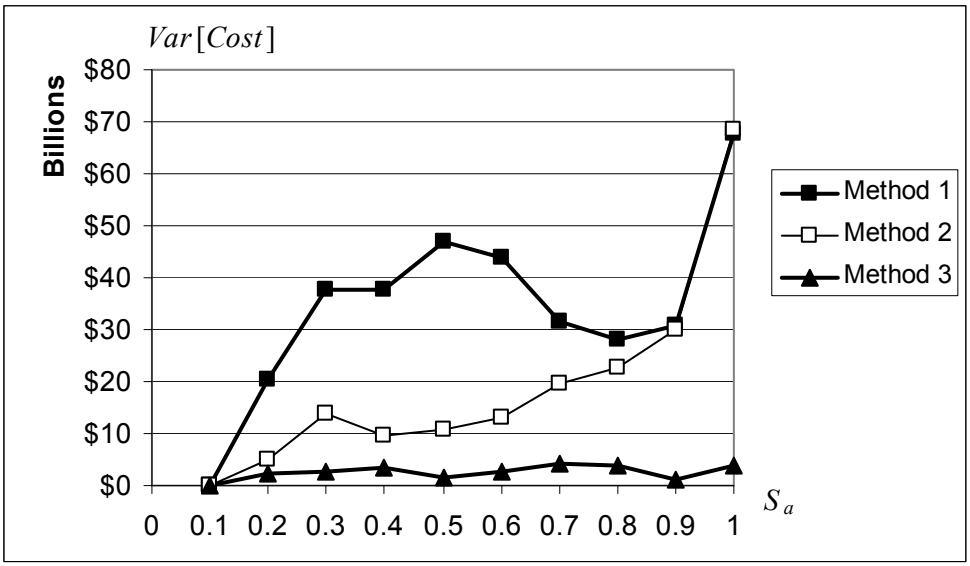

Figure 5.15 Variance of repair cost estimate for multiple damage states model with correlation of capacities 0.6, ground motion LA15.

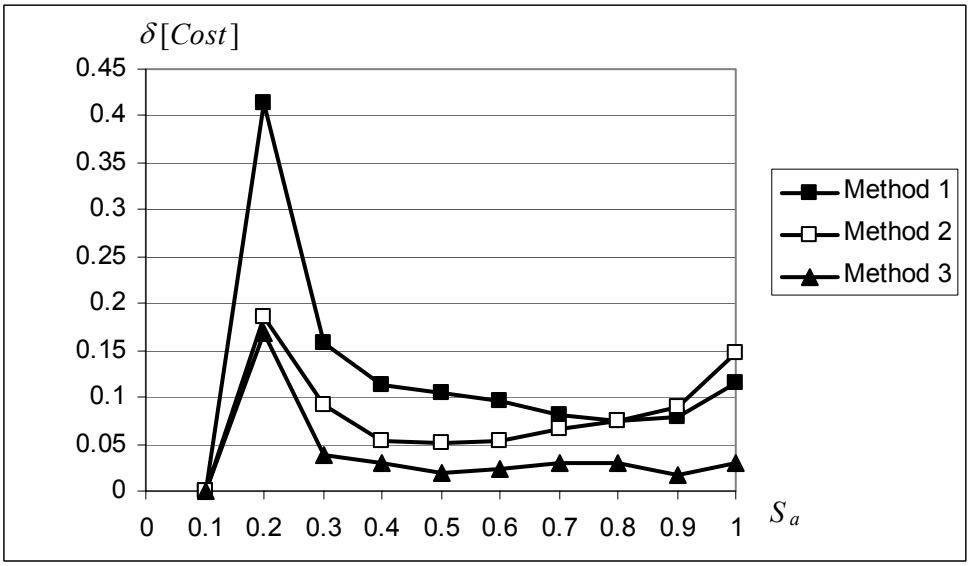

Figure 5.16 Coefficient of variation of repair cost estimate for multiple damage states model with correlation of capacities 0.6, ground motion LA15.

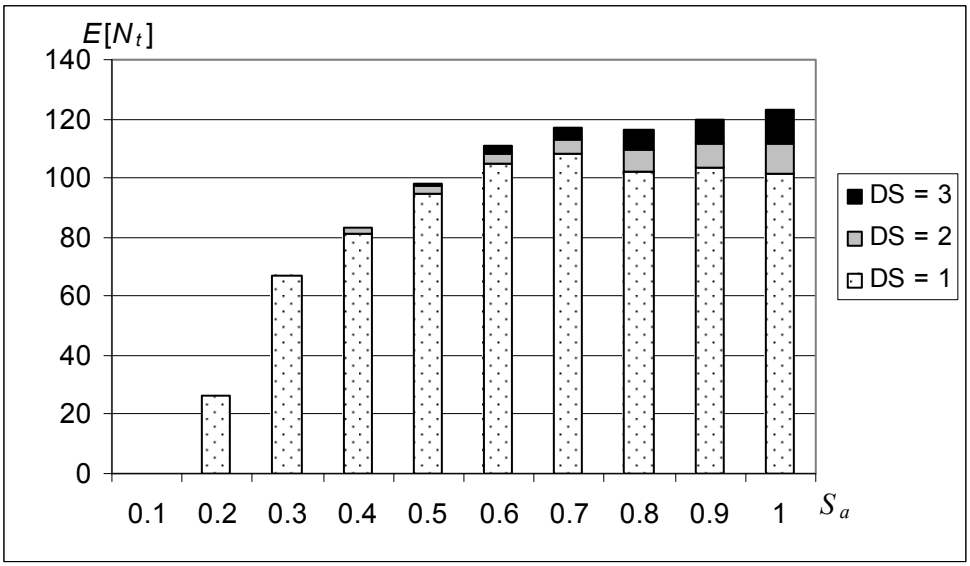

Figure 5.17 Expected number of flexural members in three damage states of interest, obtained by Method 1, correlation of capacities 0.6, set of ground motion records.

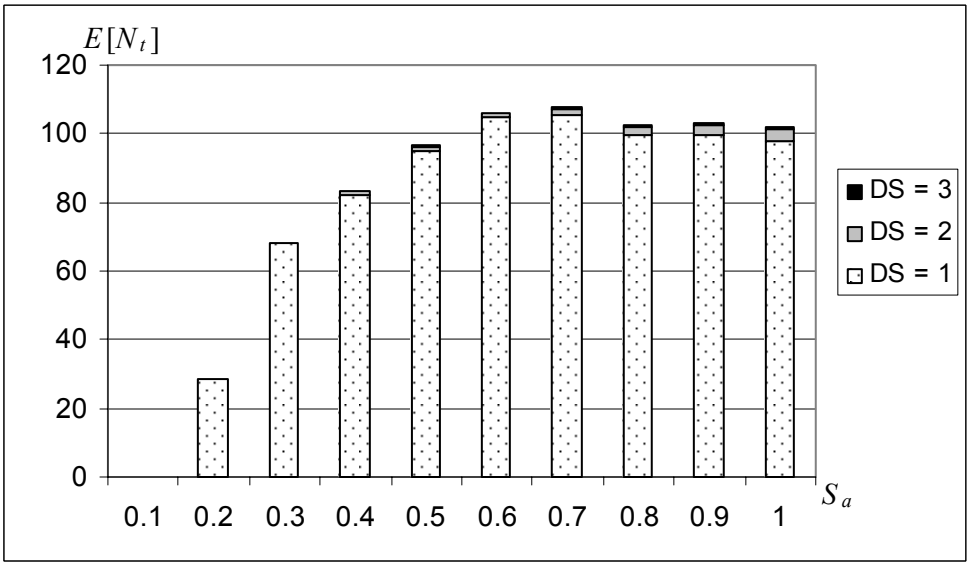

Figure 5.18 Expected number of flexural members in three damage states of interest, obtained by Method 2, correlation of capacities 0.6, set of ground motion records.

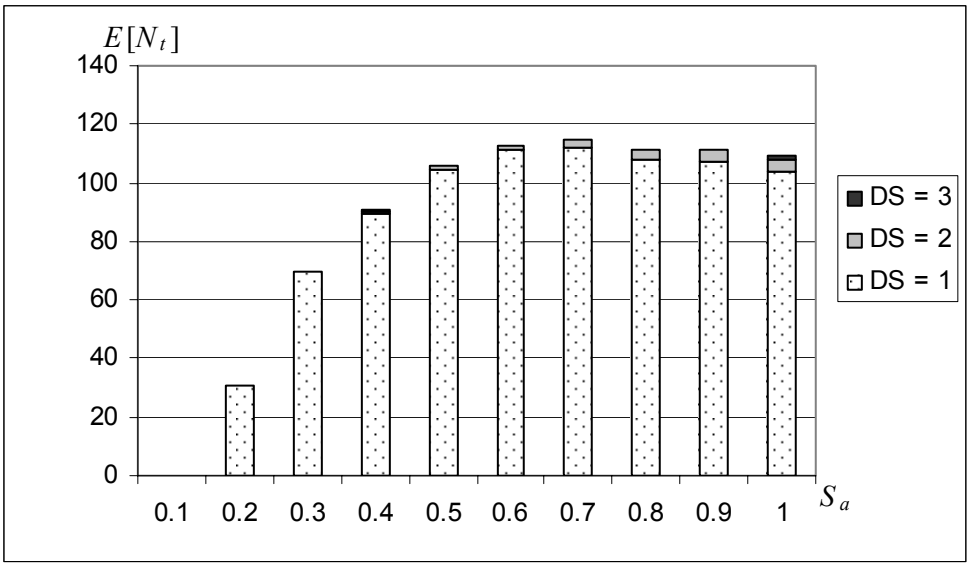

Figure 5.19 Expected number of flexural members in three damage states of interest, obtained by Method 3, correlation of capacities 0.6, set of ground motion records.

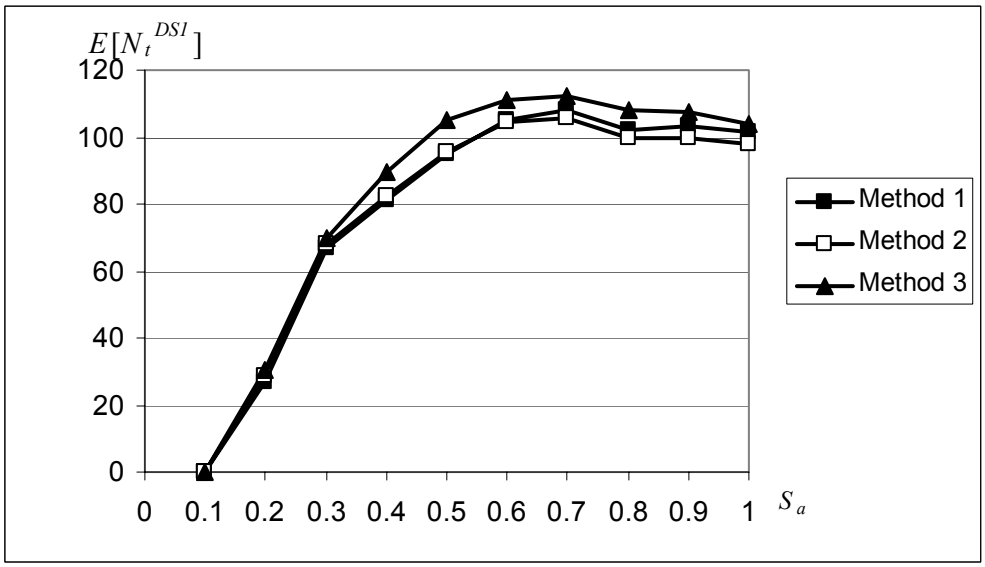

Figure 5.20 Expected number of flexural members in *DS* = 1 for multiple damage states model with correlation of capacities 0.6, set of ground motion records.

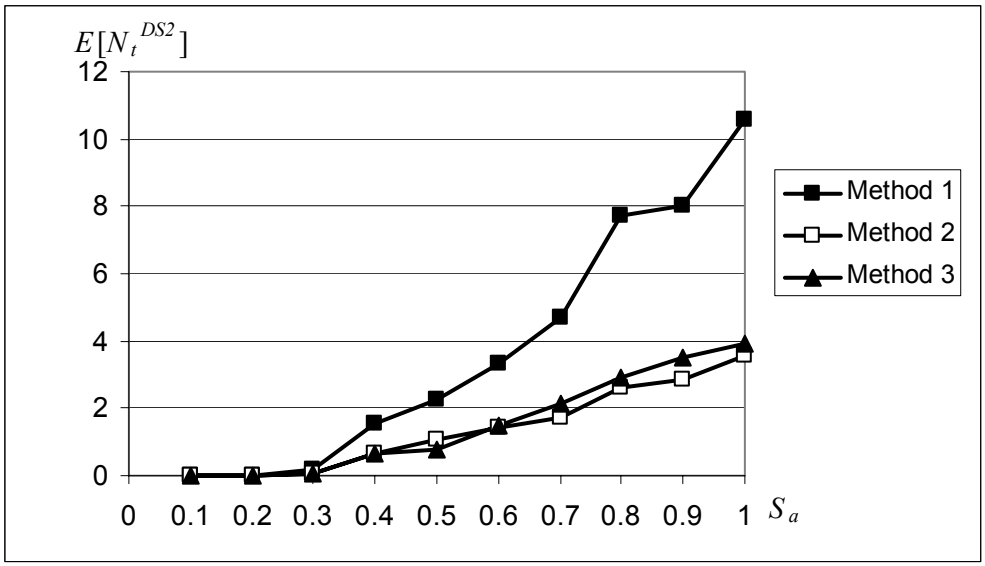

Figure 5.21 Expected number of flexural members in *DS* = 2 for multiple damage states model with correlation of capacities 0.6, set of ground motion records.

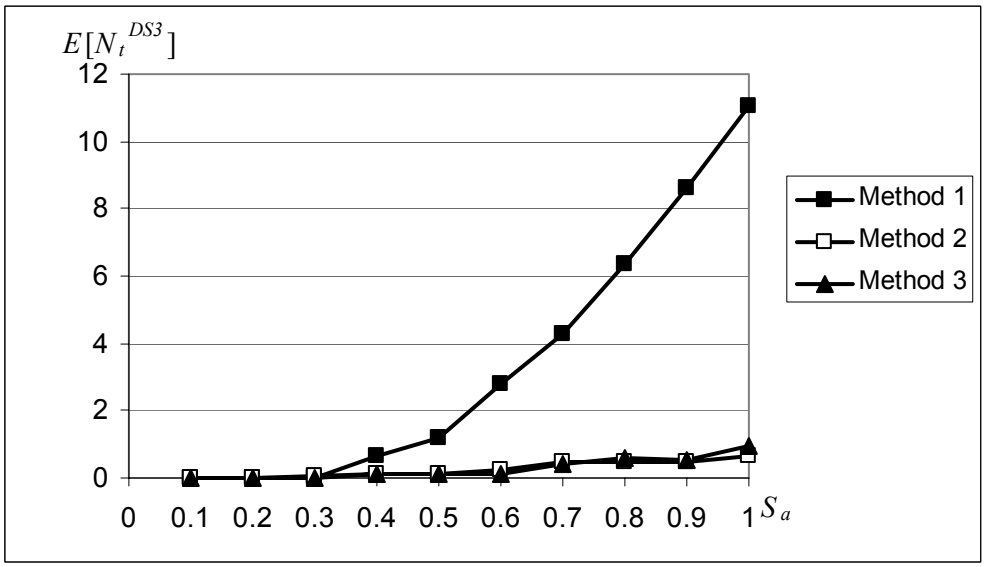

Figure 5.22 Expected number of flexural members in *DS* = 3 for multiple damage states model with correlation of capacities 0.6, set of ground motion records.

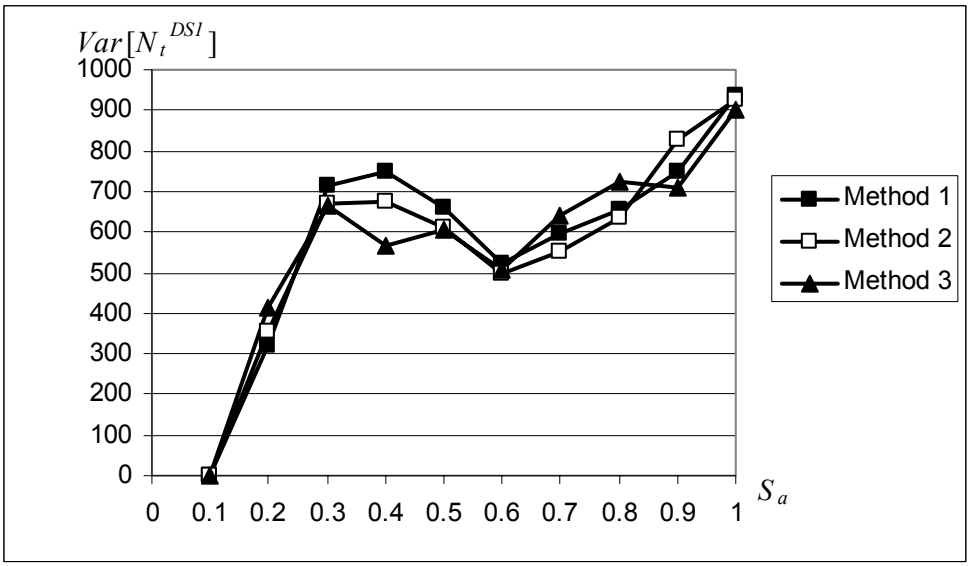

Figure 5.23 Variance of number of flexural members in *DS* = 1 for multiple damage states model with correlation of capacities 0.6, set of ground motion records.

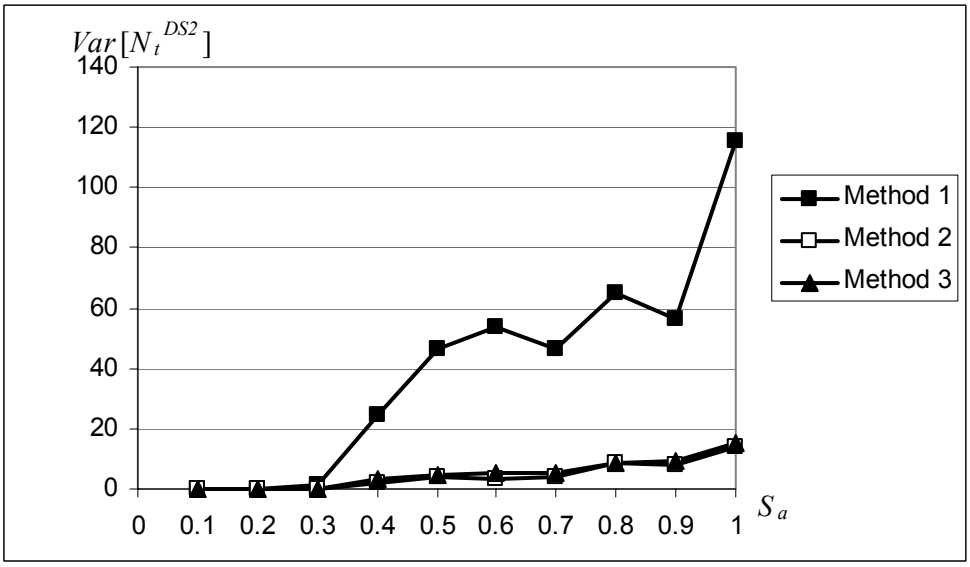

Figure 5.24 Variance of number of flexural members in *DS* = 2 for multiple damage states model with correlation of capacities 0.6, set of ground motion records.

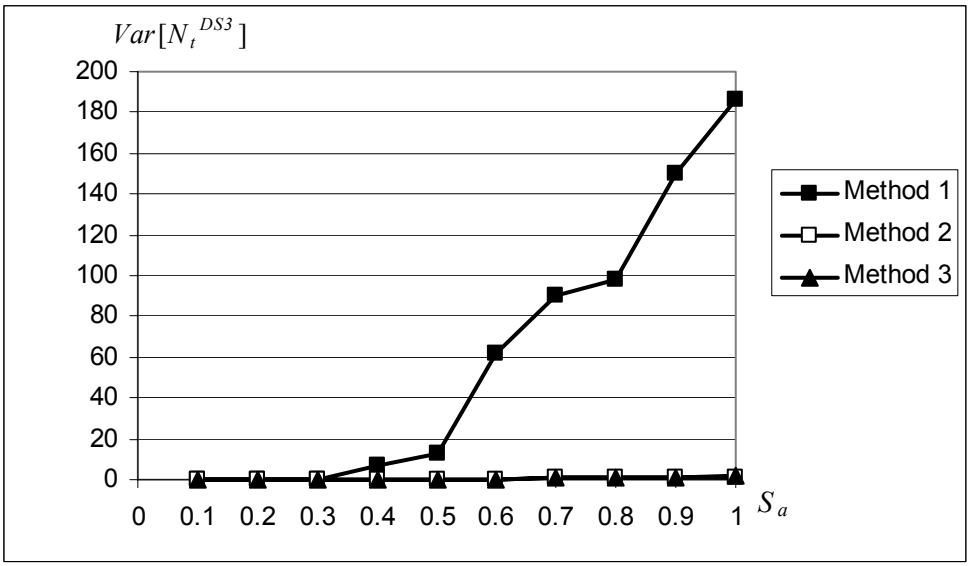

Figure 5.25 Variance of number of flexural members in *DS* = 3 for multiple damage states model with correlation of capacities 0.6, set of ground motion records.

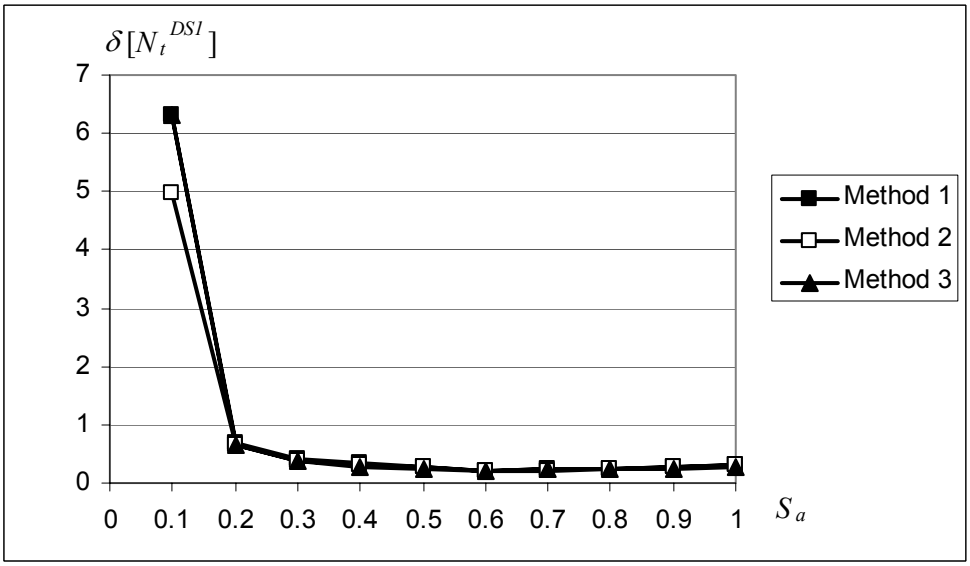

Figure 5.26 Coefficient of variation of number of flexural members in *DS* = 1 for multiple damage states model with correlation of capacities 0.6, set of ground motion records.

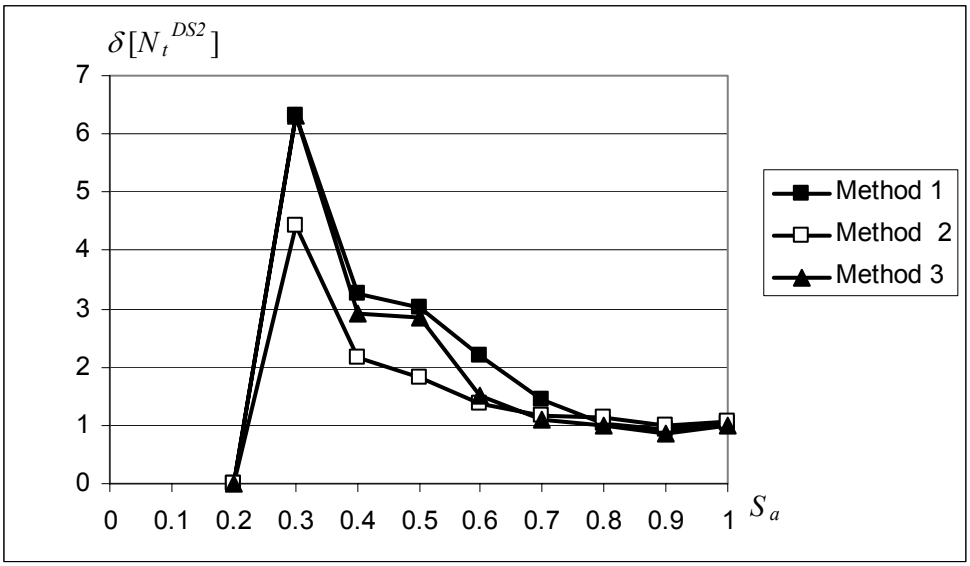

Figure 5.27 Coefficient of variation of number of flexural members in *DS* = 2 for multiple damage states model with correlation of capacities 0.6, set of ground motion records.

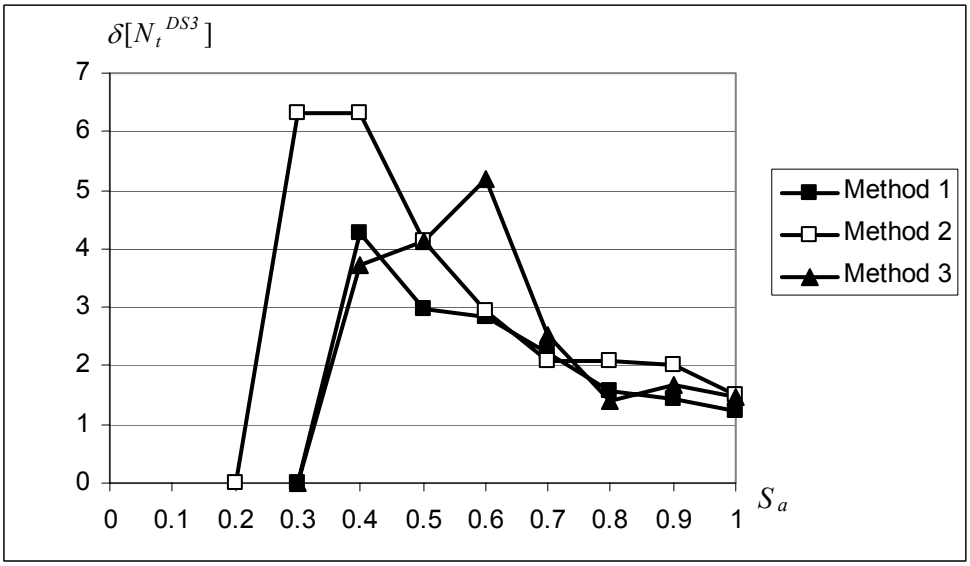

Figure 5.28 Coefficient of variation of number of flexural members in *DS* = 3 for multiple damage states model with correlation of capacities 0.6, set of ground motion records.

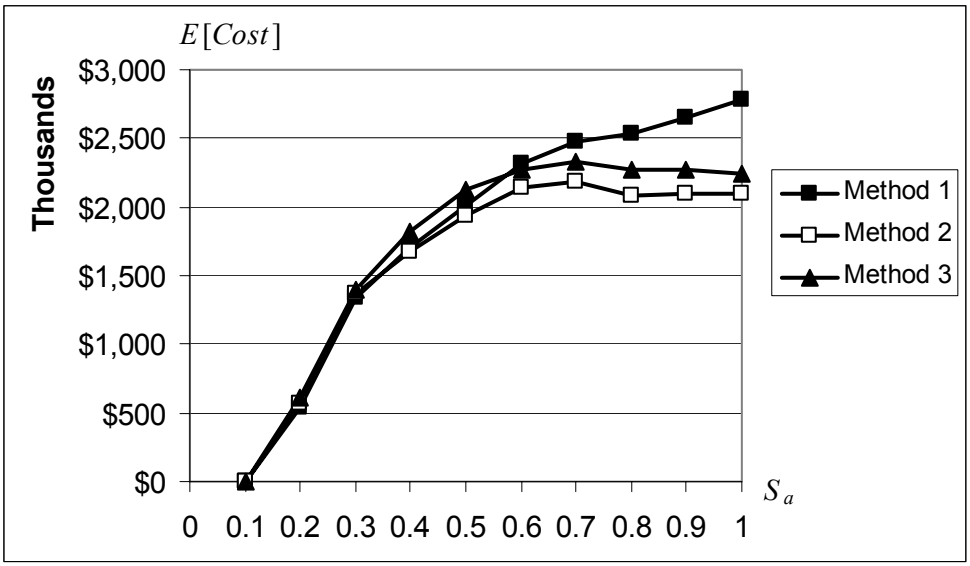

Figure 5.29 Expected repair cost estimate for multiple damage states model with correlation of capacities 0.6, set of ground motion records.

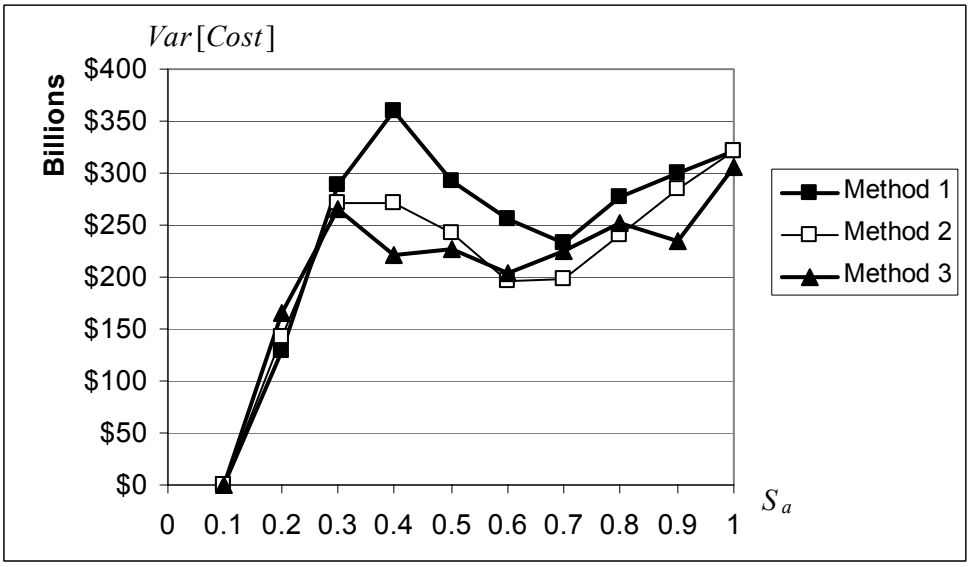

Figure 5.30 Variance of repair cost estimate for multiple damage states model with correlation of capacities 0.6, set of ground motion records.

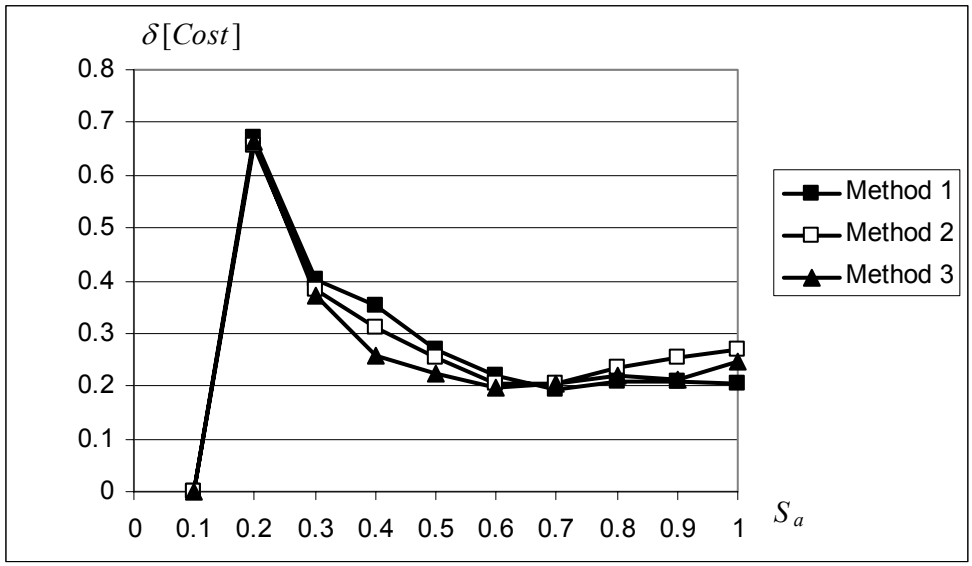

Figure 5.31 Coefficient of variation of repair cost estimate for multiple damage states model with correlation of capacities 0.6, set of ground motion records.

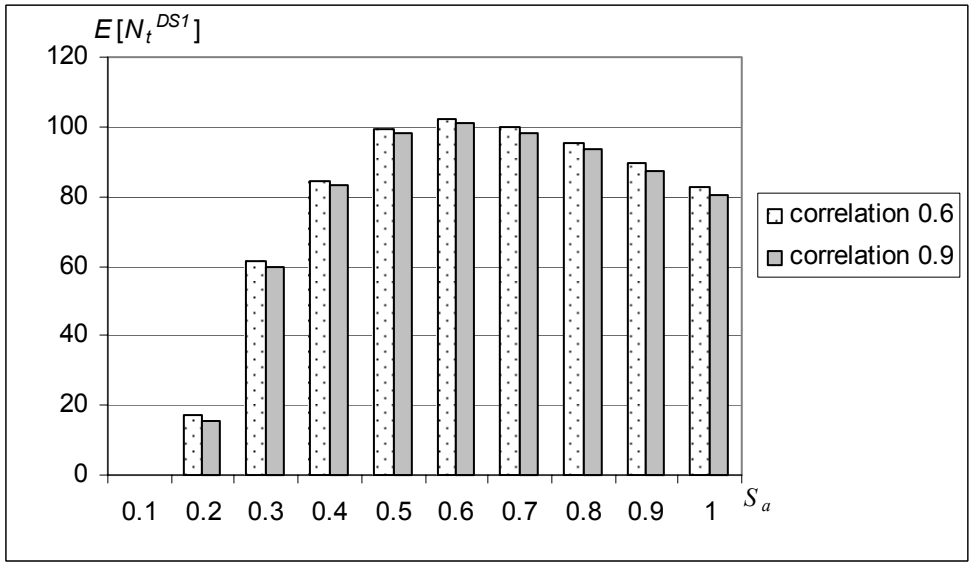

Figure 5.32 Expected number of flexural members in DS = 1 obtained by Method 1 for low (0.6) and high (0.9) coefficient of correlation of member capacities, ground motion LA15.

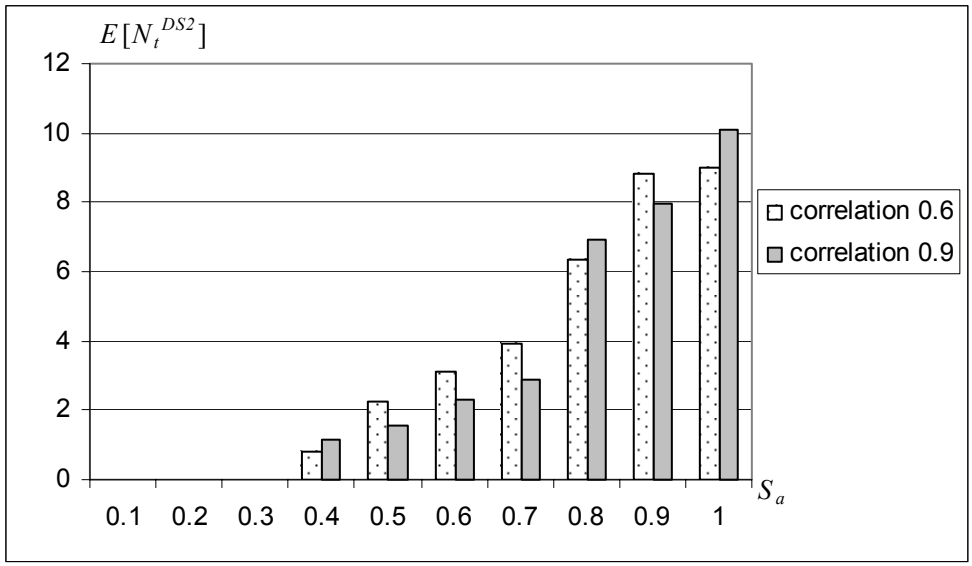

Figure 5.33 Expected number of flexural members in DS = 2 obtained by Method 1 for low (0.6) and high (0.9) coefficient of correlation of member capacities, ground motion LA15.

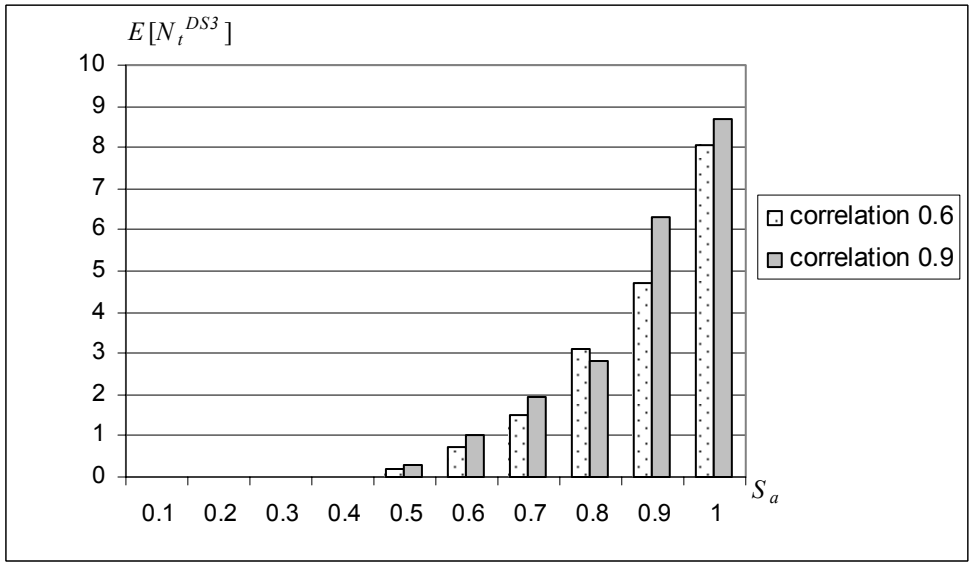

Figure 5.34 Expected number of flexural members in DS = 3 obtained by Method 1 for low (0.6) and high (0.9) coefficient of correlation of member capacities, ground motion LA15.

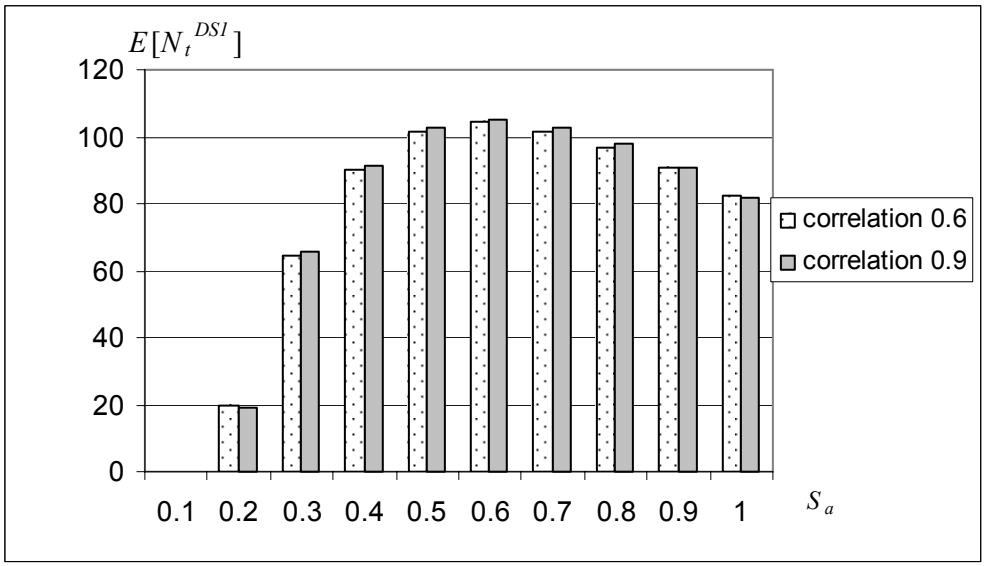

Figure 5.35 Expected number of flexural members in DS = 1 obtained by Method 2 for low (0.6) and high (0.9) coefficient of correlation of member capacities, ground motion LA15.

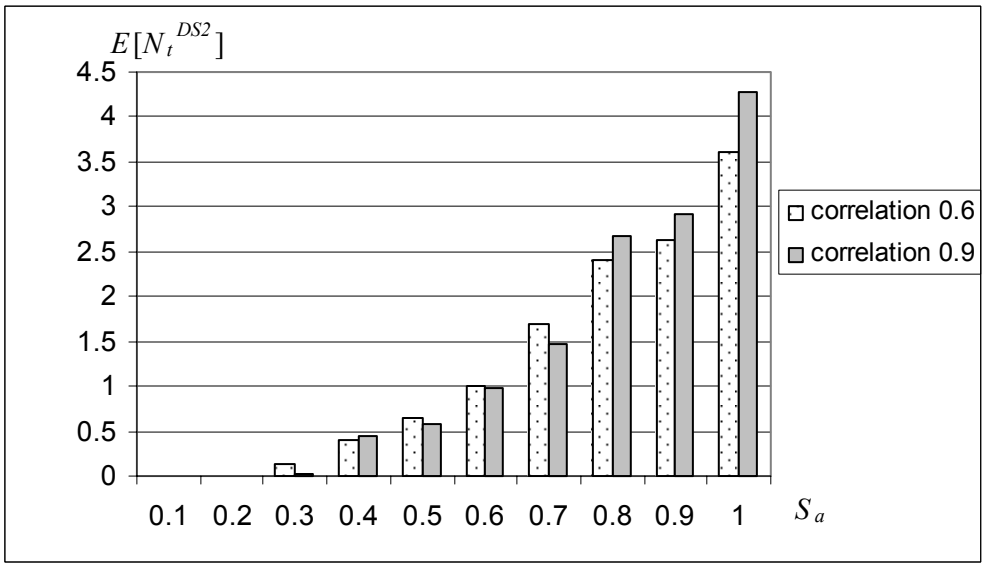

Figure 5.36 Expected number of flexural members in DS = 2 obtained by Method 2 for low (0.6) and high (0.9) coefficient of correlation of member capacities, ground motion LA15.

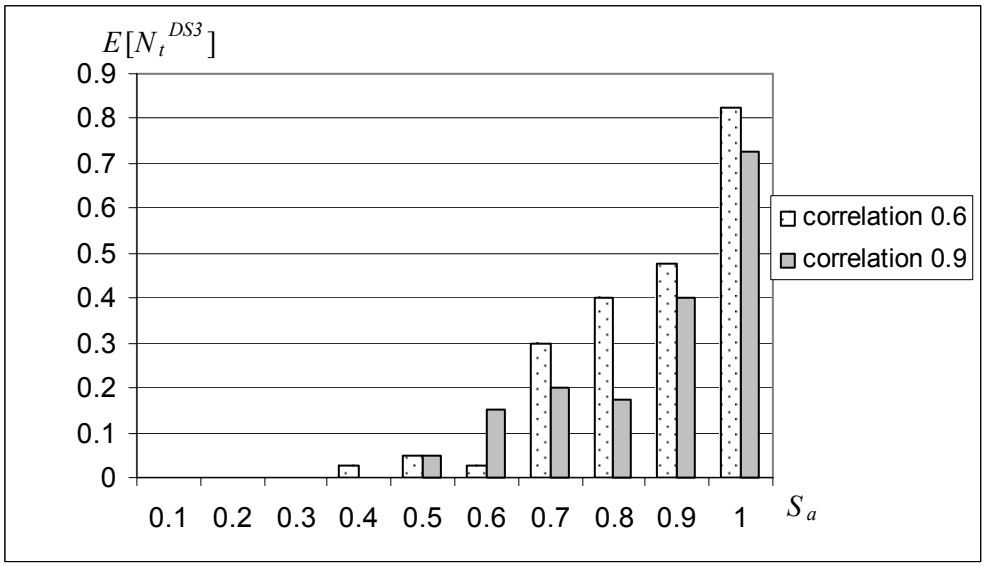

Figure 5.37 Expected number of flexural members in DS = 3 obtained by Method 2 for low (0.6) and high (0.9) coefficient of correlation of member capacities, ground motion LA15.

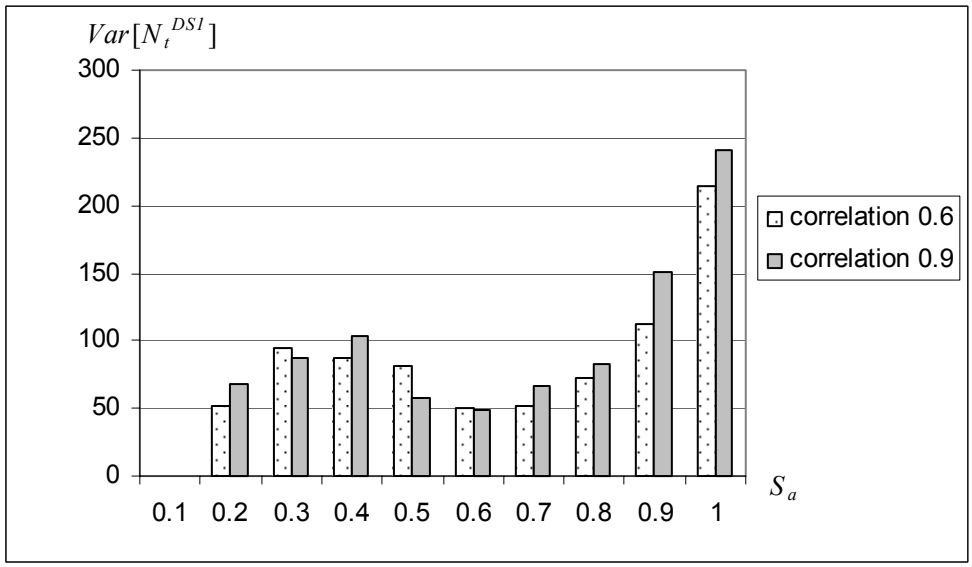

Figure 5.38 Variance of number of flexural members in DS = 1 obtained by Method 1 for low (0.6) and high (0.9) coefficient of correlation of member capacities, ground motion LA15.

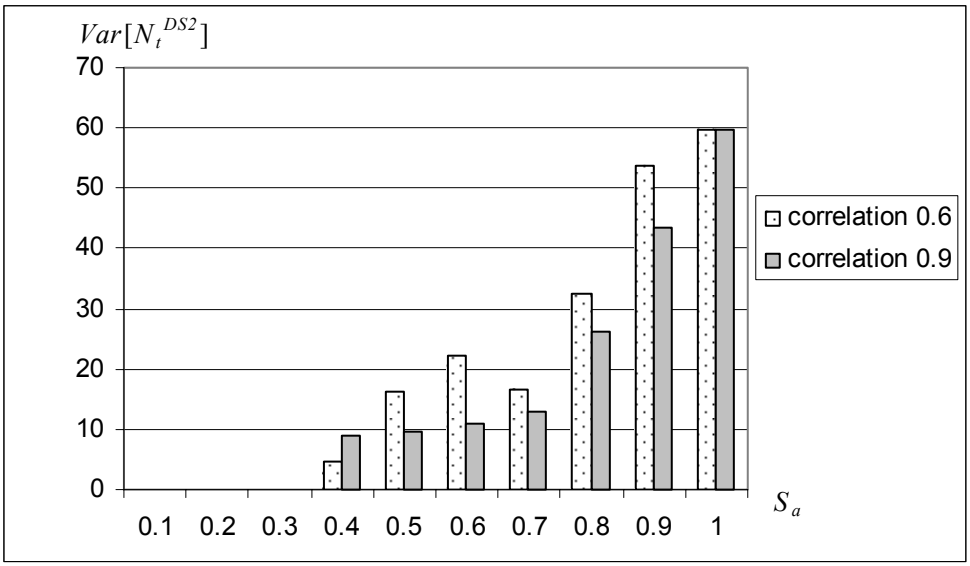

Figure 5.39 Variance of number of flexural members in DS = 2 obtained by Method 1 for low (0.6) and high (0.9) coefficient of correlation of member capacities, ground motion LA15.

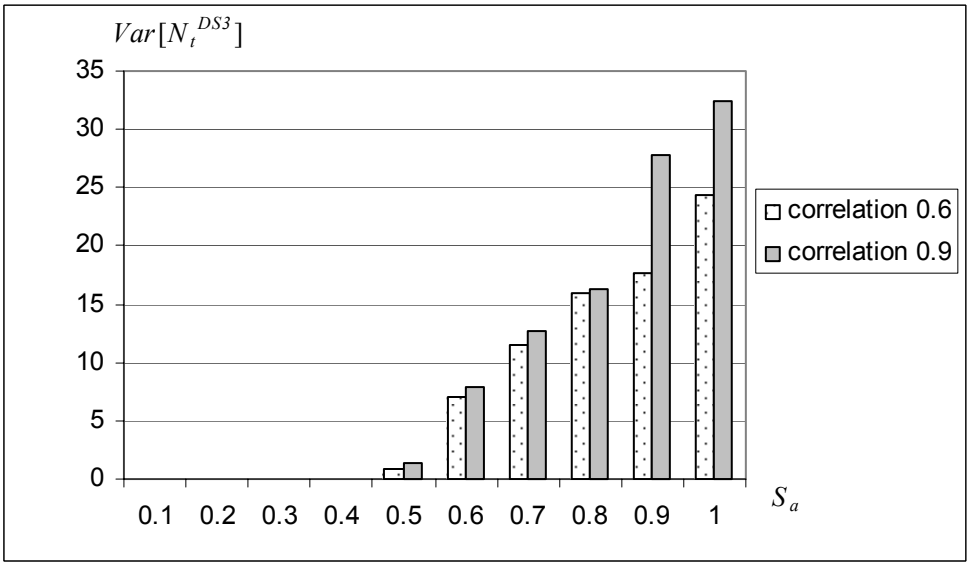

Figure 5.40 Variance of number of flexural members in DS = 3 obtained by Method 1 for low (0.6) and high (0.9) coefficient of correlation of member capacities, ground motion LA15.

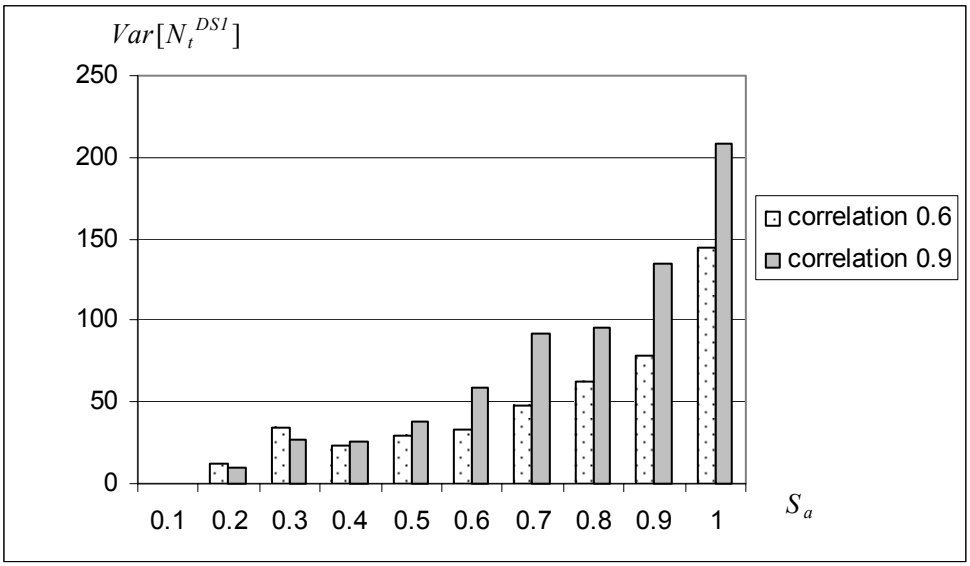

Figure 5.41 Variance of number of flexural members in DS = 1 obtained by Method 2 for low (0.6) and high (0.9) coefficient of correlation of member capacities, ground motion LA15.

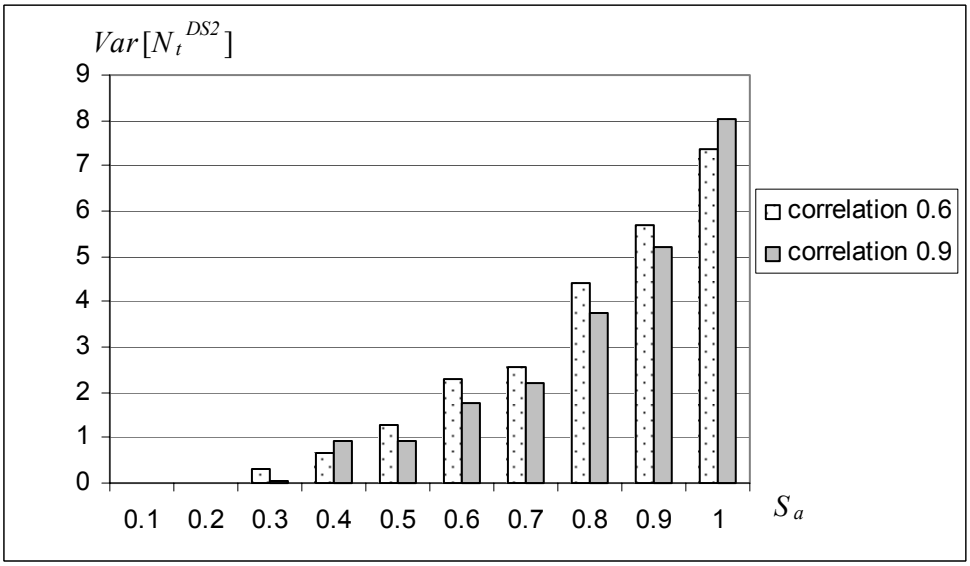

Figure 5.42 Variance of number of flexural members in DS = 2 obtained by Method 2 for low (0.6) and high (0.9) coefficient of correlation of member capacities, ground motion LA15.

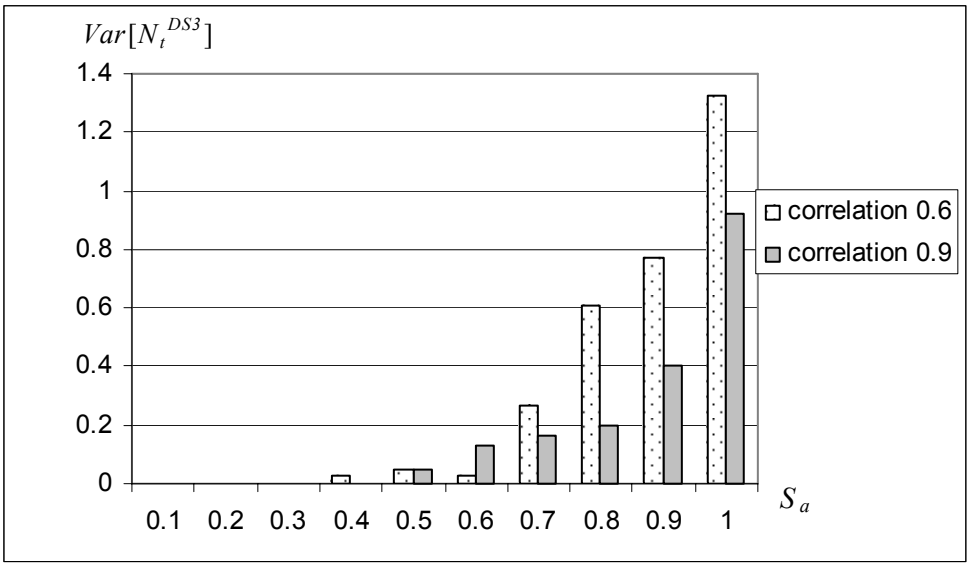

Figure 5.43 Variance of number of flexural members in DS = 3 obtained by Method 2 for low (0.6) and high (0.9) coefficient of correlation of member capacities, ground motion LA15.

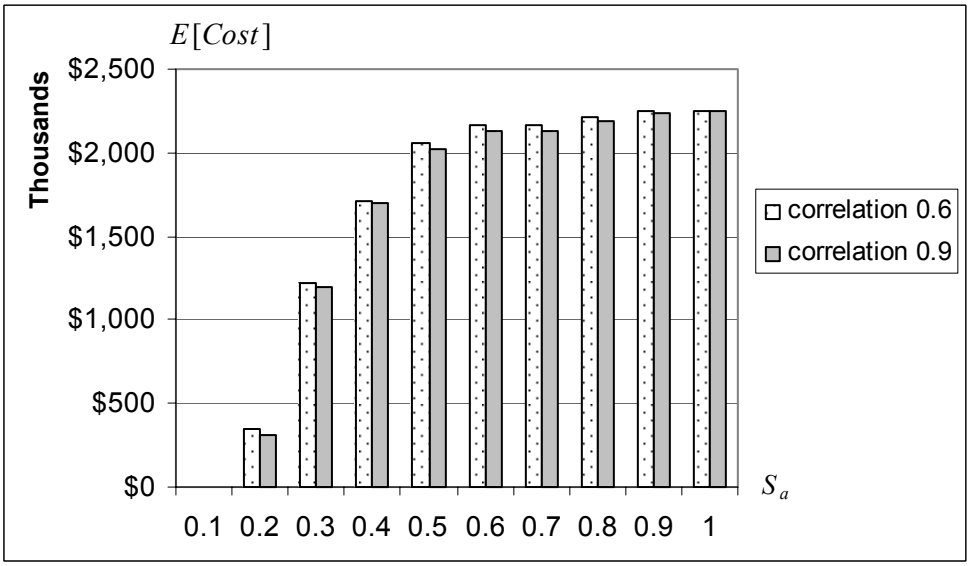

Figure 5.44 Expected repair cost obtained by Method 1 for low (0.6) and high (0.9) coefficient of correlation of member capacities, ground motion LA15.

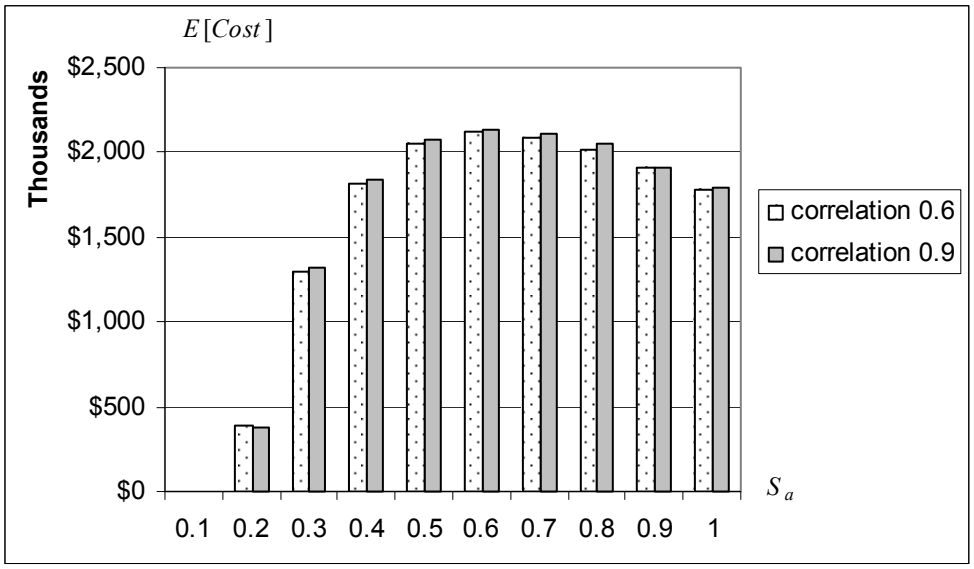

Figure 5.45 Expected repair cost obtained by Method 2 for low (0.6) and high (0.9) coefficient of correlation of member capacities, ground motion LA15.

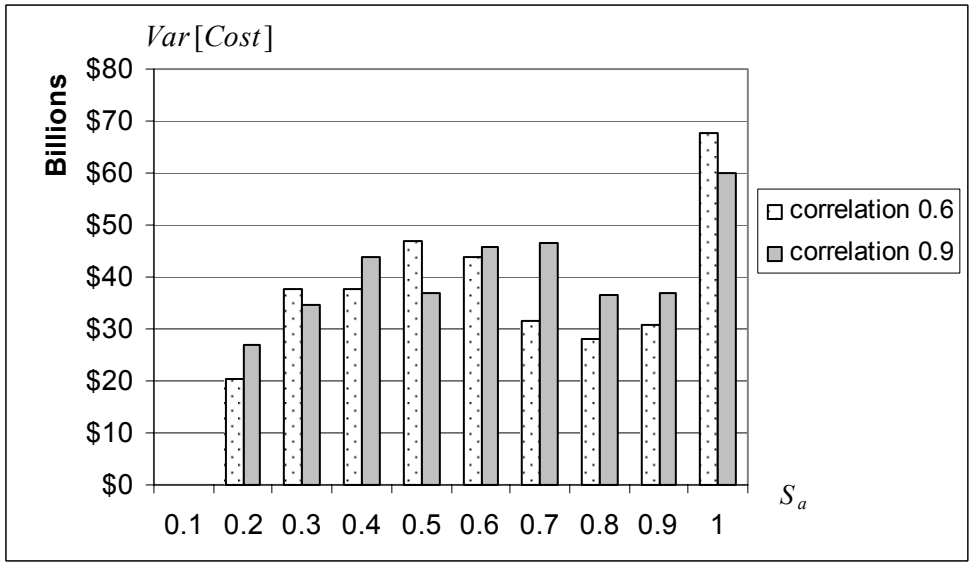

Figure 5.46 Variance of repair cost obtained by Method 1 for low (0.6) and high (0.9) coefficient of correlation of member capacities, ground motion LA15.

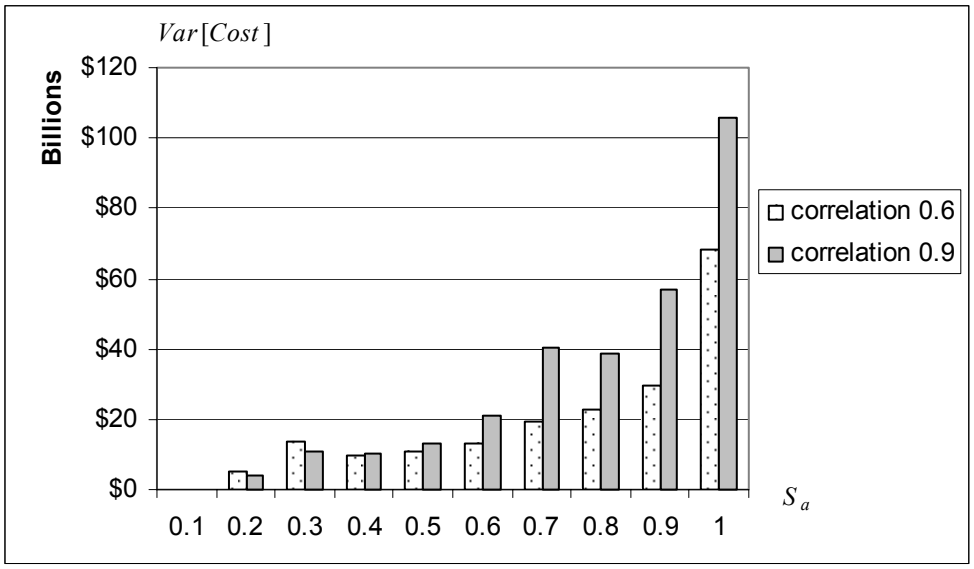

Figure 5.47 Variance of repair cost obtained by Method 2 for low (0.6) and high (0.9) coefficient of correlation of member capacities, ground motion LA15.

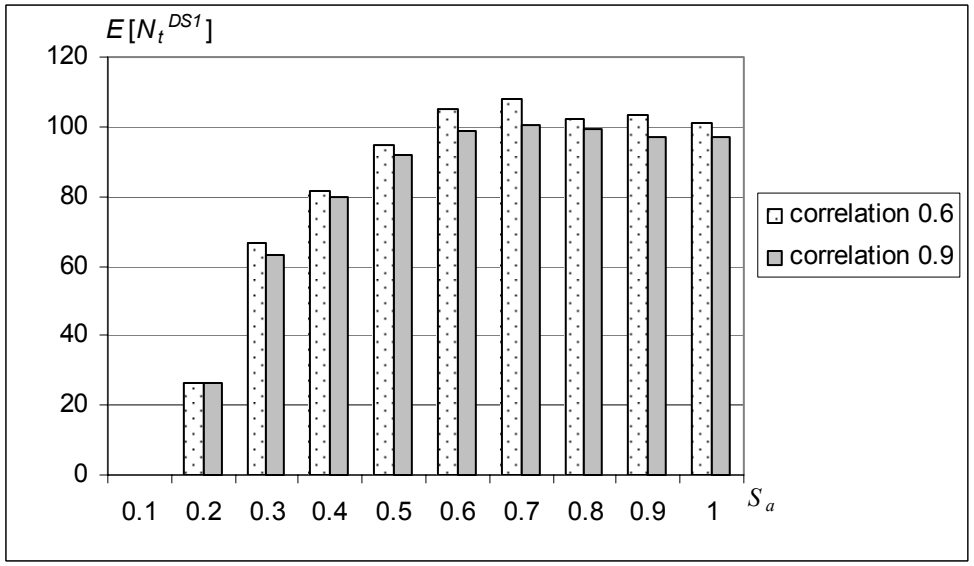

Figure 5.48 Expected number of flexural members in DS = 1 obtained by Method 1 for low (0.6) and high (0.9) coefficient of correlation of member capacities, set of ground motion records.

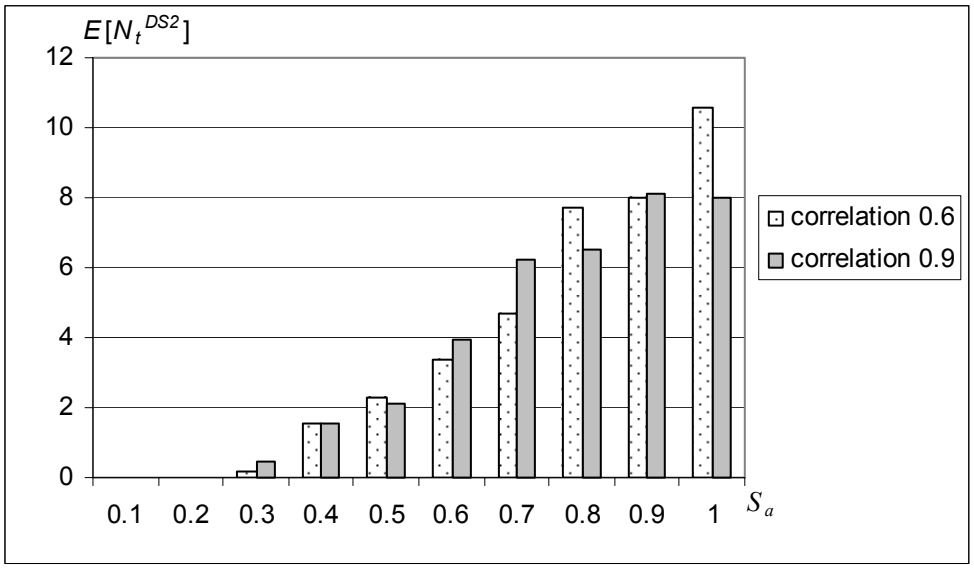

Figure 5.49 Expected number of flexural members in DS = 2 obtained by Method 1 for low (0.6) and high (0.9) coefficient of correlation of member capacities, set of ground motion records.

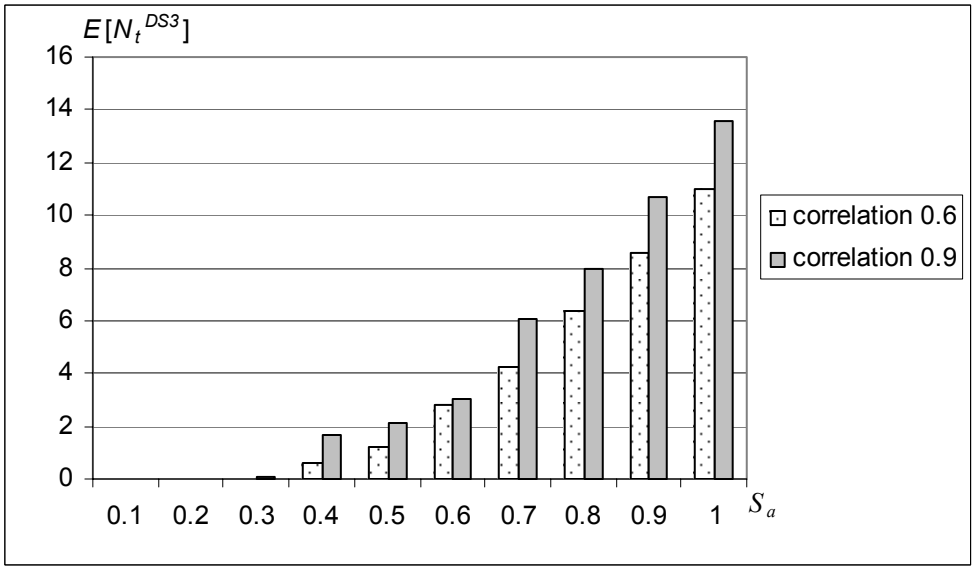

Figure 5.50 Expected number of flexural members in DS = 3 obtained by Method 1 for low (0.6) and high (0.9) coefficient of correlation of member capacities, set of ground motion records.

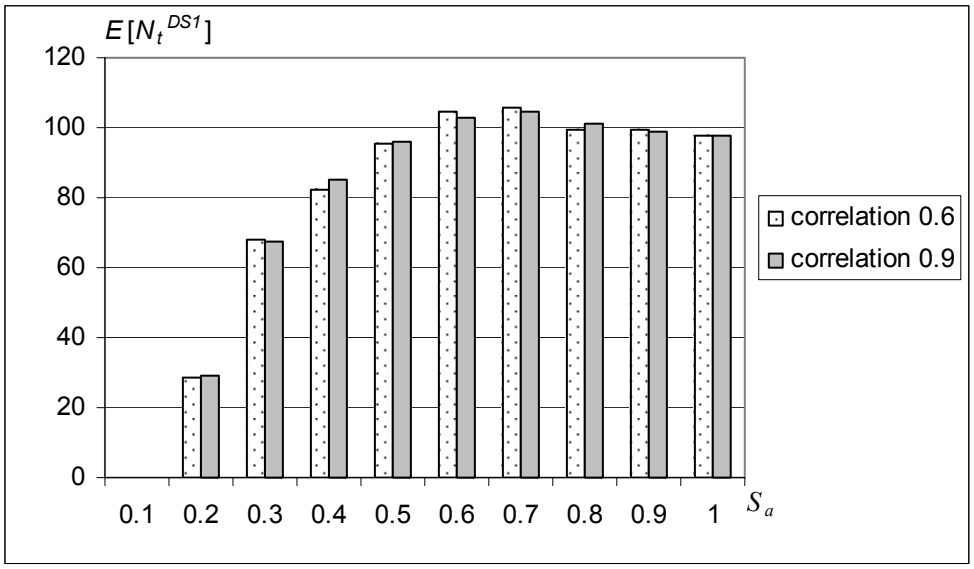

Figure 5.51 Expected number of flexural members in DS = 1 obtained by Method 2 for low (0.6) and high (0.9) coefficient of correlation of member capacities, set of ground motion records.

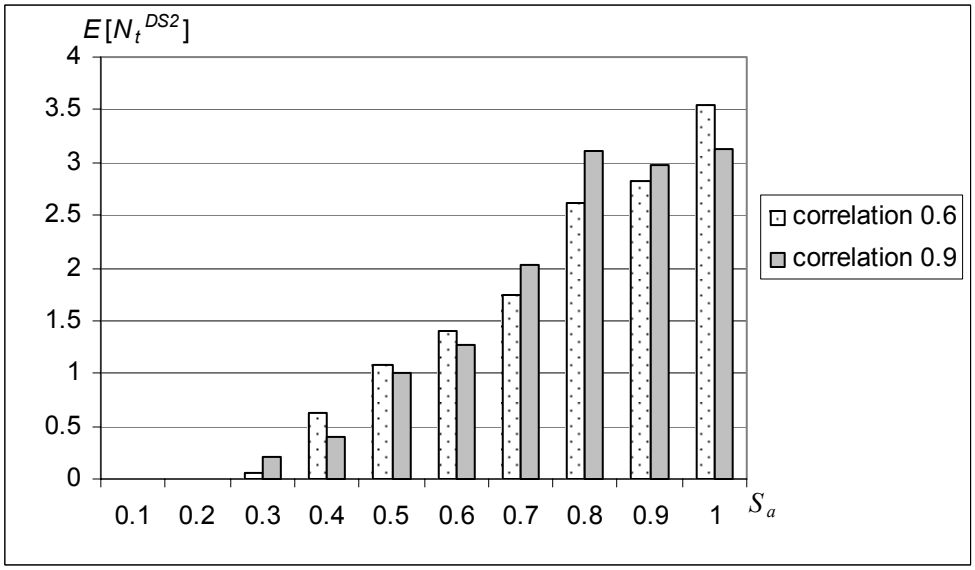

Figure 5.52 Expected number of flexural members in DS = 2 obtained by Method 2 for low (0.6) and high (0.9) coefficient of correlation of member capacities, set of ground motion records.

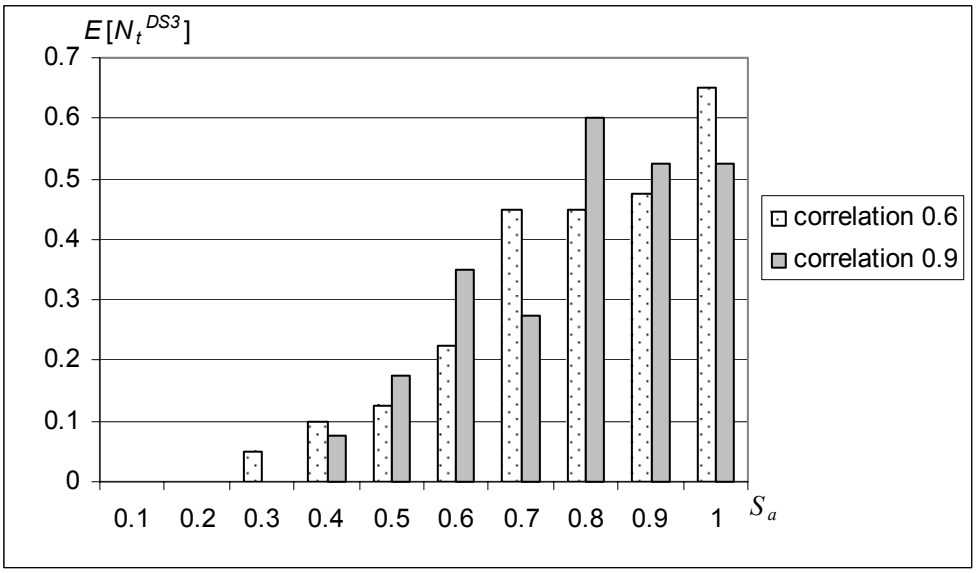

Figure 5.53 Expected number of flexural members in DS = 3 obtained by Method 2 for low (0.6) and high (0.9) coefficient of correlation of member capacities, set of ground motion records.

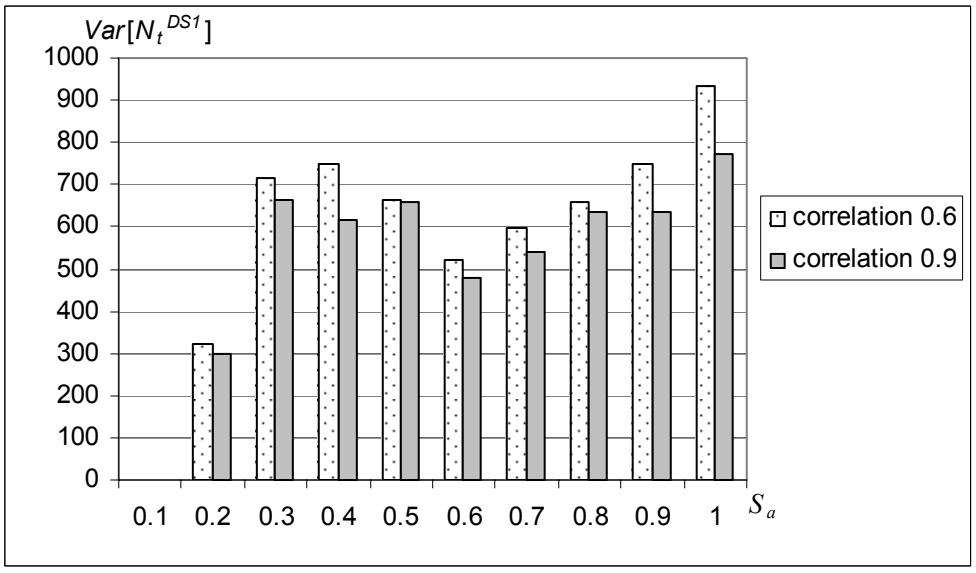

Figure 5.54 Variance of number of flexural members in DS = 1 obtained by Method 1 for low (0.6) and high (0.9) coefficient of correlation of member capacities, set of ground motion records.

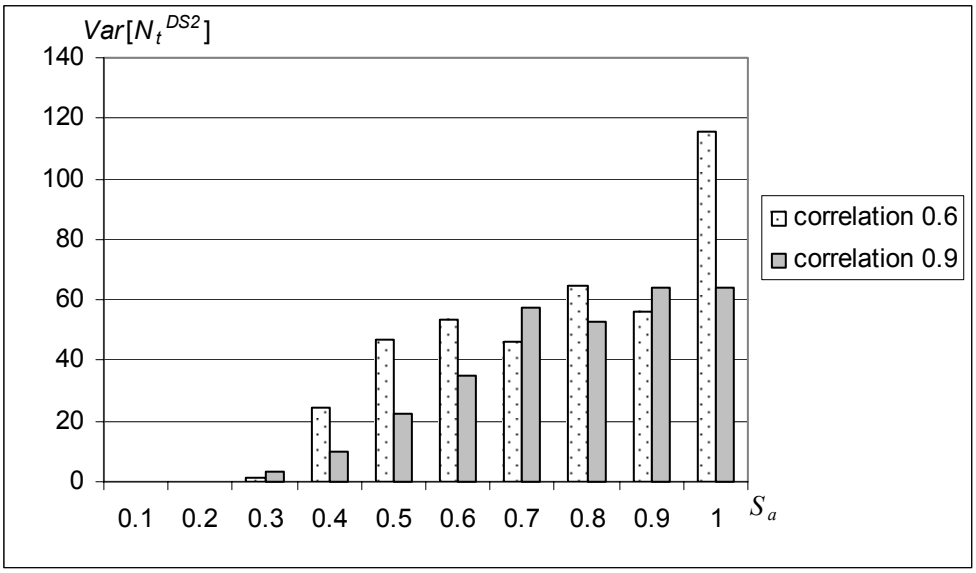

Figure 5.55 Variance of number of flexural members in DS = 2 obtained by Method 1 for low (0.6) and high (0.9) coefficient of correlation of member capacities, set of ground motion records.

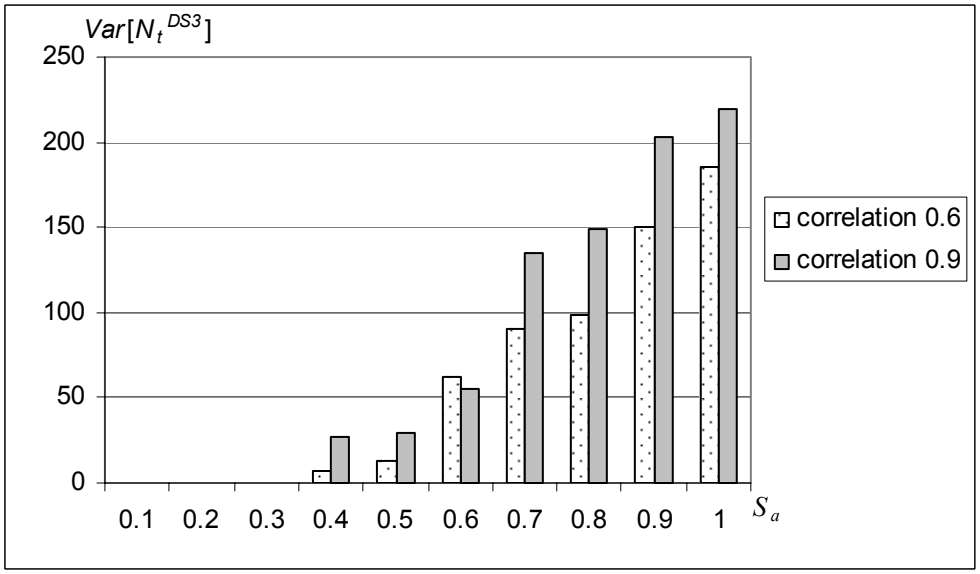

Figure 5.56 Variance of number of flexural members in DS = 3 obtained by Method 1 for low (0.6) and high (0.9) coefficient of correlation of member capacities, set of ground motion records.

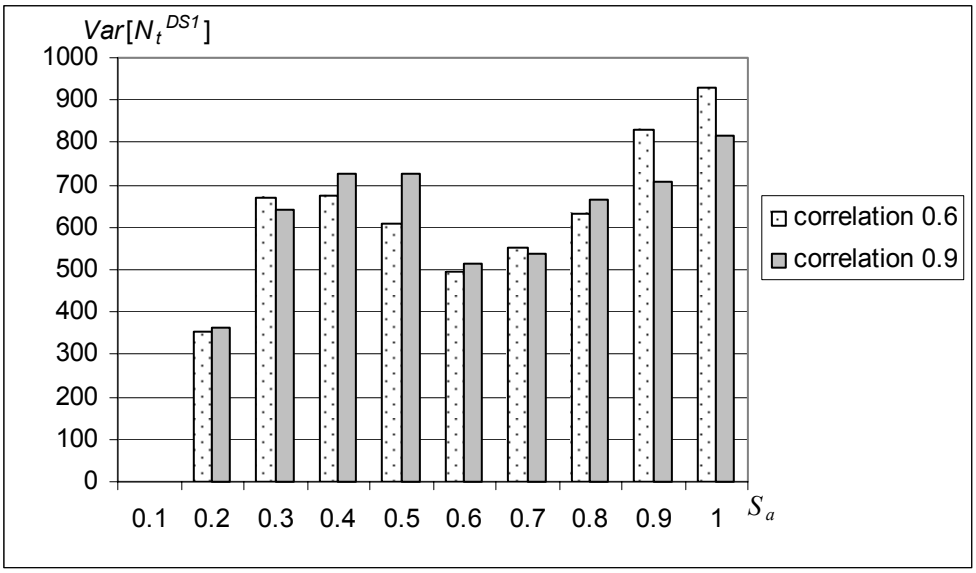

Figure 5.57 Variance of number of flexural members in DS = 1 obtained by Method 2 for low (0.6) and high (0.9) coefficient of correlation of member capacities, set of ground motion records.

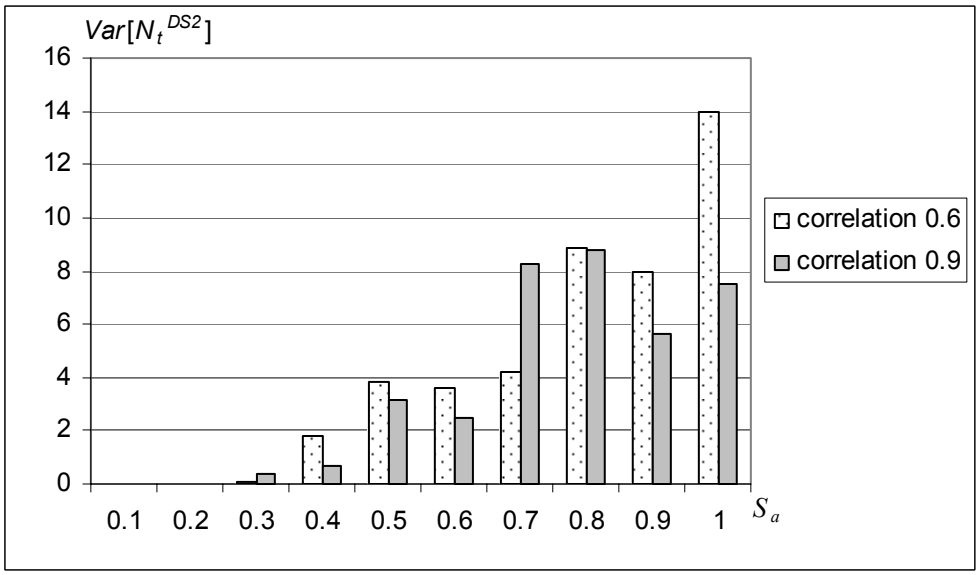

Figure 5.58 Variance of number of flexural members in DS = 2 obtained by Method 2 for low (0.6) and high (0.9) coefficient of correlation of member capacities, set of ground motion records.

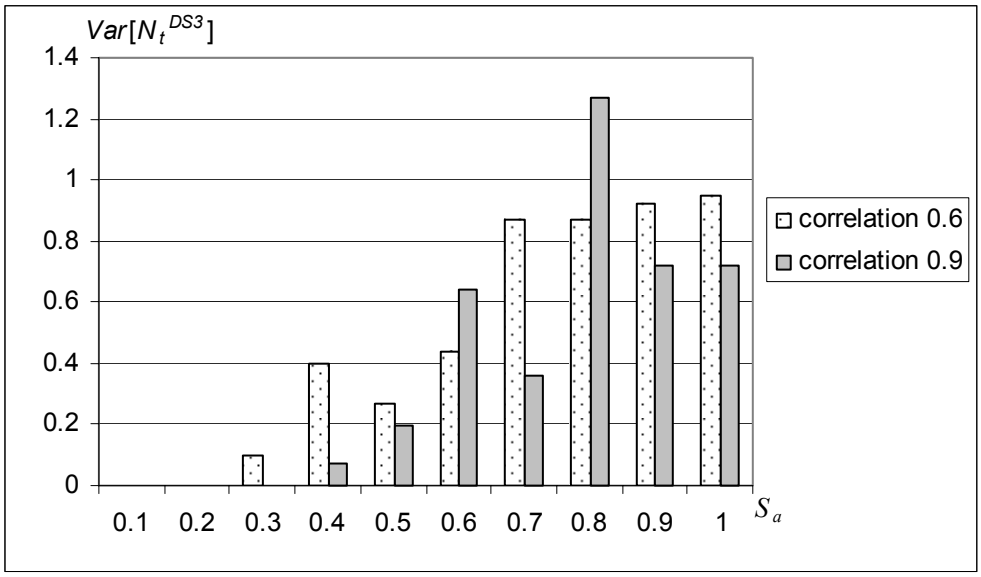

Figure 5.59 Variance of number of flexural members in DS = 3 obtained by Method 2 for low (0.6) and high (0.9) coefficient of correlation of member capacities, set of ground motion records.

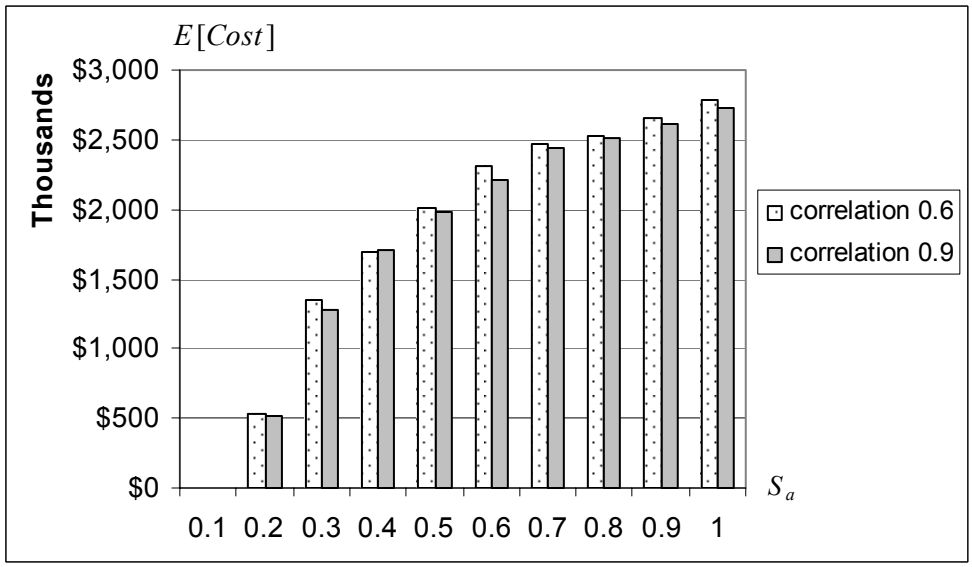

Figure 5.60 Expected repair cost obtained by Method 1 for low (0.6) and high (0.9) coefficient of correlation of member capacities, set of ground motion records.

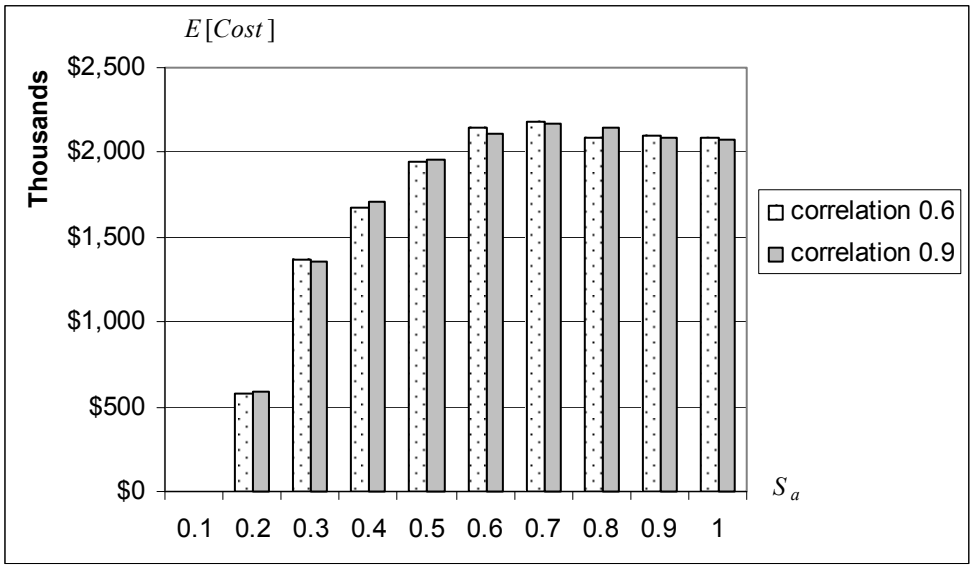

Figure 5.61 Expected repair cost obtained by Method 2 for low (0.6) and high (0.9) coefficient of correlation of member capacities, set of ground motion records.

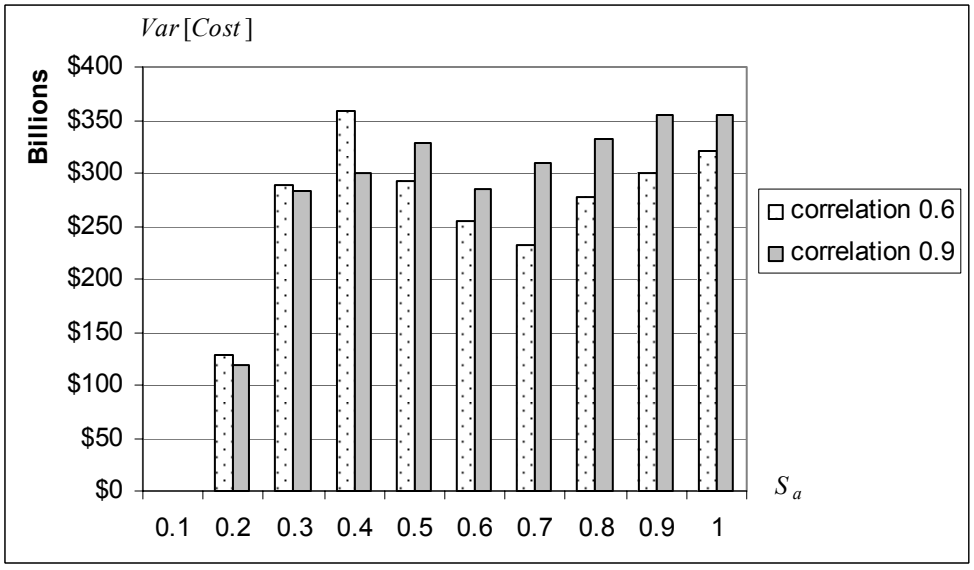

Figure 5.62 Variance of repair cost obtained by Method 1 for low (0.6) and high (0.9) coefficient of correlation of member capacities, set of ground motion records.

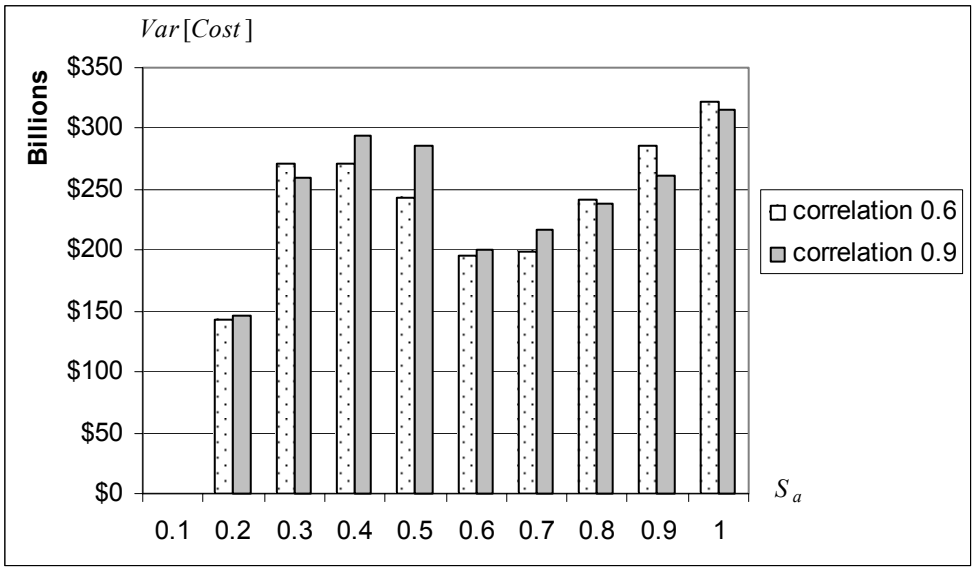

Figure 5.63 Variance of repair cost obtained by Method 2 for low (0.6) and high (0.9) coefficient of correlation of member capacities, set of ground motion records.

6 Combined methods of damage estimation

6.1 Example of application

A coupled approach to damage and structural analyses is proposed in this study as an alternative to the existing uncoupled damage and structural analyses. So far, the proposed approach is used to estimate damage that is expressed in terms of critical changes in structural behavior, such as yielding, achieving maximum strength or degrading to 80% of the maximum strength. A more common view of structural damage employs damage definitions in terms of visible or otherwise detectable degradation (e.g., concrete cracking, concrete spalling, etc.). In Section 4.1.4 we show that visible damage may be closely related to the changes in member's structural behavior. If true, it means that, for example, the damage state "first visible crushing of cover concrete" can be treated as the "yield" damage state; therefore, it can be analyzed by the coupled damage analysis as shown in Chapter 4.

However, some visible damage may not be directly related to the changes in structural behavior. In this case we can use the uncoupled damage analysis for investigating the part of visible damage that is related to the structural behavior. For example, consider significant cracking of reinforced concrete members that may necessitate the member's repair (see Beck et al. 2002), increasing the overall cost and possibly affecting some other decision variables. In general, such cracking (the "cracked" damage state) occurs before yielding of longitudinal reinforcement (the "yield" damage state). Therefore, knowledge of whether a member is in the "yield" damage state or not gives some information about being in the "cracked" damage state. This information can be obtained from the coupled damage analysis. The other factors that control onset of the

"cracked" damage state are not related to the structural properties and can be studied by the uncoupled damage analysis. The combination of the two approaches will provide the complete information about the damage state of interest. In this section, we show how such damage states (damage states that are not fully connected to the changes in structural behavior) can be treated with a combined damage analysis by extending the example considered in Chapter 5 to include the "cracked" damage state.

In the chosen damage model, the "cracked" damage state complements the three damage states used in Chapter 5, bringing the total number of damage states up to four: "cracked" ($DS = 1$), "yield" ($DS = 2$), "maximum strength" ($DS = 3$) and "ultimate" ($DS = 4$). For the three latter damage states, we use the Method 1 damage estimation technique that is applied in Chapter 5. Therefore, for each structural analysis, we know from the coupled damage analysis if the member is in damage state 2, 3 or 4; in either case the probability of being in the "cracked" damage state is zero. If the coupled damage analysis indicates no damage, the member is not yielded. In this case, the probability of being in the "cracked" damage state can be estimated by uncoupled damage analysis through appropriately defined conditional probability function: $P(DS = 1 \mid EDP = z)$. Since the onset of this damage state does not affect the structural response (implication: the damage defining properties do not overlap with structural response defining properties, $\underline{X}^{CS} = \varnothing$), the uncoupled damage analysis can be conducted without double sampling of structural properties. The key issue here is the choice of *EDP* and damage model. To avoid double sampling of the structural parameters, we need to define the *EDP* and damage model so that it does not depend on the member's properties that are used in the structural model. For this particular damage state, maximum ductility ratio D_r (ratio

of the maximum curvature to the yield curvature) can serve as the *EDP* and we define the conditional probability as follows

$$P(DS = 1 \mid D_r = z) = \begin{cases} 0, & z < D_r^{lb} \\ 1/\left(1 - D_r^{lb}\right) & D_r^{lb} \le z < 1 \\ 0, & z \ge 1 \end{cases} \tag{6.1}$$

where D_r^{lb} is the lowest ductility value providing a non-zero probability of being in the "cracked" damage state; note that for a ductility ratio greater than 1 the member is in the "yield" or higher damage state. For the present study, we set the lower threshold parameter to D_r^{lb} = 2/3, assuming that operation at lower values of ductility does not cause any damage (the design range).

The assumption of the constant part of the fragility function in (6.1) is used primarily for simplicity of implementation, since the main purpose of this chapter is to demonstrate that properly defined fragility functions can be used as part of the proposed coupled damage analysis.

We used the previously-defined four damage states to estimate the repair cost of the reinforced concrete moment frame that is described in Chapter 5.1. For this purpose the relation between damage and repair cost (5.4) is extended for the four damage states

$$\begin{gathered} DS = 1 \text{ (cracked)} \Rightarrow \ Cost = \$10{,}000 \\ DS = 2 \text{ (yield)} \Rightarrow \ Cost = \$20{,}000 \\ DS = 3 \text{ (maximum strength)} \Rightarrow \ Cost = \$30{,}000 \\ DS = 4 \text{ (ultimate)} \Rightarrow \ Cost = \$40{,}000 \end{gathered} \tag{6.2}$$

where we neglect the uncertainty in the cost to repair the members. Figures 6.1-6.3 present the results of the cost estimation. In Figure 6.1, each cross corresponds to one

dynamic structural simulation followed by a damage and loss analysis. The model with uncertain critical curvatures is used (see Section 5.2), together with a set of 40 ground motion records for each S_a level. Figure 6.2 gives the expected repair cost and one standard deviation interval about the expected value for each level of ground motion. The resulting function is usually called a seismic vulnerability function and can be conveniently used in the decision-making process (Beck et al. 2002).

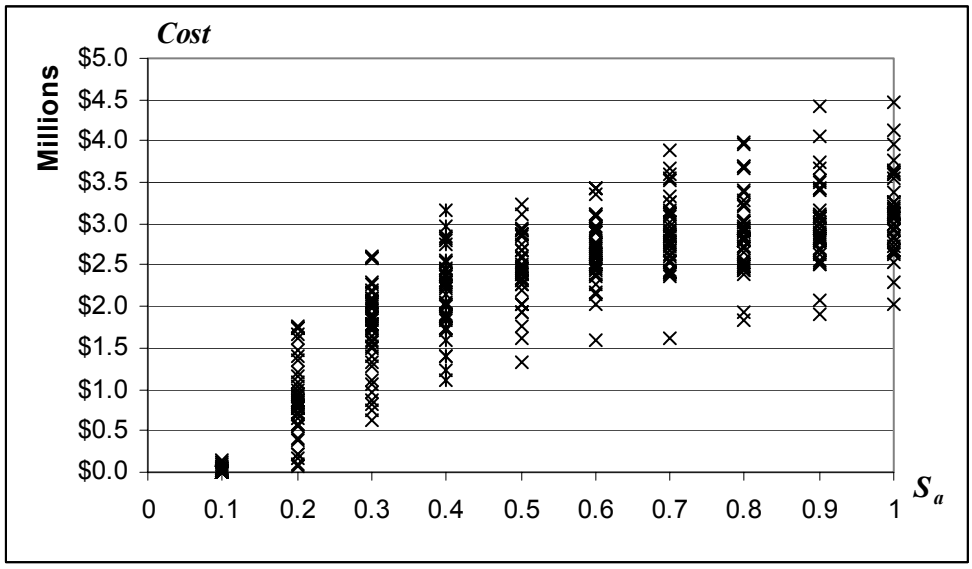

Figure 6.1 Repair cost estimates based on combined method of damage analysis, set of ground motion records.

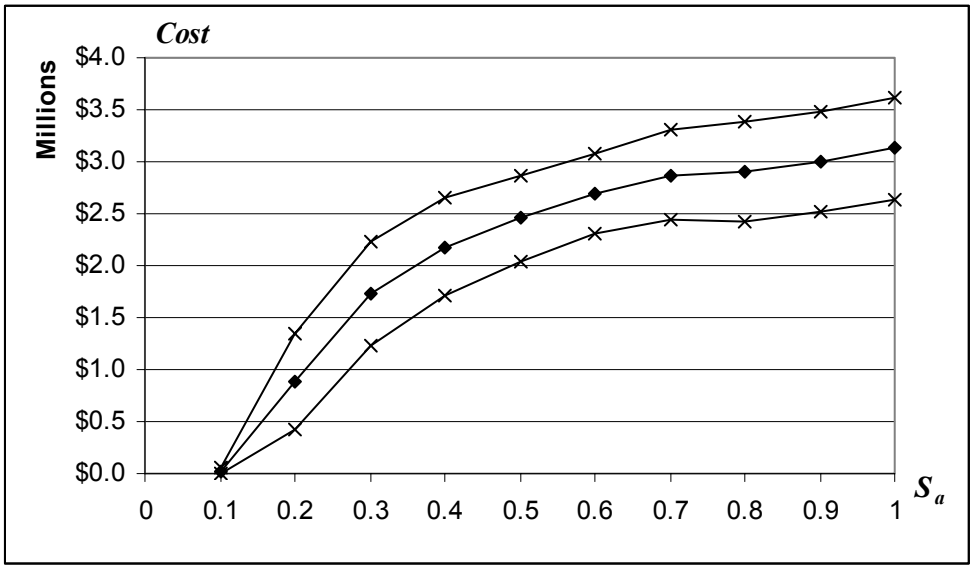

Figure 6.2 Expectation of repair cost estimate and one-sigma confidence intervals obtained by combined method of damage analysis, set of ground motion records.

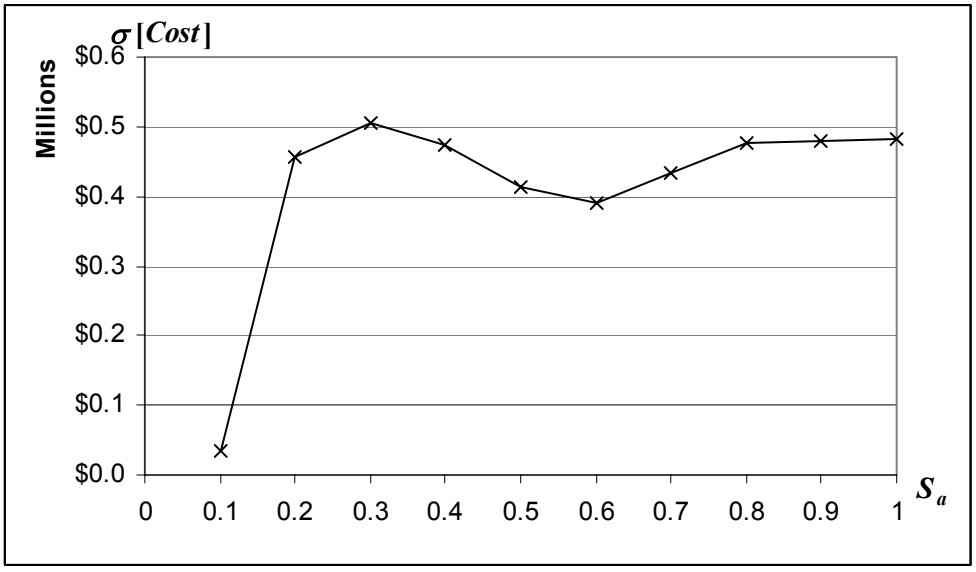

Figure 6.3 Standard deviation of repair cost estimate obtained by combined method of damage analysis, set of ground motion records.

The results presented in Chapters 5 and 6 demonstrate that a decision variable estimation can be performed by the coupled damage analysis through using damage states defined both in terms of the structural state of the members (e.g., “yield,” “maximum

strength," "ultimate") and in terms physical damage (e.g., "cracked," "first visible concrete crushing"). The combination of these damage states can provide a more accurate damage measure, improving a decision variable estimate. The proposed set of four damage states seems to be a good choice for estimating the cost of repairing the damage of reinforced concrete members. The discussion of other possible choices of damage states is presented in the next section.

6.2 Damage states of reinforced concrete members

From the previous section, we can see that there are at least two ways to defining damage measures. One of them is to define damage in terms of critical points on the force-deformation diagram like "yield," "maximum strength," etc., and another is to define damage in terms of physical damage like "concrete crushing," "concrete spalling," "buckling of longitudinal reinforcement," etc. Both these approaches to damage definition can be handled by either coupled or uncoupled damage analyses. In this study we consider in detail the difference between coupled and uncoupled damage analysis as applied to damage defined in terms of critical points on the force-deformation diagram (see Chapters 3 to 6). Now we briefly discuss the most important problems to be consider while choosing between different ways of defining damage.

First of all, the choice of damage measure should depend on how much information the chosen damage states give about the decision variable. For example, repair cost of a damaged reinforced concrete member can not be directly derived from the fact that "buckling of longitudinal reinforcement" has been detected. However, it can be derived from the fact that the member is to be repaired by reinforced concrete jacketing. Standard cost estimation techniques can be used to do this. Therefore, we need damage

states to be defined in such a way that the damage states can be related to the repair techniques that are likely to be used. Defining damage states in terms of visible or detectable damage is a viable choice, since in industry practice, the selection of a particular repair technique is based primarily on the appearance of a damaged member. Therefore, a link between visible damage and repair effort can be established. However, the same is true for the damage measure defined in terms of critical changes in structural behavior. Appendix A provides a review of existing repair methods and a qualitative relation between the four damage states used in this chapter and repair methods. Based on these qualitative relations, it is possible to derive a set of actual conditional probabilities of applying different repair methods, given one of the four damage states, providing that more empirical data from actual construction industry practice is available. We shall leave this task for future research.

The problem with using physical damage definitions is related to the fact that such descriptive damage states are not necessarily mutually exclusive. For example, breakage of longitudinal reinforcement can happen without buckling (under tensile load), and vice versa. Therefore, with uncoupled damage analysis, one would have to deal with the general case of multiple damage states, which require $2^n - 1$ fragility functions for n damage states (see Section 3.2), Obtaining that many fragility functions is expensive and impractical, rendering this approach impractical too. It is likely that the combined damage analysis (Section 6.1) would better deal with such situation. In this case, after the coupled damage analysis is performed the amount of information to be transferred through fragility functions is reduced, possibly decreasing the number of required

fragility functions. This is a mostly intuitive conclusion that is based on the example presented in Section 6.1. A rigorous proof of this statement is left for the future research.

In conclusion, we consider another possible approach to selecting damage states and compare it to the previously mentioned ones. The other way is to define damage states loosely in terms of qualitative verbal definitions of damage, e.g., "light," "moderate," "severe," etc. In this case, mutual exclusiveness of the damage states is simply insured by convention: each "heavier" damage state negates the preceding "lighter" damage state. Thus, one can use one fragility function for each damage state. However, a problem arises from the lack of clarity in the definition of these damage states. It is not clear what exactly the terms "light" or "severe" mean. One would need to define a set of unambiguously identifiable symptoms corresponding to each damage state in question. It is not easy to define such a set that would be applicable in any practical application. The most probable outcome is that all generically defined damage states ("light" etc.) will be defined either in terms of a structural state (drastic changes in structural behavior) or physical damage, reducing the problem to one that we have already addressed in this study in detail.

7 The use of in-situ information for fragility functions

In this chapter, we consider the example of an in-situ assembly consisting of a reinforced concrete column loaded in shear. We demonstrate the difference between the properly evaluated fragility function (3.3) and the case where the CDF of capacity (3.13) is used as a fragility function.

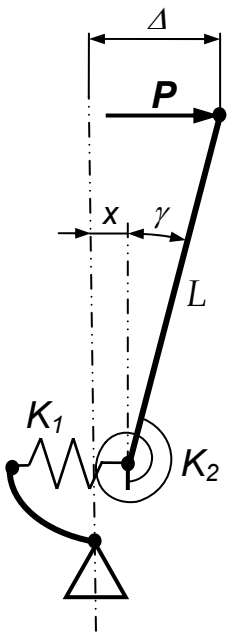

Figure 7.1 Column model

Consider the model of a column presented in Figure 7.1. This type of model is often used to imitate the behavior of real structural elements. We assume that the shear and flexural springs K_1 and K_2 have the force-deformation behavior shown in Figure 7.2. The damage state for this element is defined by degradation of the shear spring stiffness: once the stiffness of the spring has dropped to αK_1, the element is considered to be damaged (DS = "shear yield"). Note that according to ACI guidelines, this damage state is recognized as a failure in shear. The fact that for the flexural spring, an infinite strength

is assumed, means that the model is valid for columns with prevalent shear failure mode. We want to study the fragility of this column with respect to the "shear failure" damage state, in terms of the inter-story drift ratio (*IDR*). For this model: $IDR = \Delta / L$ (see Figure 7.1).

7.1 Generic fragility function (no in-situ information included)

First, we study the column disregarding possible differences in the in-situ conditions, since given the column we do not know exactly where it is going to be used. We call such a column a "general" column. For the general column, only the properties of the column itself can be taken into consideration. Therefore, the force *P* can

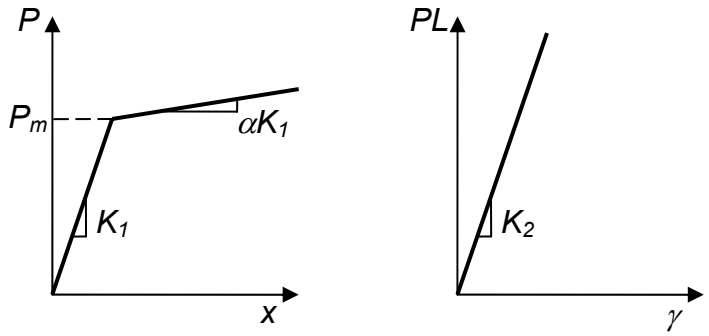

Figure 7.2. Force-deformation characteristics of the shear spring (left) and flexural spring (right).

not be included into analysis, since in practice the force depends on external loading and the properties of the structure which are assumed to be unknown. Suppose that the only uncertain property of the column is its shear strength (P_m). Suppose further, that this parameter is distributed lognormally: $P_m \sim LN\ (\mu_{Pm},\ \sigma_{Pm})$, where $\mu_{Pm},\ \sigma_{Pm}$ are parameters of the corresponding normal probability distribution ($log(P_m) \sim N\ (\mu_{Pm},\ \sigma_{Pm})$). Then for every given value of $IDR = z$, the state of the column is uncertain. Depending on the applied load P_m, the column might be either undamaged (shear stiffness is K_1) or

damaged (shear stiffness is αK_1). This means that for every value of $IDR = z$, there are two regions of values of P_m: the failure region $\Omega_{\text{"shear failure,"}z}$, corresponding to the damaged state and its complement, the safe region $\Omega^C_{\text{"shear failure,"}z}$, corresponding to the undamaged state. These regions for the present model can be found as follows. First,

$$\Delta = x + \gamma L$$

$$\Delta = \frac{P}{K_1} + \frac{PL^2}{K_2} = \frac{P\left(K_2 + L^2 K_1\right)}{K_1 K_2}$$

where this relation is valid for the undamaged states (initial stiffness state). Given that $IDR = z = \Delta / L$, the force is equal to

$$P = \frac{zLK_1K_2}{K_2 + L^2K_1} \tag{7.1}$$

This relation is only true if $P < P_m$ (undamaged state), otherwise the stiffness of the shear spring would be αK_1 and the whole expression would be different. This means that (7.1) is valid if and only if P defined by (7.1) is less than P_m. Therefore, the following is true

$$0 \le P_m \le \frac{zLK_1K_2}{K_2 + L^2K_1} \text{ - failure region}$$

$$\frac{zLK_1K_2}{K_2 + L^2K_1} < P_m \text{ - safe region}$$

Note that the failure and safe zones depend only on the properties of the column and IDR and do not depend on the force P, as it should be for a generic analysis.

Since the failure region is known, we can find the probability of failure for each value of IDR. The probability of failure is the integral of the probability density function of P_m over the failure region. For the present case, this probability takes the form

$$P(DS = \text{“shear failure”} \mid IDR = z) = F_{Pm}(z\varphi), \tag{7.2}$$

where $F_{Pm}(.)$ is the cumulative distribution function of P_m (lognormal) and $\varphi = \dfrac{LK_1K_2}{K_2 + L^2K_1}$. The fragility function (7.2) is what one can obtain by studying the fragility of the column in a general way, disregarding differences in real in-situ conditions.

7.2 Fragility function with in-situ information included

Now we consider the case where some information about the in-situ conditions is known that leads to a probability distribution on the shear force P. Clearly, for such a column, the probability distribution for the force P will, in general, depend on the structure and the site it is located in.

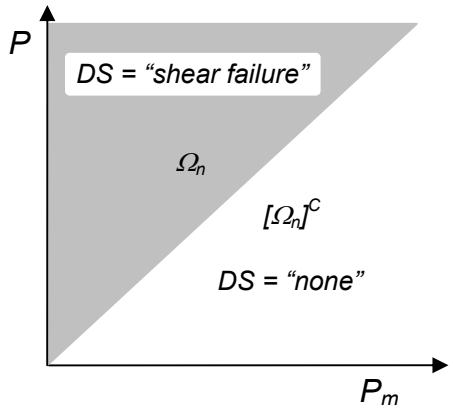

Figure 7.3 Failure region and safe region in the Ω space.

Suppose that P is a lognormally distributed random variable: $P \sim LN(\mu_P, \sigma_P)$. All the remaining properties of the column are exactly the same as in the first case. We want to find a fragility function for the column using this information about P: $P(DS = \text{"shear failure"} \mid IDR = z)$.

First, we have to find a failure region corresponding to the event $DS = \text{"shear failure"}$ (Ω_n) in the space of the uncertain parameters: $\Omega = P \times P_m = [0, \infty) \times [0, \infty)$. Since *"shear failure"* is defined as a reduction of the shear spring stiffness to αK_1, it is easy to see that $DS = \text{"shear failure"}$ is equivalent to $P \geq P_m$. This failure region is shown as the shaded area in the Figure 7.3.

Second, given that event $IDR = z$ has happened, parameters P and P_m can not take arbitrary values in the space Ω, because equality $IDR = z$ imposes restrictions on the possible values of the external force P and maximum shear strength P_m. Therefore, we have to identify the region Ω_z that corresponds to the event $IDR = z$. For the safe region, the external force P is found, as before, by (7.1). It is easy to see that P does not depend on P_m in this region. Therefore, within the safe region, Ω_z is defined by

$$P = \frac{zLK_1K_2}{K_2 + L^2K_1}, \quad P_m \in \left[\frac{zLK_1K_2}{K_2 + L^2K_1}, \infty\right) \tag{7.3}$$

In the failure region, the forces and deformations are related as follows

$$\Delta = \left[\frac{P_m}{K_1} + \frac{P - P_m}{\alpha K_1}\right] + \frac{PL^2}{K_2}$$

Therefore, the relation between P and P_m is easily derived as

$$P = \frac{(1-\alpha)K_2}{K_2 + \alpha K_1 L^2} P_m + \frac{z\alpha L K_1 K_2}{K_2 + \alpha K_1 L^2} \;,\; P_m \in [0,\; \frac{zLK_1K_2}{K_2 + L^2 K_1}] \tag{7.4}$$

Equations (7.3) and (7.4) define the region Ω_z, which is a 1-D surface in the space Ω. Equation (7.4) defines the section of surface Ω_z that lies within the failure zone.

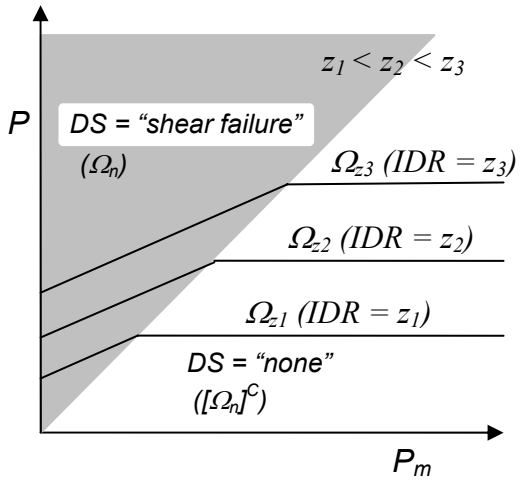

Figure 7.4 Surface Ω_z for different values of IDR

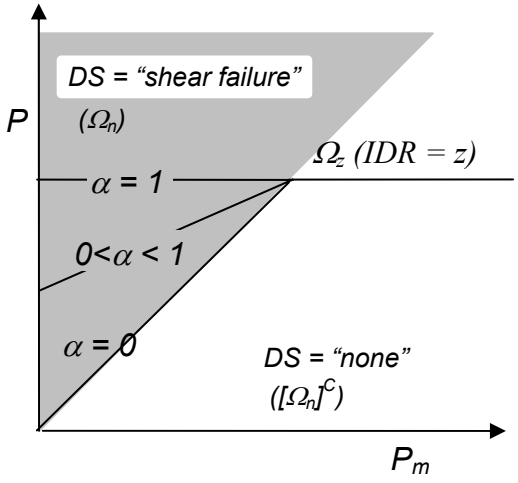

Figure 7.5 Surface Ω_z for different values of α

Figure 7.4 shows surface Ω_z for several values of IDR. Since α ranges within the interval [0, 1], the tangent of the line (7.4) also changes within the interval [0, 1]. Figure 7.5 shows surface Ω_z for different values of α and the same value of IDR.

If the surface Ω_z is a straight line (α = 1), then the fragility function will coincide with the CDF of capacity (because P and P_m are independent). Therefore, it should be true that the more Ω_z deviates from a straight line, the more the site-specific fragility function should differ from general fragility function (CDF of capacity). Thus, for better demonstration it is desirable to take α = 0. However, as shown latter, taking α = 0 causes mathematical difficulties. Therefore, we pick α by observing the following conditions: α ≠ 0 and α << 1.

The procedure for estimating the fragility function is outlined in Equations 3.18 - 3.20. In order to be able to perform this procedure, we need to know the joint probability function of the vector $\underline{X}^*$ that for the present case is equal to [P_m, P]. Since P and P_m are taken as independent random variables with lognormal probability distributions, the joint probability density function is just the product of their probability density functions

$$f_{\underline{Y}}(\underline{y}) = f_{Pm,P}(p_m, p) = f_{Pm}^{LN}(p_m) f_P^{LN}(p) \tag{7.5}$$

We define a new coordinate system as follows: $\underline{Y}$ = [P_m, IDR], then transformation of variables $\psi^{-1}(\underline{Y})$ takes the form

$$\underline{X}^* = \psi^{-1}(\underline{Y}): \quad \begin{cases} P_m = P_m \\ P = IDR\varphi \end{cases} \qquad IDR\varphi < P_m$$

$$\begin{cases} P_m = P_m \\ P = \dfrac{(1-\alpha)K_2}{K_2 + \alpha K_1 L^2} P_m + \dfrac{\alpha L K_1 K_2}{K_2 + \alpha K_1 L^2} IDR \end{cases} \qquad 0 < P_m < IDR\varphi \tag{7.6}$$

Therefore, the Jacobian (3.20) of the transformation $\psi^{-1}(\underline{Y})$ is equal to

$$J = \begin{vmatrix} 1 & 0 \\ 0 & \varphi \end{vmatrix} = \varphi, \qquad IDR\varphi < P_m$$
$$J = \begin{vmatrix} 1 & 0 \\ \dfrac{(1-\alpha)K_2}{K_2 + \alpha K_1 L^2} & \dfrac{\alpha L K_1 K_2}{K_2 + \alpha K_1 L^2} \end{vmatrix} = \frac{\alpha L K_1 K_2}{K_2 + \alpha K_1 L^2}, \quad 0 < P_m < IDR\varphi \tag{7.7}$$

Now we can see that in the case $\alpha = 0$, the Jacobian becomes zero, making the PDF for a certain area to be equal to zero too. Although there is nothing non-physical about this situation, we choose to avoid such an extreme case in this example.

The fragility function is given by (3.18). The safe region for the present case is expressed in terms of P_m and, given that $IDR = z$, is defined as before: $z\varphi < P_m$. Then, the fragility function is calculated as

$$P(\,DS = \text{“shear failure”} \mid IDR = z) = \int_0^{z\varphi} f_{P_m|IDR}(\,p_m \mid z)\,dp_m \tag{7.8}$$

where the conditional PDF of P_m is found as $f_{P_m|IDR}(\,p_m \mid z) = f_{P_m,IDR}(\,p_m, z) / f_{IDR}(z)$. The PDF of *IDR* is obtained according to the second equation of (3.19) that for the present case takes the particular form

$$f_{IDR}(z) = \int_0^{\infty} f_{P_m,IDR}(p_m, z)\,dp_m \tag{7.9}$$

where the joint PDF of P_m and IDR is found according to (3.19) and in the present case takes the form

$$f_{P_m,IDR}(p_m,z)=\begin{cases} f_{P_m,P}(p_m,z\varphi)\varphi & z\varphi < p_m \\ f_{P_m,P}\left(p_m,\dfrac{(1-\alpha)K_2}{K_2+\alpha K_1L^2}p_m+\dfrac{\alpha LK_1K_2}{K_2+\alpha K_1L^2}z\right)\dfrac{\alpha LK_1K_2}{K_2+\alpha K_1L^2} & 0<p_m<z\varphi \end{cases} \quad (7.10)$$

where the joint PDF $f_{Pm,P}(\circ,\circ)$ is given by (7.5).

Equations 7.8 – 7.10 provide the algorithm for estimating the fragility function of the in-situ column. We use this algorithm to calculate the fragility function for a sample column. The parameters of the sample column are chosen based on the parameters of the columns of a seven-story hotel in Van Nuys, California. The general stiffness parameter φ = 10000 kips, length of the column L = 100 in, the translational (in shear) stiffness K_1 = 6000 kips/in, the rotational stiffness is derived as $K_2 = L^2K_1(\varphi/L)/(K_1-\varphi/L) \cong 1000000$ kips·in, and the expected shear strength $E[P_m]$ = 60 kips. The coefficient of variation of the shear strength is assumed to be δ_v^{Pm} = 0.15. The parameters of the probability distribution of the force P are chosen to provide a probability of failure (unconditional on IDR, given only that a seismic event has happened) to be 2% with coefficient of variation δ_v^P = 0.6. The estimate of the coefficient of variation is based on the assumption that the force P is produced by natural hazard and has higher uncertainty than material properties. The estimate of the probability of failure is based on the result of two earthquakes that happened at the site. The building has 150 columns in the lateral force resisting frame; none of them failed during the first earthquake and 6 of them failed in shear during the second one, giving an estimate of the probability of failure of 6/(2*150) = 0.02. Assuming that the Van Nuys building is a typical example of the structural design of its time, we call the assembly with 2% probability of failure the "normal strength" design. The stiffness parameter φ is not used for estimating parameters of the probability

distributions. Using $E[P_m]$, δ_v^{Pm}, δ_v^{P}, and the probability of failure, the four parameters of the probability distributions are estimated as: $\mu_{Pm} = 10.991$, $\sigma_{Pm} = 0.1492$, $\mu_P = 9.8116$, $\sigma_P = 0.5545$, where the units of both P_m and P are pounds (lb).

7.3 Results and conclusions

The results for the two fragility functions are presented in Figures 7.6-7.7. Figure 7.6 shows the fragility functions for the case of "normal strength" design and $\alpha = 0.01$. The relative difference in the shear failure probability estimate is also shown for the case where the CDF of capacity in (7.2) is used instead of the site-specific fragility function in (7.8).

It can be seen that relative difference in the estimates is 100-150% at the lower end, where the probability of shear failure is nearly zero, making the discrepancy insignificant for practical purposes. For the range of practically meaningful values of failure probability, the relative difference is on average 50%. It can also be concluded that the CDF of capacity gives a consistently higher probability of failure of the column than when the in-situ condition (load probability distribution) is taken into account.

Note that the same results hold even if a cyclic load is applied. Using the maximum applied force instead of P, along with the maximum IDR, and assuming that the shear failure does not depend on the load history and there is no strength degradation due to dissipated energy, all the results are valid.

It is also interesting to see how the value of stiffness degradation α affects the fragility function. Figure 7.7 shows the CDF of capacity together with site-specific fragility functions for several values of α.

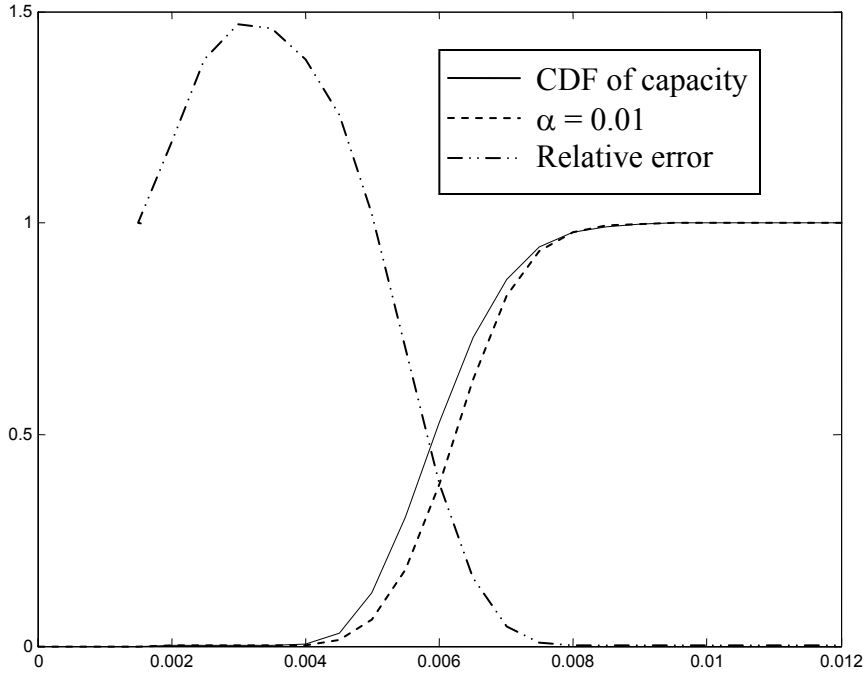

Figure 7.6 Site-specific fragility function and CDF of capacity for the "normal strength" design.

First note that our initial guess is correct: as α goes to one, the fragility function approaches the CDF. Indeed, the fragility function for $\alpha = 0.1$ practically coincides with the CDF of capacity and for the range of values of α between 0.1 and 1, the fragility functions do not noticeably change and stay approximately equal to the CDF of capacity. For the values of α in close proximity to 0 ($\alpha<0.1$), a different behavior can be observed. The fragility function turns out to be quite sensitive with respect to the value of α. Figure 7.7 shows the fragility functions for $\alpha= 0.1, 0.01, 0.001, 0.0001$. We can see that as α goes to 0, the fragility function moves further and further to the right, with fragility function for $\alpha = 0.0001$ positioned at a significant distance from the CDF of capacity.

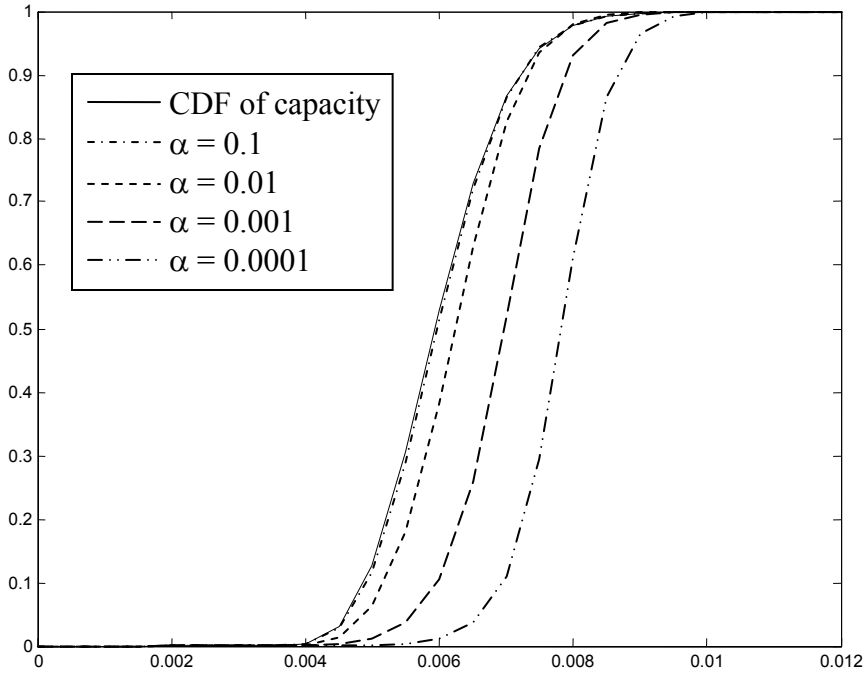

Figure 7.7 Site-specific fragility functions for "normal strength" design for different values of α

Clearly, for the present example, the difference between the general fragility function (CDF of capacity) and the site-specific fragility function for the near zero values of α can hardly be ignored. For instance, if the value of α is 0.0001 and a group of 100 columns is considered, then given that IDR = 0.6%, the probability of shear failure is practically zero (as estimated by the site-specific fragility function), while the CDF of capacity predicts that more than 60% of the columns will fail, implying a huge difference in the corresponding recovery efforts. This shows the importance of using in-situ information, if available, in developing fragility functions.

So far we have dealt only with the case of "normal strength" that is defined as a 2% probability of failure in the case of a seismic event. In practice, such a design is not always implemented. It is conceivable that requirements for safety and reliability are

different for different types of structures. Therefore, the probability of failure could be different. We consider two more cases of the structural design. One of them represents a very strong and reliable member: the probability of failure is taken to be 0.1%. We call this case an "over-strength" design. The other case corresponds to a weak member: the probability of failure is assumed to be 10%. We call this case an "under-strength" design. Figures 7.8 – 7.11 shows the results of a comparison of the CDF of capacity and various site-specific fragility functions for these two cases.

For all three cases of the column design, we can observe a similar picture; that is, for $\alpha > 0.1$, the site-specific fragility functions practically coincide with the CDF of capacity, moving to the right as α goes to zero. However, the strength of the design has some effect upon the fragility functions shape; that is, the stronger the column is (the lower the probability of failure), the more to the left the fragility functions are located. In general, this amounts to less discrepancy between the CDF of capacity and the other fragility functions for the stronger columns. We can see that for the case $\alpha = 0.01$, the "over-strength" design has the lowest relative difference and "under-strength" design has the highest relative difference. Figure 7.12 shows the fragility functions for $\alpha = 0.0001$ for the three design cases.

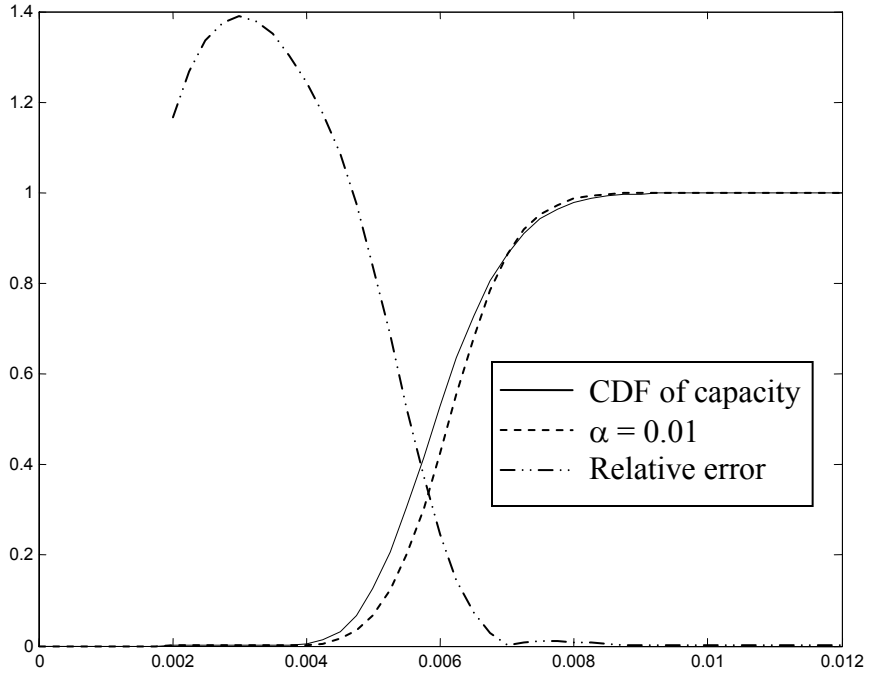

Figure 7.8 Site-specific fragility function and CDF of capacity for the "over-strength" design.

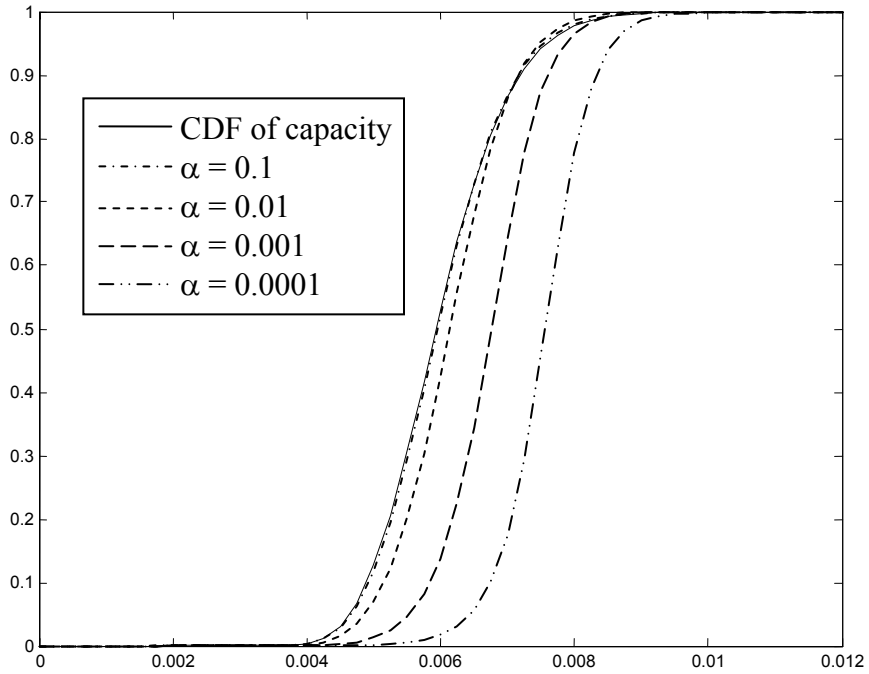

Figure 7.9 Site-specific fragility functions for "over-strength" design for different values of α

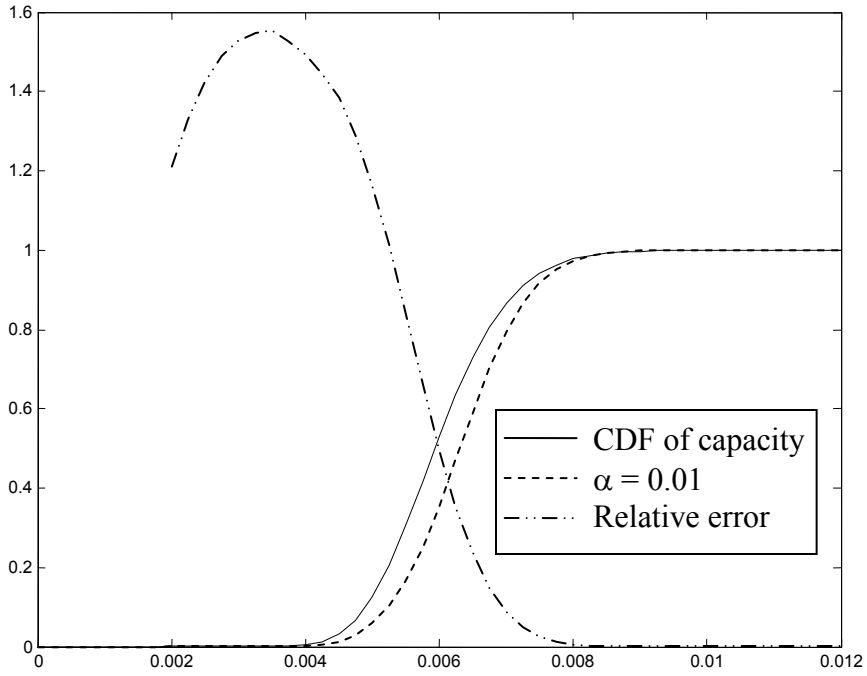

Figure 7.10 Site-specific fragility function and CDF of capacity for the "under-strength" design.

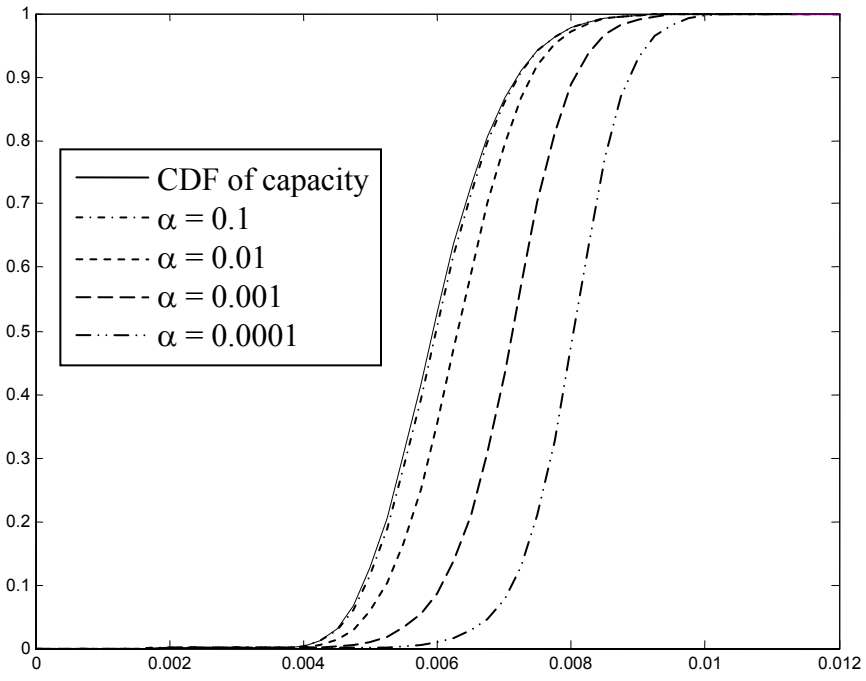

Figure 7.11 Site-specific fragility functions for "over-strength" design for different values of α

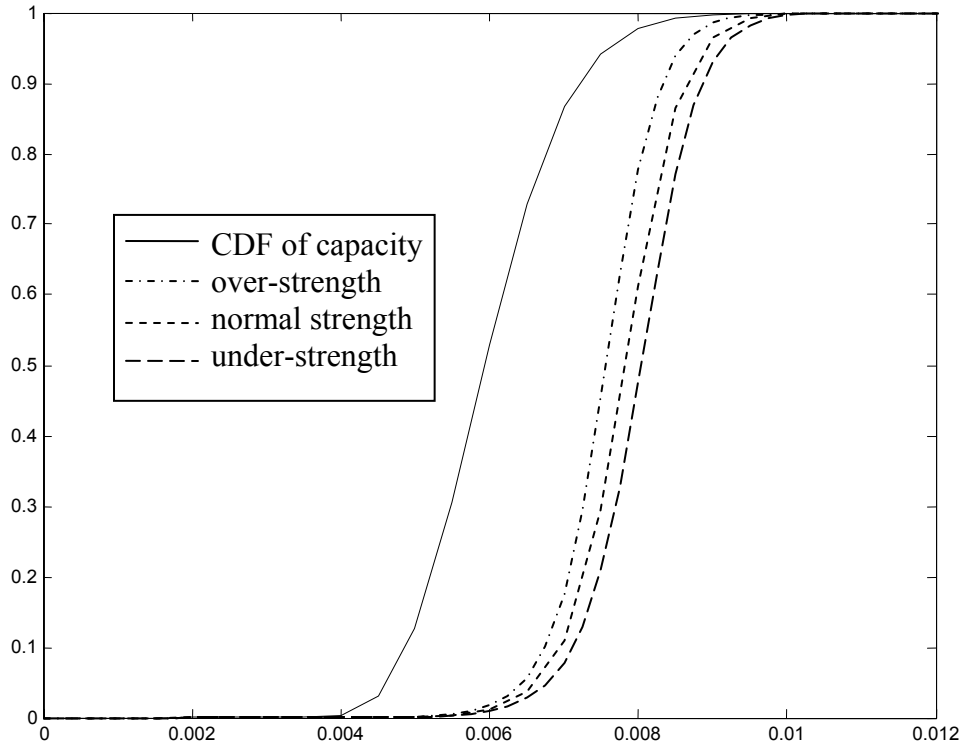

Figure 7.12 Site-specific fragility functions for the "normal strength," "under-strength" and "over-strength" design (α= 0.0001).

8 Conclusions and future research

The conventional approach to damage estimation is based on fragility functions that relate some chosen parameters of structural response, usually referred to as engineering demand parameters (*EDP*), to incurred damage. In the present study, it is shown that for structural damage estimation based on structural analysis, the uncoupled approach based on usual fragility functions (3.13) has deficiencies that lead to less accurate damage prediction. These shortcomings originate from two sources: first, dependence of practically all *EDP*s on the damage of structural members and second, inexact limit-state functions that are used for damage description.

It is shown that in case of damage analysis uncoupled from structural analysis (*EDP*s are obtained from structural analysis and then are used as input for fragility functions), dependence of *EDP* on structural damage results in using two samples of structural properties instead of one during estimation of decision variables. The associated error is studied by comparison of the results of damage estimation obtained by the uncoupled methods and a new technique that implements coupled damage and structural analyses and does not have double sampling. The proposed coupled approach, besides using an *EDP*, uses all information available from structural analysis that is relevant to the damage to be assessed. It is shown that the discrepancy can be significant in some cases. In particular, for the case of a fixed ground motion and ignoring uncertainties in the structural properties during structural analysis, double sampling associated with the uncoupled approach leads to significant underestimation of damage variability (variance); also, it has been shown for the multiple damage state model that

double sampling leads to significant underestimation of the level of more severe damage (after-yield damage states).

The other shortcoming of uncoupled damage and structural analyses: inexact mathematical damage description (inexact limit-state functions) has also been studied. In practice, the exact limit-state functions are rarely available. It is shown in this study that in case of structural damage the inexact damage description may cause significant errors in damage estimates.

Both this weaknesses of the uncoupled damage estimation are the particular examples of practically inevitable inconsistencies between structural and damage analyses if they are separated (uncoupled) from each other. The proposed approach using coupled structural and damage analyses helps to overcome the deficiencies of uncoupled damage estimation techniques by eliminating these inconsistencies. Indeed, it eliminates the double sampling and corresponding errors altogether. It also helps to alleviate the problem of inexact damage description, since it allows utilizing more complicated and accurate limit-state functions. The difference between the two approaches is studied by comparison of results of damage estimation performed for a 2-D structural model of a reinforced-concrete frame. The result show that errors of the fragility function based damage estimates could be significant and they depend on specific characteristics of the chosen structural model and the damage model in a complex way, preventing the possibility of estimating the errors in a general form that is applicable to all practically possible cases.

There are some problems that have not been fully addressed in this study that could be interesting subjects for future research. One of them is sensitivity of the effects

of double sampling to the various factors. For example, in this study, the level of uncertainty of structural parameters has been set to 0.08 (as measured by the coefficient of variation). It is possible that for higher levels of uncertainty, the effects of double sampling may be more pronounced. Also, we have assumed a lognormal distribution for the parameters, but the shape of distribution can possibly affect the difference in the results between the two approaches, which may be worth some future research. The other factor that could affect the damage estimation results is redundancy of the structural model under consideration. The model used in present study is highly redundant, which is typical for buildings. It is possible that for less redundant systems, such as bridges, the difference between the two approaches will be more prominent, which is another possible subject for future studies. An important observation of the present study is the significant underestimation of severe damage in case of uncoupled damage analysis. The causes of this discrepancy need to be understood better and are worthy of further investigation.

A case is also studied where structural damage prediction is not based on an *EDP* obtained from a structural analysis but on an *EDP* obtained from observation of real structure behavior, where a structural model is not employed. It is shown that incorporating site-specific information can significantly change the damage estimates and, therefore, can be worth doing.

A close relation between structural states (“yield,” “maximum strength,” etc.) and visible or detectable damage (“concrete crushing,” “spalling,” etc.) is assumed in this study. A general consensus in the earthquake engineering community and some experimental studies support this claim. However, researchers that perform test programs rarely record signs of visible damage at various stages during of their testing, which

makes it difficult to relate force deformation history to visible damage. Collection of such information is recommended in future testing so that the damage analysis can be built in into the structural analysis.

The other interesting problem that has not been fully addressed in this study but might be a subject of future research is the problem of defining a proper limit-state function for damage description. Currently, damage is usually defined by a "capacity less than demand" limit-state function. It is a conventional and intuitively understandable idea but it still brings about some questions and doubts that are related to the concept of "capacity." The fragility functions are often defined as cumulative distribution functions of capacity, but in many situations the very existence of capacity is questionable due to the fact that damage can be caused by several independent factors. In that case, the term capacity with respect to just one of the multiple factors is not well-defined. It is believed that capacity can be well-defined in cases where the fragility function is an increasing function of *EDP*. The problem of finding sufficient conditions for a fragility function to be an increasing function can be an interesting and challenging problem for future research.

9 References

Aboutaha, R. S., Engelhardt, M.D., Jirsa, J.O., and Kreger, M.E., 1993, "Seismic Strengthening of R/C Columns Using Steel Jackets," ***American Society of Civil Engineering Structures Congress***, Irvine, CA.

Aguilar, J., Juarez, H., Ortega, R., and Iglesias, J., 1989, "The Mexico Earthquake of September 19, 1985 -- Statistics of Damage and Retrofitting Techniques in Reinforced Concrete Buildings Affected by the 1985 Earthquake," ***Earthquake Spectra, Vol. 5, No. 1***, Oakland, CA: Earthquake Engineering Research Institute, pp. 145-151.

Altin, S., Ersoy, U., and Tankut, T., 1992, "Hysteretic Response of Reinforced Concrete Infilled Frames," ***Journal of Structural Engineering, Vol. 118, No 8.***

American Concrete Institute (ACI), 1996a, ***ACI 224.1R-96, Causes, Evaluation, and Repair of Cracks in Concrete Structures***

American Concrete Institute (ACI), 1996b, ***ACI 546R-96, Concrete Repair Guide***

American Institute of Steel Constructions (AISC), Inc., 1997, ***Seismic Provisions for Structural Steel Buildings,*** Chicago, IL

Aoyama, H., Kato, D., Katsumata, H., and Hosokawa, Y., 1984, "Strength and Behavior of Postcast Shear Walls for Strengthening of Existing Reinforced Concrete Buildings," ***Eighth World Conference on Earthquake Engineering, San Francisco CA, Vol. 1***

Au, S.K., Beck, J.L., 2001a, "First Excursion Probabilities for Linear Systems by Very Efficient Importance Sampling," ***Probabilistic Engineering Mechanics, 16***, pp. 193-207.

Au, S.K., Beck, J.L., 2001b, "Estimation of Small Failure Probabilities in High Dimensions by Subset Simulation," ***Probabilistic Engineering Mechanics, 16***, pp. 263-277.

Basoz, N., Kiremidjian A. S., 1999, ***Development of Empirical Fragility Curves for Bridges***, 5th U.S. Conference on Lifeline Earthquake Engineering, Seattle, Wash. August 12-14, pp. 693-702.

Beck, J.L., Kiremidjian, A.S., Wilkie, S., Mason, A., Salmon, T., Goltz, J., Olson, R., Workman, J., Irfanoglu, A., and Porter, K.A., 1999, ***Social, Economic and System Aspects of Earthquake Recovery and Reconstruction, Final Report for CUREe-Kajima Phase III Project***, Richmond, CA: Consortium of Universities for Research in Earthquake Engineering

Beck J.L., Porter K.A., Shaikhutdinov R.V., S. K. Au, T. Moroi, Y. Tsukada, and M. Masuda, 2002 ***Impact of Seismic Risk on Lifetime Property Values, Final Report,*** Richmond, CA: Consortium of Universities for Research in Earthquake Engineering

Bonacci, J.F., and Maalej, M., 2000, "Externally Bonded FPR for Service-Life Extension of RC Infrastructure," ***Journal of Infrastructure Systems, Vol. 6, No. 1,*** pp. 41-51.

Bush, T.D., Talton, C.R., and Jirsa, J.O., 1976, "Behavior of Structure Strengthened Using Reinforced Concrete Piers," ***ACI Structural Journal***

Carr, A.J., 2001, ***Ruaumoko,*** Christchurch, New Zealand: University of Canterbury

Corazao, M., and Durrandi, A.J., 1989, ***Repair and Strengthening of Beam-to-Column Connections Subjected to Earthquake Loading, Technical Report NCEER-89-0013,*** Buffalo, NY: National Center for Earthquake Engineering Research, State University of New York

Cornell, A., and Krawinkler, H., 2000, ***Progress and Challenges in Seismic Performance Assessment***, PEER Center News 3(2): 1-3.

Ellingwood, B., Galambos, T.V., MacGregor, J.G., and Cornell, C.A., 1980, ***Development of a Probability-Based Load Criterion for American National Standard A58, Special Publication 577,*** National Bureau of Standards, Washington, DC, 222 pp.

Ersoy, U., 1992, "Repair and Strengthening of R/C Structures – Research at METU," ***International Symposium on Earthquake Disaster Prevention, Vol. 2***

Ersoy, U., Tankut, A.T., and Suleiman, R., 1993, "Behavior of Jacketed Columns," ***ACI Structural Journal, Vol. 90, No 3.***

Goel, S.C., and Lee, H.S., 1990, "Seismic Strengthening of R/C structures by Ductile Steel Bracing System," ***Proceedings of Fourth U.S. National Conference on Earthquake Engineering, Palm Springs CA, Vol. 3***

Hachem, M.M., 2003, ***BiSpec 1.2***, Berkeley, California: University of California at Berkeley

Hart, G.C., Srinivasan, M., ***Typical costs for seismic rehabilitation of existing buildings***, FEMA (Series) 156-157, Washington, D.C., Federal Emergency Management Agency, 1994

Hipley, P., 1997, "Bridge Retrofit Construction Techniques," ***Second National Seismic Conference on Bridges and Highways, Sacramento, California, July 8 -11***

Gardoni, P., Kiureghian, A., Mosalam K.M., 2001, ***Probabilistic Capacity Models and Fragility Estimates for RC Columns Based on Experimental Observations***, ASCE Journal of Engineering Mechanics

Irfanoglu, A., 2000, ***Structural Design under Seismic Risk Using Multiple Performance Objectives***, Report No. EERL 2002-02, Pasadena, CA: Earthquake Engineering Research Laboratory, California Institute of Technology

Islam, M.S., 1996, "Holiday Inn," ***1994 Northridge Earthquake Buildings Case Study Project Proposition 122: Product 3.2,*** Sacramento CA: Seismic Safety Commission, 189-233.

Jennings, P.C., 1971, ***Engineering Features of the San Fernando Earthquake of February 9, 1971, Report EERL 71 – 02,*** Pasadena, CA: California Institute of Technology

Kiureghian, A., 1999, ***Fragility Estimates for Electrical Substation Equipment***, 5th US Conference on Lifeline Earthquake Engineering, Seattle, Wash. August 12-14, pp.643-652.

Krawinkler, H., 2002, "A General Approach to Seismic Performance Objectives," ***International Conference on Advances and New Challenges in Earthquake Engineering Research***, First Annual Meeting of ANCEER, Hong-Kong, August 19-20, Hong-Kong, China

Li, Y.R., and Jirsa, J.O., 1998, "Nonlinear Analyses of an Instrumented Structure Damaged in the 1994 Northridge Earthquake," ***Earthquake Spectra, 14 (2),*** Oakland, CA: Earthquake Engineering Research Institute, pp. 245-264.

Miranda, E, and Aslani, H., 2003, ***Probabilistic response assessment for building-specific loss estimation***, Report No. PEER-2003/03, Berkeley, CA: Pacific Earthquake Engineering Research Center, University of California

Moehle, J.P., Nicoletti, J.P., and Lehman, D.E., 1994, ***Review of Seismic Research Results on Existing Buildings, Report No. SSC 94-03,*** Sacramento, CA: California Seismic Safety Commission

Mosallam, A.S., 2000, "Strength and Ductility of Reinforced Concrete Moment Frame Connections Strengthened with Quasi-isotropic Laminates" ***Composites Part B – Engineering, Vol. 31***, pp. 481-497.

Ozaka, Y., and Suzuki, M., ND, "Study on Shear Failure and Repair Method of Reinforced Concrete Beam," ***Japanese Society of Civil Engineers, Concrete Library International, No 9.***

Pacific Earthquake Engineering Research Center (PEERC), 2004, ***Open System for Earthquake Engineering Simulation,*** (OpenSees), Berkeley, CA: Pacific Earthquake Engineering Research Center, (http://opensees.berkeley.edu/)

Porter, K.A., 2000, ***Assembly-Based Vulnerability of Buildings and Its Uses in Seismic Performance Evaluation And Risk-Management Decision-Making***, Doctoral Dissertation, Stanford University, Stanford, CA, published by ProQuest Co., Ann Arbor, MI, pub. 99-95274, 196 pp.

Porter, K.A., Kiremidjian, A.S. and LeGrue, J.S., 2001, "*Assembly-Based Vulnerability of Buildings and Its Uses in Performance Evaluation*," Earthquake Spectra, 17 (2), 291-312.

Public Works Research Institute (PWRI), 1986, ***Manual For Repair Methods of Civil Engineering Structures Damaged by Earthquakes***, (Japanese version, 1986) The Public Works Research Institute, Ministry of Construction, Vol. 45, (English version, 1988) Buffalo, NY: National Center for Earthquake Engineering Research, State University of New York

Resnik M.D., 1987, ***Choices: an Introduction to Decision Theory,*** University of Minnesota Press, Minneapolis

Rissman and Rissman Associates, 1965, ***Holiday Inn Van Nuys Structural Drawings,*** Pacific Palisades, CA

Rodriguez, M., and Park, R., 1992, "Lateral Load Response of Reinforced Concrete Columns Strengthened by Jacketing," ***International Symposium on Earthquake Disaster Prevention, Vol. 2***

Saadatmanesh, H., and Malek, A.M., 1998, "Design guidelines for Flexural Strengthening of RC Beams with FRP Plates," ***Journal of Composites for Construction, Vol. 2, No 4,*** pp. 158-164.

Saiidi, M., and Sozen, M.A., 1979, ***Simple and Complex Models for Nonlinear Seismic Response of Reinforced Concrete Structures, Report UILU-ENG-79-2031,*** Urbana, IL: Department of Civil Engineering, University of Illinois

Sharpe, R.D., 1974, ***The Nonlinear Response of Inelastic Structures., Ph.D. Thesis,*** Christchurch, New Zealand: Department of Civil Engineering, University of Canterbury

Stone, W.C., and Taylor, A.W., 1993, ***Seismic Performance of Circular Bridge Columns Designed in Accordance With AASHTO/CALTRANS Standards, NIST Building Science Series 170,*** Gaithersburg, MD: National Institute of Standards and Technology

Stoppenhagen, D.R., Jirsa, J.O., and Wyllie, L.A., 1995, "Seismic Repair and Strengthening of a Severely Damaged Concrete Frame," ***ACI Structural Journal, Vol. 92, No 2.***

Tanaka, H., Park, R., 1990, ***Effects of Lateral Confining Reinforcement on the Ductile Behavior of Reinforced Concrete Columns***, Report 90-2, University of Canterbury, Christchurch, New Zealand, June

Williams, D., 2000, ***Weighing the Odds: A Course in Probability and Statistics***, Cambridge University Press, Cambridge, UK

Williams, M.S., Villemure, I., and Sexsmith, R.G., 1997, "Evaluation of Seismic Damage Indices for Concrete Elements Loaded in Combined Shear and Flexure," ***ACI Structural Journal, Vol. 94, No. 3***, pp. 315-322.

Woodward-Clyde Federal Services, 1997, ***Suites of Earthquake Ground Motions for Analysis of Steel Moment Frame Structures,*** Pasadena, CA (http://nisee.berkeley.edu/data/strong_motion/sacsteel/ground_motions.html)

ZEvent, 2000, ***UCFyber Version 2.4.1,*** Berkeley, CA

Appendix A. Probabilistic relation between damage states and repair methods.

A.1 Available repair methods

(1) Epoxy injection. This requires filling the cracks with epoxy grout under pressure. According to ACI (1996b) Section 22.6.6.3, this procedure can prevent all movement at an opening and restore the full strength of a cracked concrete member. Ozaka and Suzuki (ND) support this statement by an experimental study of specimens repaired with epoxy injection of specimens with shear cracks less than 1 mm. The method is simple and widely used. Jennings (1971) gives examples of its application for buildings that were lightly damaged after 1971 San Fernando earthquake. However, some researchers report that the method is not always effective. Corazao and Durrandi (1989) repaired beam-to-column connections with cracks less than 1/8 in wide, and found that epoxy injection by itself might not be adequate for restoring strength and stiffness. In particular, restoring the bond and anchorage of bars can be difficult and unreliable. This is likely to restrict the method to light damage states where deterioration of bonds is negligible. Otherwise, the method is difficult to implement and its effectiveness depends greatly on the quality of the work.

The Japanese Ministry of Construction Manual (PWRI, 1986) gives a good description of damaged concrete members that can be repaired by this method. This description agrees well with the light damage state given by Williams *et al.* (1997) and "cracking" damage state used in this study. Recommendations and requirements for epoxy material choice, surface preparation, application techniques and equipment are also given in American Concrete Institute (1996a and 1996b).

(2) Replacement of damaged concrete. This usually involves shoring of the structure, removal of the damaged concrete and replacement with new concrete. The bond between the old and the new concrete is ensured by applying an epoxy-based bonding agent to the old concrete surface. Corazao and Durrandi (1989) study the performance of two beam-to-column joints repaired with this technique. Damage was characterized by concrete spalling, penetrating cracks, deterioration of bond between longitudinal reinforcement and the concrete, and intact reinforcement. This type of damage can be recognized as the "yielding" damage state. The technique is shown to be effective for restoring strength, stiffness and energy dissipation characteristics of the subassembly. Guidelines for removal of concrete, surface preparation and choosing epoxy bondage is given by the American Concrete Institute (1996b).

(3) Interior reinforcing. A common method of providing additional reinforcement across cracked surfaces is to install new dowels in holes drilled perpendicular to the crack surfaces. The entire length of the dowel is fixed to the concrete by the use of a bonding matrix. Epoxy injection is commonly used to fill all cracks after installation of the dowels and their adhesive. The methodology and examples are described by the American Concrete Institute (1996b). The procedure is simple and uses commonly available equipment, but its applicability for seismic repair is doubtful. First, for severe damage states, the cracks penetrate in various directions and develop in large number, so there is no perpendicular direction for all of them. Second, for light damage, space constraints from the outside of the member may not permit drilling holes transverse to the crack. This situation would be typical for buildings. Third, the seismic performance of members repaired with this technique is not confirmed experimentally.

(4) Exterior reinforcing by reinforced-concrete jacketing. This involves encasement with a reinforced concrete jacket together with additional reinforcement. Stoppenhagen *et al.* (1995) investigate the behavior of upgraded columns acting in moment-resisting frame. Their results show that the method effectively prevents shear failure. Corazio and Durrandi (1989) demonstrate that strength, stiffness and energy dissipation capabilities can be effectively restored by jacketing the columns along with the beam segments adjacent to the columns, even in case of very severe damage. In particular, one test involved a column damaged to the point that its contribution to lateral load resistance was considerably reduced. Stoppenhagen *et al.* (1995) also show the effectiveness of this repair technique. Heavily damaged columns with shear failure, extensive spalling, bent longitudinal bars, and ½-in cracks, were encased with new columns containing longitudinal and shear reinforcement. The lateral capacity of the repaired frame increased by a factor of five, preserving the original stiffness. Ersoy *et al.* (1993) obtained similar results. They tested specimens in two damage states: one in which initial signs of concrete crushing were observed, and the other where considerable crushing and rebar buckling occurred. After repair, the columns had strength about 10% less than the corresponding monolithic column but with considerably less deformation capacity. The authors also emphasize that members repaired without unloading performed significantly worse. Rodriguez and Park (1992) repaired and tested specimens that were damaged beyond the failure damage state as classified by Stone and Taylor (1993) that is called “ultimate” in this study. The repaired unit demonstrated an increase in strength and stiffness about three times those of the original specimen.

(5) Exterior reinforcing by steel jacketing. This involves encasement of a member in steel plates, with epoxy resin used to bond the plates to the concrete. Ersoy (1992) points out that merely bonding plates to the concrete provides inadequate improvement, but that strengthened beams behaved well when the end of the plate was either welded to the main bar or was both clamped and epoxied to the beam. The technique is less laborious than concrete jacketing and is commonly used. Aboutaha *et al.* (1993) demonstrated that the method is effective for increasing shear strength of short columns. They tested original intact columns that were strengthened with steel jackets. They performed no tests involving damaged specimens. Tests with lightly damaged specimens were performed by Corazao and Durrandi (1989), who conclude that the method can be quite effective in restoring and improving the structural performance of beam-column connections provided that design details properly address the transfer of forces through the joint.

(6) Exterior reinforcing by steel bracing. This involves supplementing an exiting reinforced concrete frame with a steel frame. Goel and Lee (1990) studied a repaired reinforced concrete frame that was damaged to the point close to maximum loading capacity (2% drift). They find that response of the repaired frame was stable with increased stiffness, strength and energy dissipation.

(7) Combined methods. Corazao and Durrandi (1989) report a combination of several techniques for repairing heavily damaged beams. The damage was in the form of severe flexural and diagonal cracks accompanied by the spalling of the cover concrete and buckling of the longitudinal reinforcement steel. Repair efforts included injection of resin, splicing the buckled portion of the reinforcement with new bars, and replacement

of damaged concrete with epoxy mortar. The repaired specimens exhibited increased strength, ductility and energy dissipation capabilities along with reduced stiffness. Overall performance proved quite satisfactory, and specimens suffered much less damage after the repairs were performed.

Ozaka and Suzuki (ND) repaired six specimens with epoxy injection accompanied by steel plates attached to the beam webs. Damage before repair was characterized by shear cracks 2 mm wide. The yield load after repair was 15% higher. The authors conclude that the steel plates increase the shear strength and member deformability.

(8) FRP jacketing. This involves encasing in fiber-reinforced polymers (FRP), an innovative technique that has only recently been an object of experimental studies. Mosallam (2000) used specimens damaged to the point beyond yielding and then repaired them with epoxy injection, carbon-epoxy and E-glass-epoxy quasi-isotropic laminates. The ductility and strength of the repaired specimens were increased up to 42% and 53% respectively, as compared to the control specimens.

(9) Infill walls and wing walls. Quite a number of researchers studied the performance of this type of reinforcement e.g., Bush *et al.* (1976), Altin *et al.* (1992), Aoyama *et al.* (1984). For a more complete list, see Moehle *et al.* (1994). Although these methods are widely accepted within the industry and were generally reported as satisfactory for retrofitting existing buildings, no tests with previously damaged frames have been conducted, which poses a question about the adequacy of this technique for repair.

A.2 Statistics of application of repair techniques

Given the variety of repair methods available, the next question to be addressed is how frequently each is used. Aguilar et al. (1989) studied 114 buildings that were damaged during 1985 Mexico City earthquake. They created a database containing descriptions of the buildings, types of damage and the repair techniques used. The level of damage for all buildings is described as severe. For the present study, the point of particular interest is the frequency of usage of different repair techniques for reinforced concrete moment frames. The relevant statistics are given in Table A.1.

Table A.1 Frequency of usage of different repair techniques for reinforced concrete frames after 1985 Mexico City earthquake.

Repair and strengthening technique	Number of times used
Epoxy resin	3
RC jacketing	35
Steel jacketing	9
Infill walls, wing walls	22
Steel bracing	7
Replacement	12

Bonacci and Maalej (2000) present a comparative study of the usage of steel jacketing and fiber reinforced polymer (FRP) jacketing. Their paper summarizes the results of a comprehensive survey of field applications of both steel plates and FRP composites as external reinforcement for the life extension of deteriorating RC flexural members. The authors demonstrate a trend toward using FRP jacketing rather than steel

jacketing. This trend should be accounted for when evaluating the likelihood of using these methods in the future.

A.3 Relating damage states to repair efforts

There are no universally accepted standards for choosing repair methods for damaged reinforced-concrete flexural members. Even if a damage state is clear, there are several techniques that can be used, and it is difficult to predict the repair procedure an unknown engineer will specify in any future application. The engineer's decision depends not only on the damage itself but on a number of uncertain circumstances such as availability of materials, equipment, personnel, and company expertise. Table A.2 relates common repair techniques to damage.

Because more than one possible repair technique is associated with each damage state, a qualitative probabilistic relationship is proposed in Table A.3. The table gives the approximate likelihood that a particular damage state would be repaired in a particular way. The estimates are based on statistics of application and modern trends in the industry together with considerations addressed by Table A.2: the apparent acceptance by the engineering and construction industry, the availability of standards, the labor required to perform the repair, and any design difficulties. Methods employed to address the "ultimate" damage state are assumed to be applicable to the "maximum strength" damage state as well. The difference between "maximum strength" and "ultimate" damage states is reduced to increasing likelihood of replacement for "ultimate" damage state. Qualitative probabilities given in the table can form the basis for assigning a set of quantitative probabilities to repair events.

There is another factor that could affect the choice of repair techniques: overall repair objectives. If the owner's final goal is not merely to restore the structure but to improve its strength above its pre-earthquake condition, then methods that are unable to provide additional strength can be ruled out, reducing the available choices and altering the probabilities for remaining repair techniques.

Table A.2 Characteristics of repair techniques.

Technique	Damage states	Performance	Other remarks
Epoxy injection	Cracking or Yielding	Good results for light damage. For heavier damage it is difficult to insure proper filling of every crack.	Commonly used (PWRI, 1986). Standards available (ACI 1996a, ACI 1996b). Easily implemented for light damage states. No design requirements. Requires care and high quality of the work for moderate damage.
Replacement of damaged concrete	Yielding	Provides full restoration of all member loading characteristics (strength, stiffness, energy dissipation). Does not provide strengthening. Requires full unloading of the member.	Every step (removing of damaged concrete, surface preparation, replacing with new concrete) is well documented by ACI standards (ACI 1996b). No design requirements. Laborious. No data on acceptance of the method as a whole within the industry
R/C jacketing	Yielding to Ultimate	Provides full restoration or increasing of strength, stiffness and energy dissipation up to five times of original level, depending on repair details. May require unloading of the structure.	Standards available (ACI 1996b, building codes). Requires design. Very laborious. Accepted within the industry (Corazao and Durrandi, 1989).

Technique	Damage states	Performance	Other remarks
Steel jacketing	Cracking to Yielding	Effective for restoring and strengthening R/C structures providing proper design. Usually accompanied by epoxy injection.	Standards available (Hipley, 1997). Requires design. Less laborious than R/C jacketing. Well accepted within the industry (Bonacci and Maalej 2000).
Steel bracing	Yielding	Could effectively restore and strengthen the whole structure providing proper design. Applied to the whole frame.	Standards available (AISC, 1997). Qualified designer required. Laborious. Accepted within the industry.
Steel bracing	Yielding	Could effectively restore and strengthen the whole structure providing proper design. Applied to the whole frame.	Standards available (AISC, 1997). Qualified designer required. Laborious. Accepted within the industry.
FRP jacketing	Yielding	Reported to be effective for recovery and increasing load capacity.	Standards and guidelines are available (Hipley, 1997, Saadatmanesh and Malek, 1998). Easy to implement. Composite-materials designer is required. Method is finding increasing popularity in the industry. It is usually used as an alternative to steel jacketing (Bonacci and Maalej, 2000).

Technique	Damage states	Performance	Other remarks
Infill walls and wing walls	No data	Shown to be effective as strengthening-retrofitting technique. Is applied to the whole column (wing walls) or to several bays (infill walls)	Some standards and guidelines for design are available from Caltrans (Hipley, 1997). Requires design. Laborious. Well accepted within the industry.

Table A.3 Proposed relation between damage states and repair techniques.

Damage state	Possible repair methods	Probability of usage*
Cracking	Epoxy injection	High
	FRP jacketing	Low
Yielding	Infill walls or wing walls	Low
	Steel bracing	Low
	R/C jacketing	Average
	FRP jacketing	Average
	Steel jacketing	Below average
Maximum strength	Replacement	Above average
	R/C jacketing	Average
	Infill walls or wing walls	Average
Ultimate	Replacement	High
	R/C jacketing	Below average
	Infill walls or wing walls	Below average

* Scale: low – below average – average – above average – high; applied independently to each damage state.